UNIVERSITY OF SOUTHAMPTON

FACULTY OF ENGINEERING AND APPLIED SCIENCE
INSTITUTE OF SOUND AND VIBRATION RESEARCH

THE USE OF DAMPING MATERIAL IN INDUSTRIAL MACHINES

by

ARCANJO LENZI

July, 1985

UNIVERSITY OF SOUTHAMPTON

ABSTRACT

FACULTY OF ENGINEERING AND APPLIED SCIENCE
INSTITUTE OF SOUND AND VIBRATION RESEARCH

Doctor of Philosophy

THE USE OF DAMPING MATERIAL IN INDUSTRIAL MACHINES

by Arcanjo Lenzi

Structural damping has become an important parameter in L_{eq} reduction of machines. Its use is particularly important in the medium frequency range (500 Hz to 3000 Hz) from where most of the acoustic energy is radiated. Studies on a new and useful damping technique, the filling of cavity components with granular materials, is presented in this thesis. Experimental studies show regions of maximum damping caused by standing wave formation in the material. The first maximum occurs when the internal dimension of the cavity is equal to one quarter of the longitudinal wavelength. The tuning of optimum damping to any desirable frequency requires accurate knowledge of wave speed. Experiments show that wave speeds also decrease with amplitude when strains reach values higher than about 10^{-6}. This is caused by gross slip taking place at contacts which breaks the main structure of grain-grain contacts responsible for the propagation of elastic waves. Waves speed whose amplitude produce strains smaller than 10^{-6} were observed being independent of amplitude. Is is concluded that the effective elasticity of the granular material, for these small strains, is given by the elasticity of actual grains themselves in the chain of grain contacts; local deformations at contacts are negligible. Loss factors of granular materials also present identical variation with strain. At large strains ($> 10^{-6}$) energy is totally dissipated at grain contacts, by dry friction in partial and gross slip forms. For low strains, as insignificant amount of energy is dissipated at grain contacts compared to the amount of energy dissipated by hysteresis inside the grains themselves.

ACKNOWLEDGEMENTS

The author gratefully acknowledges the guidance provided by Professor E.J. Richards during the course of this project, and is also indebted to the following:

The Federal University of Santa Catarina (UFSC) and Conselho Nacional de Desenvolvimento Científico e Tecnológico - CNPq (both in Brazil) for the financial support;

Mr. G. Stimpson, for suggesting so many improvements in the English;

To all the staff of the ISVR who freely gave much advice during this project;

And his wife, Maria Helena, for the constant encouragement and motivation.

The superb typing of the manuscript by Mrs. Maureen Strickland is also gratefully acknowledged.

TABLE OF CONTENTS

LIST OF SYMBOLS

A	- Weighting function; constant;
B	- Constant;
C	- Speed of waves;
C_ℓ	- Longitudinal wave speed;
d	- Thickness
E	- Young's (Elastic) modulus;
E_{gm}	- Young's modulus of granular material;
Emax	- Maximum vibratory energy;
E_{vib}	- Vibratory energy of structure;
f	- Frequency;
Δf	- Frequency bandwith;
f_n	- Resonant frequency;
fo	- Central frequency band;
F(t)	- Time history force;
F(f)	- Force spectrum;
g	- Acceleration due to gravity, 9.81 $\square/s^2$;
G	- Shear modulus;
h	- Length;
H(f)	- Point response function spectrum;
I	- Inertia moment of Area;
Im{ }	- Imaginary part of;
k	- Wavenumber (ω/C); constant; stiffness;
ℓ	- Length; dimension of cavity;
Leq	- Equivalent sound pressure level;
m	- mass;
M	- Flexure moment;
N	- Normal compression force of spheres;
p	- Pressure;
$\overline{P}$	- Force;
P_c	- Clamping pressure;
Q	- Quality factor used for damping representation;
r	- Radius;
r_o	- Radius of contact area;
R	- Radius of sphere;
Re{ }	- Real part of;

S - Area;

t - Time;

T - Tangential fore; Reverberation time;

V - Velocity response;

x - Displacement; axis of cartesian coordinate system;

$\overline{X}$ - Displacement amplitude;

Y - Axis of cartesian coordinate system;

ω - $2\pi f$ - Angular frequency (rad/s)

W_{in} - Input power;

W_{diss} - Power dissipated;

$\overline{Z}$ - Complex impedance;

α - Normal displacement;

γ - Poisson's ratio;

ξ - Beam wall displacement;

ζ - Particle displacement;

ϕ - Phase difference; porosity;

η - Loss factor;

η_{gm} - Loss factor of granular material;

η_s - Structural loss factor;

ρ - Material density;

σ - Normal tension;

σ_f - Fatigne limit;

σ_{rad} - Radiation efficiency;

σ_o - Hydrostatic pressure;

θ - Tangential displacement;

μ - Friction coefficient.

CHAPTER 1

INTRODUCTION

Noise in industry has become a matter of increased concern in recent years and its hazardous effects on hearing are now well known. It is estimated that in Great Britain alone some half a million workers are subjected to noise levels which may cause hearing damage. Impending legislation, specifying limits for noise in industrial environments, has provided a new stimulus for research into ways of reducing levels. Noise control at source is obviously the most desirable, though most difficult method, rather than the more common solution of enclosures. This thesis concentrates on the former area, with particular reference to machine structures, mechanical processes and handling noise (noise associated with the transport of workpieces and materials inside factories).

The relative importance of the several parameters influencing the noise radiation from machine structures can be seen from Richard's equation[1]

$$L_{eq}(A, \Delta f, f_o) = 10 \log F_c'(f_o) + 10 \log \mathrm{Re}\{- jH_c(f)\} + 10 \log \frac{\Delta f}{f_o}$$

$$+ 10 \log \frac{A\sigma_{rad}}{f_o} - 10 \log \eta_s - 10 \log d + C$$

where L_{eq} is the equivalent level of the sound power radiated, filtered in a band Δf and centred at f_o; F_c is the impulse force; H_c is the point response function (defined as displacement/force); d is a typical thickness of the structure; $A\sigma_{rad}$ is the A-weighted radiation efficiency; η_s is the structural loss factor and C is a constant.

Richards was able to show the importance that medium frequencies (500 Hz to 3000 Hz) have on the total noise energy radiated from machines. This is due to the way the frequency related parameters, such as force derivatives, radiation efficiency, A-weighting function and point response, combine and maximise L_{eq} in this region. Other parameters have a flat spectral shape.

The total noise radiated is considered as a sum of terms each related to individual structural parameters and to the excitation. Some terms of the equation have been quite extensively studied, radiation efficiency[2] and the point response function[3], for instance, while others are still not properly understood. This is the case for structural damping; the mechanisms of energy dissipation which exist in machine structures at medium frequencies have not been fully explained. The importance of damping as a noise control parameter can be seen from the above equation which shows that as L_{eq} is negatively proportional to the logarithm of the loss factor, a tenfold increase in η_s (at mid-frequencies where most of the sound is radiated) reduces L_{eq} by 10 dB. Hence, this thesis has been aimed towards finding ways of improving the damping of machine structures.

The damping of a structural component is the term usually employed to describe the dissipation into heat (or otherwise) of vibratory energy. Energy flow to other structural components is another way in which energy is removed from a vibrating component. However, this is difficult to quantify so that heat dissipation mechanism only will be discussed in this thesis. The most common mechanisms by which vibrational energy is dissipated in industrial structures are internal friction in metals (material damping), friction at joints (interfacial damping) and additive treatments such as viscoelastic materials attached to the surface of the structure (additive damping). Oil films or air trapped at joints and gaps and the filling of the cavities in components with granular materials can also provide considerable amounts of energy dissipation. Sound radiation from structures is a form of damping (acoustic damping) but its contribution is usually insignificant compared to other mechanisms.

The usual form of specifying the level of damping that exists in a component is by the loss factor defined as

$$\eta_s = \frac{\text{Energy dissipated per radian of oscillation}}{\text{Total vibratory energy in the system}} .$$

The loss factor thus defined is convenient because it represents a ratio of energies and can be employed to both simple and complex structural vibrators. Another form of damping representation often found in the literature is the Quality Factor (Q) defined as the reciprocal of the loss factor,

$$Q = 1/\eta_s .$$

Each machine obviously has its own particular and simplest method of noise control, the forcing function being the most important parameter because it is in fact the primary cause of the noise problem. It is not always possible, however, to reduce the force input to desirable levels as this may adversely affect the efficiency of the machine or process. Thus, other parameters must be considered. This is the stage where damping becomes an essential parameter in noise reduction. An example of this can be seen in noise reduction of drop forges. Four main noise sources are apparent: (a) acceleration noise from the impulsive movement of several components, particularly the tup, anvil and the billet as it deforms plastically in a very short time at each blow; (b) noise due to air emission at very high speed from the impact area; (c) small explosions in the impact area due to combustibility of the oil and sawdust thrown into the die area; (d) the vibratory energy stored in the various components after each blow. Source (d) above is perhaps the dominant noise source in drop forges, because although surface velocities may not reach values as high as those during the initial impacts (constituting the acceleration noise which lasts for milliseconds only) their continuing transient vibrations are a major contribution to the overall L_{eq} before they finally die away. The columns of a drop forge are components where structural damping can be applied quite simply because of their hollow construction. Their walls have panels which can be damped by viscoelastic layers, and also cavities which can be filled with granular materials. Tup guides bolted to them provide further increases in the damping by energy dissipation in dry friction-form at contacting parts and joints of connection with other components (anvil and head gear, for instance) also contribute significantly to the overall damping due to the presence of rubber inserts. This example shows the importance of different forms of damping usually found in machine structures. Chapter 2 of this thesis presents a description of the physical phenomena associated with their mechanisms.

The filling of cavities in components with granular materials is a new technique which has some advantages over more conventional techniques. For instance, it is easy to apply and granular materials such as sand are cheap and have high internal damping. They can also resist high temperatures.

Although very few studies have so far been carried out on this particular damping technique, results were encouraging enough to start a research program seeking an understanding of the mechanisms of energy dissipation and the parameters to them associated. Wolf[27] reports experimental studies on a large I - beam having steel boxes filled with sand attached to it. Damping levels varied from 0.01 to 0.2 depending upon the amplitude of vibration. Measurements made at three frequencies (40 Hz, 110 Hz and 220 Hz) showed higher damping levels at 220 Hz and lowest at 40 Hz, despite acceleration levels of the beam did not vary significantly. Wolf's results show an interesting dependence upon amplitude i.e., an increase in the damping at higher order modes of the beam where its actual displacement amplitude is reduced. This leads one to conclude that amplitude of vibration may not be the parameter directly associated to the loss factor increase with frequency.

The work of kuhl an Kaiser[29] on damping of short concrete bars and aluminium tubes filled with sand, shows regions of maximum damping at about 1000 Hz. This was latter explained by Cremer and Heckl[21] in terms of resonances in the sand itself.

These results indicate that granular materials such as sand, may provide high levels of structural damping when applied to machine structures and contribute to a significant reduction in noise radiation.
This thesis therefore presents experimental and theoretical studies on the determination of parameters related to the mechanisms of energy absorption (and dissipation) from the structure in which the granular material is contained. A first part of the study (chapter 3) consists of a series of experiments designed to determine the influence of parameters such as amplitude of vibration, grain sizes, external pressure and cavity dimension upon the damping of beams. Internal damping and speed of waves have also been the subject of detailed studies - chapters 4 and 5 respectively - which originated from the necessity for accurate information about these particular parameters for the production of the damping of structures filled with granular materials. Such predictions are presented in chapter 6.

CHAPTER 2

DAMPING MECHANISMS COMMONLY FOUND IN MACHINE STRUCTURES

2.1 Introduction

Richards'[1] work showed the importance of the medium frequency acoustic energy radiation from machinery. This is due to a combination of structural and acoustical parameters, as was described in Chapter 1. Increasing structural damping levels especially in this frequency range is an important method of reducing the levels of noise radiation.

This chapter presents a brief physical description of the several mechanisms of damping found in most industrial machines, involving mainly material damping, frictional damping existent in joints, damping due to viscoelastic layers and due to air pumping at gaps of assembled plate-like components.

Results of measurements made in several machines and components, such as rods of rock drills, presses and drop forges are also presented to show the relevance of damping as a parameter for noise control.

2.2 Structural Damping Measurement Methods

2.2.1 Decay rate method

Perhaps the most common method of measuring damping is the decay rate method due to its simplicity. The rate of decay of vibrations after the excitation is suddenly turned off is measured and expressed in the form of reverberation time (T) which represents the time taken for the vibratory energy to decay to one millionth (60 dB) of its initial value. The loss factor is determined from the relation

$$\eta = \frac{2.2}{f\,T}$$

where f is the measurement bandwidth central frequency. Despite its popularity, the method has several drawbacks which must be remembered during

measurements. The first is related to the damping level up to which it is applicable. A structure whose loss factor is of 0.16, performing free vibrations, will dissipate all its vibratory energy in one cycle. Thus the decay rate readings (and consequently loss factor determination) are very inaccurate. The method is usually not recommended for structures having loss factor greater than 0.08 - 0.1.

Measurements are usually made in bands isolating distinct structural resonances. Machine components because of their sizes and bulky shapes, have distinct resonances only in the low and medium frequency regions. Resonant peaks are often closely spaced and amplitudes of one frequency band may influence readings taken in neighbouring bands. In such cases, filters of very sharp roll-off slope are required (48 dB/Dec or so) and results should be checked with measurements made by other methods, for instance, the half-power bandwidth.

2.2.2 Half-power bandwidth method

Loss factor determination by the half-power bandwidth method consists of plotting the response spectrum and measurement of the frequency bandwidth for values 3 dB down the peak (whose resonant frequency is f_n). The loss factor is calculated from the relationship:

$$\eta = \frac{\Delta f}{f_n} .$$

The modal density of flexual vibrations is constant with frequency, but, as the response halfpower bandwidth increases linearly with frequency for constant damping, the spectrum of highly damped structures has overlapping resonances which restricts the application of this method. On typical machine components its use is limited mainly to low frequencies. Alternatively, if the structure is poorly damped, resonances are so sharp that analysers frequency resolution is not sufficient if zooming facilities are not available.

2.2.3 Input power measurement method

A third method, the input power method, follows more closely the definition of loss factor. This involves measurement of the power dissipated (W_{diss}) by the component (which can be assumed equal to the power supplied to it assuming no energy is transmitted to other parts of the structure) and the structure's vibratory energy (E_{vib}). The loss factor is determined from the expression

$$\eta = \frac{W_{diss}}{2\pi f E_{vib}} .$$

The method has enormous potential because the power dissipation measurements (after conversion into energy dissipation per cycle) provides valuable information about damping mechanism and especially their variation with amplitude. Loss factors can be measured for different amplitudes of vibration in a very controlled way. This method is particularly useful in the research of new damping mechanisms. It enables measurements in highly damped structures, but it also has its drawbacks: it is time consuming, phase matching between force and response signals may present problems and resonances at contacts and in connectors limit the frequency range to below a few kiloHertz.

2.3 Material Damping

Although the inherent damping by internal friction in metals and alloys is small compared to that which can be instilled by special damping techniques, highly damped materials are desirable to provide a contribution to the overall damping of components in cases where additive damping treatments fail to succeed. Viscoelastic materials have been extensively used for many years and more recently studies on granular materials have shown that their use in industrial structures can significantly improve loss factors. An understanding of their mechanisms of internal energy dissipation is then essential to aid the design of quieter machines.

2.3.1 Damping in metals

Internal damping in metals is characterised by several relaxation peaks occurring over the spectrum which are associated to various microstructural mechanisms. A hypothetical spectrum suggested by Zener[5] shows regions of maximised loss factors caused by different forms of relaxation (fig. 2.1).

Point defect relaxation is a form of damping commonly found in crystalline materials. Impurities and point defects breaks the symmetry within the crystals giving an anelastic characteristic to the material when sound waves propagate through them.

Grain boundaries usually present viscous-like properties yielding a constant loss factor with amplitude (linear damping). Because of the freedom grains have for moving relative to each other, the damping provided by the grain boundaries is higher than that provided by the grains themselves. Point defect relaxation is a distinct case of relaxation. This is because at higher frequencies grains have no time to move relative to each other and little energy can be dissipated. Also only small amounts of energy are dissipated at low frequencies because the large period of vibration allows elastic relaxation of grains to take place. Intermediate conditions, however, maximise the energy dissipation and gives a so-called relaxation peak.

The frequency range covered by such peaks can be several decades often including the whole audio frequency range. Another equally important parameter related to the internal damping of metals is the amplitude of vibration. Fatigue stresses are always considered in the design of machines and so have been used here to represent the parameter amplitude. Below the fatigue limit (σ_f), the mechanisms of damping are found to be almost linear for the vast majority of metals used in industry. Some regions of a material may have stresses high enough to cause plastic flow or shear of some grains, but on a small scale without affecting the overall linearity of the damping mechanisms (fig. 2.2). As stresses in the material approach the fatigue limit (and even exceeding it) the high degree of plastic flow in the microstructure makes the loss factor strongly amplitude-dependent (but still frequency independent). Thus, at stresses higher than σ_f there is a sudden jump in the loss factor curve against strain.

Machine components are designed to operate with stresses smaller than σ_f and so this nonlinear region can generally be ignored and linear damping only should be observed.

Based on measurements made[5] in several materials commonly used in industry (1020 steel, grey iron, magnesium alloy, aluminium, sandwich steel, glass laminate, titanium alloy and others) at stresses below the fatigue limit, loss factors were all found to be approximately linear ($\eta \propto \sigma^n$, where n varies between 0 and 1). The deviation from linearity can be neglected in practical cases.

The effect of dynamic stress distribution over components has been studied in detail by Lazan and found that for linear damping mechanisms the loss factor of the component can be assumed to be identical to the loss factor of the material and independent of the stress distribution (i.e., independent of components' mode shapes of vibration).

Damping levels of different materials vary according to the degree to which each material is capable of dissipating energy in its microstructure. Cast iron, for instance, has a high percentage of carbon in graphite form and is a material with relatively high damping.

Typical loss factors of some of the materials usually found in industry are listed below.

Material	Loss Factor η
Aluminium	10^{-4}
Copper	2×10^{-3}
Cast iron	10^{-3}
Manganese/ Copper alloy	$3\text{-}7 \times 10^{-2}$
Steel	$1\text{-}6 \times 10^{-4}$
Tin	2×10^{-3}
Tungsten	2×10^{-4}

The damping level of a material in the absence of any other damping mechanism affects its dynamic characteristics, particularly at resonances. Resonant vibration levels are then totally controlled by the internal damping. In order to account for the internal damping of a component in the calculation of its dynamic response, the material elasticity modulus is usually written in the form

$$\overline{E} = E(1 + j\eta)$$

where E is the elasticity modulus obtained from static tests.

2.3.2 Damping of polymers (viscoelastic) materials

Polymer is a class of materials which exhibit high internal damping due to the nature of their long chain molecules which gives a combination of elasticity and viscosity. As a result the dynamic performance is between that of a crystalline solid and a liquid. The most important feature of this type of material is the dependence of damping on frequency and temperature. The amplitude of vibration does not affect the damping.

Molecules of polymers are composed of long chains of segments[6]. Each segment is made of a primary chemical structure (fig. 2.3). The overall combination of such segments is what differentiates one polymer from another. The way the segments are connected, size and numbers of branches, cross linkings, the addition of fillers, etc., are all factors which affect that damping of the material. In fact, special polymers can be "designed" to achieve particular damping qualities.

At low frequencies, stresses applied to the material deform the molecules by rotation and bending of not only the branches but also the whole segments too. This is a slow process allowing time for the molecule to readjust itself to a constant equilibrium state. Deformations follow in phase with slow change of stresses. Low frequency vibrations do not dissipate very much energy and this region is called the "rubbery" region of the spectrum.

At intermediate frequencies, chain segments perform coiling and uncoiling motions (chain segments are smaller than the macro-molecule and larger than primary chemical structures or the chain length of a monomer

group). The inertia of the whole molecule restrains its motion allowing bendings and coiling of chain segments only. In this region high damping occurs. Frequencies are high enough not to permit relaxation of the segments of the molecule, also strain and stress are out-of-phase.

At very high frequencies the bending and stretching of primary chemical structures at the outside of the molecule (forming its tips) provide its main source of deformation. The main structure of the molecule remains underformed and gives stiff characteristics to the material, called the "glassy" region on the spectrum. This process is also accompanied by very little energy dissipation.

Material loss factors are at a maximum in the intermediate frequency range of the spectrum called the "transition region".

Figure 2.4 shows typical loss factor and Young's modulus shapes for polymetric materials. Transition regions spread over several frequency decades so that loss factors can be constant and at a maximum throughout the audio spectrum. Special viscoelastic damping materials having loss factors of the order of unity can be obtained. Figure 2.5 shows measurements made on samples of standard PVC supplied by ICI. Values of $\eta = 0.2\text{-}0.3$ are typical of general purpose plastics and PVC materials available on the market in the form of tubes or sheets.

2.3.3 Standard material damping measurement methods

2.3.3.1 Metallic materials

Damping of metallic materials is usually measured by suspending samples in the form of bars on very thin wires (or silk thread whenever possible) to minimise the flow of energy through the suspension. The bar should also be suspended at nodal points for the same reason. For materials of very low damping ($\eta \leq 10^{-4}$) it is recommended that they are tested in a vacuum chamber to eliminate the damping supplied by the air surrounding the test specimen (acoustic damping). The usual test method is the decay rate method, unless damping is nonlinear. Transducers recommended are non-contacting devices, usually magnetic, which are readily available on the market. A laser velocimeter has recently been successfully used for loss factor measurements[25,26] of the damping of metals. Its main advantage is that it does not require careful positioning of transducers close to the

specimen surface. Accelerometers are not applicable for small samples of material as energy flowing through the cable leads to erroneous measurements.

2.3. .2 Viscoelastic materials

Damping measurements of viscoelastic samples is commonly performed by the use of the OBERST bar. It consists of attaching a layer of the material to be tested to a metallic (steel or aluminium) bar and the damping levels and resonant frequencies before and after attaching the viscoelastic material are measured. Elasticity and shear modulus of elasticity as well as longitudinal and shear loss factors of the material can be determined by this method. It has now become a draft proposed standard recommended by the Acoustical Society of America[18]. Figure 2.5 shows an example of its application[7], in the measurement of shear loss factors of three different ICI plastics. The OBERST bar is a simple and efficient technique which could in due course be used by all researchers in this field.

2.4 Structural Damping Techniques

After measurements on several industrial machines, one of the main conclusions was that almost all the damping was localised at the joints. That makes essential a deep understanding of the several mechanisms of energy dissipation, the parameters directly related to it as well as their importance. The effectiveness of more conventional damping techniques such as constrained layers of viscoelastic materials and vibrational absorbers will also be discussed. Two new damping techniques - air pumping and damping by granular materials - have recently been studied. A discussion of their applications will be presented.

2.4.1 Frictional damping at joints

2.4.1.1 Mechanism of friction

A joint is defined as the region of contact between two surfaces. Surfaces are never absolutely smooth; magnification would reveal many tiny tips and valleys. When surfaces are pressed together, the tips of the asperities carry all the applied forces producing high stress concentrations

which causes plastic deformation and forms cold-welded junctions between the metal surfaces. Frictional resistance to tangential forces is made up of two components[9]. One component overcomes the shear resistance of the welds before sliding begins - the shear component. As relative sliding begins, the opposing asperities tend to "plough" through one another, creating a second type of additional resistance - the ploughing component (only observed when one metal is very soft compared to the other). It may be expected that the application of a tangential load initiates plastic flow and junction growth before junction shearing begins. In practice, a "strain hardening" effect of the asperities is observed causing shearing to occur behind the junction rather than at the welds themselves.

Plastic deformation and strain-hardening are irreversible processes of energy conversion and are the mechanisms by which energy is dissipated at dry friction joints.

The overall friction coefficient is defined as the ratio of the total shear resistance to the normal load.

2.4.1.2 The normal load effect

The real area of contact is the summation of all the small junction areas and is proportional to the normal load and independent of the size of the bodies.

In an experiment reported by Andrew et al[10], the normal force versus deflection curve was plotted for different values of normal load. The loading and unloading sequences followed identical paths except for the initial loading sequence during which the joint behaved somewhat differently. This has been attributed to an initial "bedding-in" due to plastic accommodations of the asperities. It was concluded that normal loads do not dissipate enough energy to be explored for structural damping purposes.

2.4.1.3 The effect of tangential loads on displacement

The relative tangential displacement between two bodies is a summation of elastic deformation of the bodies and the actual relative slip between surfaces in contact[9]. The contribution of the asperities' plastic deformation to the tangential displacement has been shown to be negligible,

even in the first tangential loading where plastic flow of the junctions takes place.

2.4.1.4 The mechanism of fretting

The surface damage that takes place when two surfaces slide relative to each other is due to two major factors. Alternate tangential forces cause shearing close to the junctions so that for a continuous cyclic tangential load contacts are subjected to successive welding and shearing. Asperities are then flattened and the fragments thus formed are deposited in the valleys. Asperities under plastic deformations are also susceptible to corrosion, forming oxide particles on the surface. The surface is weakened by this double process of material removal, i.e., mechanical forces and chemical reactions, which makes it very susceptible to crack propagation as well as wear of the joint.

Shotpeening and metal spraying are common procedures to reduce wear of joint surfaces. Also, work on the cyanide hardening technique[11] has shown it to be very efficient and cheap.

2.4.1.5 Effect of impurities on dry friction

If metal surfaces are very clean and ductile, a superposition of tangential and normal load produces growth of the junction, reaching a total contact area almost equal to the geometric area. Tabor[12] reports that friction coefficient values of 50 to 100 or more (tending to infinity) can be reached. Small amounts of contaminants, however, are sufficient to reduce the shear strength of the interface to a few percent of that for perfectly clean surfaces reducing the friction coefficient to values of the order of unity. The presence of lubricant films between the surfaces eliminates entirely the formation of junctions and the friction is then determined by the shear strength of the lubricant film itself.

It has been experimentally observed that normal load, apparent contact area and velocity of sliding between surfaces do not affect significantly, the friction coefficient values, so that for most practical situations, dynamic friction coefficients lay in the range 0.3 to 0.5. Based on a large compilation of practical cases, static friction coefficients have been also found to be about 40% higher than dynamic

coefficients. Rabinowicz[13] recommends as good approximations for dynamic coefficients the following: $\mu_d = 0.3$ for unknown conditions, $\mu_d = 0.15$ for mild sliding conditions, and $\mu_d = 0.6$ for severe sliding conditions.

2.4.2 Analysis of Ideal Joints

2.4.2.1 Simple flat joint- partial slip condition

Consider a joint consisting of three members with the centre one of relatively small cross section. It is assumed in this analysis that shear stress at the interfaces occurs only where relative slip occurs and that in all members, sections parallel to the axis remain parallel during application of a cyclic load. The application of a force P to the centre member produces a relative slip at the interface (originally at $x = 0$), and extends inwards to an extent that the shear resistance equals P. As long as P is less than the total shear resistance the joint can offer, gross slip is prevented and a partial slip condition is said to occur. Analytical estimations[14] of the energy dissipated per cycle lead to an expression of the form:

$$E_{diss}/cycle = \frac{(1 - K)^2 \bar{P}}{24 \mu K_c P_c}$$

where μ is the friction coefficient, p_c, the clamping pressure, K_c, the stiffness of the centre member, K, the stiffness of outer members and $\bar{P}$ the average load applied to the centre member.

The energy dissipation is then proportional to the cube of the load and inversely proportional to the coefficient of friction, clamping pressure and stiffness of centre member.

2.4.2.2 Simple flat joint - gross slip condition

As the applied load exceeds the shear strength limit, surfaces can slide relative to each other in gross slip form. Predictions of the energy dissipated per cycle have lead to the following expression:

$$E_{diss}/cycle = \frac{2\ell^2 p(\bar{P} - p_s}{K_s} + E_{ps},$$

where p_s is the maximum force which causes partial slip only. Any slight increase in the load produces gross slip. E_{ps} is the energy dissipated per cycle in partial slip which takes place because of the cyclic nature of the external load.

E_{diss}/cycle is now a linear function of the applied force P, the coefficient and the clamping pressure.

Analysis of joints involving Coulomb damping (dry friction) has shown that there exists an optimum interface pressure for which damping is maximized. For very high interface pressure there occurs no slip and, consequently, no energy dissipation; for very low interface pressure slip can easily occur but the low frictional forces dissipated little energy.

In between these two extremes there is an optimum pressure for which damping is maximised. Studies of the damping of a few typical joints are discussed next.

2.4.2.3 Bolted joints

Bolted joints are one of the most common joints in machines and other structures. Such joints when optimised from the damping point of view, can contribute significantly to the overall loss factor of the structure.

The exact distribution of the normal stresses in a bolted joint is very difficult to estimate because it varies with the dimensions of the joint. Rotscher's cone, however, provides a simple and accurate enough description of the stresses. This assumes that the pressure is maximum at the radius of the bolt and drops linearly to zero at a distance of about three times the bolt diameter. Application of a tangential load produces relative slip at the outer part of the cone and consequently energy is dissipated. This process can be optimized. Ito and Masuko[15] have experimentally established the optimum pressures for a bolted joint, shown in Fig. 2.6. It is interesting to mention that their orders of magnitude were from 1 to 3 N/mm^2. (Optimum loss factors, $\eta_{op} = 0.045$ were found to be about three times higher than the non-optimized, $\eta = 0.015$.)

Measurements were carried out on a cantilever beam whose clamping end was bolted to a larger mass. Ito and Masuko also noticed some influence spacing had on the damping levels which were higher when the distance between bolts was about three times the bolt diameter (this produced an overlap of pressure cones of about half their volumes).

2.4.2.4 Double-leaf cantilever

The double-leaf cantilever as studied by Goodman and Klumpp[16] consists basically of two identical beams positioned one on the top of the other and pressed together by a constant uniformly distributed pressure p, fig. 2.7. A harmonic force F is applied at the free end in order to produce bending deformations. As the composite beam deforms, relative slip takes place at the interface and energy is dissipated.

Theoretical study[16] of the energy dissipation per cycle resulted in an expression, as follows:

$$E_{diss}/cycle = \frac{4}{3}\left(\frac{\mu t p \ell^2}{E}\right)\left[\frac{6F\ell}{th^2} - \frac{8\mu p\ell}{h}\right]$$

where μ is the friction coefficient; t the width of the beams (and interface); ℓ the beam length; E the Young's modulus of the material of the beams; and h the height of the cross section of each beam.

The optimum pressure can be shown to be $p = 3F/8th$, and the corresponding energy dissipation is:

$$E_{diss}/cycle = \frac{32}{3}\mu^2 p^2 (t\ell^3/Eh).$$

Figure 2.7 shows a comparison between theoretical and experimental results. Loss factors of about 0.1 can easily be achieved (near optimum pressure). The maximum (optimum) loss factor measured was 0.25.

As the pressure deviates from optimum values, loss factor values are reduced. It was noticed $\eta = 0.05$ for pressures equal to one quarter and equal to double the optimum one.

2.4.2.5 Frictional damping at free end of a cantilever

The case of a cantilever with its free end pressed against a surface, providing a frictional force, has been studied by Earls and Beards[17]. A harmonic force P was applied at a point along the length of the beam inducing vibrations. It was assumed that gross slip was occurring at the joint. Figure 2.8 shows a comparison between theoretical and experimental results. The optimisation of frictional damping is again apparent. Contact pressures were limited to below 0.05 N/mm^2 and the maximum loss factor achieved was 0.025 which is one order of magnitude lower than in the case of double leaf cantilevers.

2.4.3 Damping by inserts at joints

The introduction of inserts of high internal loss factor in joints can result in superior damping performance to that of dry friction joints. This section summarises the extensive work carried out by Mentel[18,19] into this particular topic. His work is mainly devoted to predictions and measurements of damping of beams and plates vibrating in their fundamental mode of vibration. All conclusions reported here are thus valid for frequencies below a few hundred Hertz.

Beams in which slipping occurs at joints dissipate energy by dry friction and when optimised, loss factors (for the fundamental mode) are about one order of magnitude higher than the internal damping of the beam material (the total expected loss factor is of the order of 5×10^{-2}).

The introduction of viscoelastic inserts between the interfaces (if the geometry of the joint allows only shear motion in the insert) can, by optimum design, produce higher loss factors than that obtainable from dry friction, but still of the same order of magnitude (total expected loss factor is of the order of 10^{-2}). If the vibratory motion of the joint is such that shear and rocking motions are possible, then the total loss factor can be increased further by a full order of magnitude ($\eta = 10^{-1}$). Such damping levels were measured even for very small vibration levels - an advantage over dry friction damping. Experimental work into the effect of inserts upon the damping of a bolted joint has been carried out by Ito and Mazuko[20]. Rubber, polyester plate and two types of oil were used as inserts. It is shown in this report that the generally accepted

assumption that oil can increase the damping of joints, may not always be true. Viscoelastic inserts were observed to provide constant damping with amplitude of vibration with slightly higher values than for the case of no inserts which means that its effects is significant. The behaviour of oiled joints is at present difficult to predict. For low clamping pressures, clamping is influenced by the oil film damping. As the pressure increases, oil is forced out of the joint and the joint damping is provided by metallic contact only. Permeable oils capable of infiltrating themselves throughout the whole joint interface are desirable. Doubts regarding the amplitude dependence of oily joints still remain, however.

The analyses and studies of damping of joints so far presented refers mainly to low frequency resonances of structures. This is sufficient for applications such as turbine blade and machine tool vibrations. The new field of damping of industrial structures for noise control requires also information about loss factors in the high frequency range. At high frequency the amplitude of vibrations may make some of the previously discussed methods inapplicable. Richards[1] has shown that the majority of the energy of industrial sounds is concentrated at medium frequencies (roughly from 500 Hz to 3000 Hz). This is due to a combination of factors, such as coincidence frequency, A-weighting and force spectrum. It is in this frequency range where damping techniques must be efficient; unfortunately, this is still an obscure area.

2.4.4 Damping by attached viscoelastic layers

This damping technique has been used successfully for many years and can be very effective in light beams and plate-like structures. The method consists of attaching a layer of high damping viscoelastic material to the surface of the structure. The technique has been extensively studied and analyses can be found in many references. In this section a short review of the capability and approximate equations for prediction are presented.

The first applications deal with structures having an added layer only, and vibrating in longitudinal and flexural modes. The resultant loss factor for the longitudinal modes is given by[21]:

$$\eta_L = \eta_2 \frac{E_2 d_2}{E_1 d_1 + E_2 d_2}$$

and for the case of bending waves

$$\eta_B = \eta_2 \frac{E_2 d_2 A^2}{B}$$

where $A \simeq (d_1 + d_2)/2$ and $B \simeq \frac{E_1 d_1^3}{12} + E_2 d_2 A^2$

η_2 is the viscoelastic material loss factor; E_2 its Young's modulus; d_2 the thickness of the applied layer; E_1 the structure material Young's modulus; and d_1 the structure thickness. Both expressions show the structural loss factor to be directly proportional to the product $\eta_2 E_2 d_2$ and independent of frequency and amplitude of vibration. One of the most important observations regarding this result is that a good viscoelastic damping material should have a modulus of elasticity as high as possible as well as a high loss factor.

For the bending case, it should also be noted that the loss factor is dependent upon the square of the parameter A which represents the distance between the neutral fibre (of this combined system) and the centre line of the layer. The use of spacers to place the damping layer as far as possible from the neutral axis is desirable. It should also be noted that in applications where damping material is attached all over the external surface of a symmetric structure (such as a circular rod), the parameter A will tend to zero, resulting in no damping.

A comparison between the damping provided by a damping layer to different modes of vibrations has shown that about ten times more damping is imparted to bending waves than to longitudinal waves. This is an important feature and suits many practical cases because bending waves are normally unwanted vibrations (radiating sound) and longitudinal waves may transmit the mechanical work of the structure.

The configuration discussed so far is of unconstrained type, in which damping is provided by longitudinal deformations in the viscoelastic material. If a stiff constraining layer is attached to the top of the viscoelastic material, bending will cause shear deformation in the visco-

elastic layer. This sandwich configuration is capable of even higher dissipation than the simple unconstrained case.

Theoretical analysis shows that this loss factor for bending vibration is given to a reasonable accuracy by:

$$\eta_{opt} = \frac{E_3 d_3 A^2}{B} \quad \frac{\eta_2}{2(1 + \sqrt{1 + \eta_2^2})}$$

where E_3 is the Young's modulus of the constraining layer material and d_3, its thickness. For thin constraining layers and thick basic structures, it reduces to

$$\eta_{opt} = \frac{3}{2} \frac{E_3 d_3}{E_1 d_1} \frac{\eta_2}{1 + \sqrt{1 + \eta_2^2}}$$

Unlike loss factors of unconstrained layers, constrained ones exhibit some frequency dependence, with an optimum value at a frequency given by

$$f_{max} \simeq \frac{1}{22} \frac{c_{L_1} d_1 G_2}{d_2 d_3 E_3} \sqrt{1 + \eta_2^2}$$

where c_{L_1} is the speed of longitudinal waves, in the base plate material, and G_2 is the shear modulus of the viscoelastic material.

Although damping is frequency dependent, this variation is small (the "half power bandwidth" extends over five octaves), thus once f_{max} is set to any medium range frequency of interest, η_{opt} can be assumed constant. The damping in the unconstrained configuration is directly proportional to the product $\eta_2 E_2$, whereas damping for constrained configurations is virtually independent of G_2. Its effect is only observed at the frequency for maximum damping. In the selection of a viscoelastic material for constrained configurations the magnitude of the other shear modulus may be ignored. The major requirement is to have η_2 as high as possible.

In the case of two plates of equal dimensions with a viscoelastic interlayer, η_{opt} and f_{max} are given by

$$\eta_{opt} = \frac{3\eta_2}{5 + 4\sqrt{1 + \eta_2^2}},$$

and

$$f_{max} = \frac{2}{11} \frac{G_2 c_{L_1}}{E_3 d_2} .$$

2.4.5 Tuned dampers

Tuned dampers or as they are also called, vibration absorbers, are essentially a single degree of freedom system which is attached to the vibrating structure at a point of maximum displacement (anti-nodal point). The force exerted on the structure by the vibration absorber can be very large reducing resonance responses to a minimum. This characteristic makes it a very efficient device for structural damping purposes. Assuming the damper unit has a mass m, stiffness k and loss factor η and that the structural response at the application point is $Xe^{i\omega t}$, the solution to the equation of motion for mass m is given by

$$x = \frac{X\, e^{i\omega t}}{1 - \frac{m\omega^2}{k(1 + i\eta)}}$$

and the force F transmitted back to the structure can be shown to be

$$F = - \frac{mW^2 Xe^{i\omega t}}{1 - \frac{m\omega^2}{k(1 + i\eta)}} .$$

Studies[22] of applications on beams and plates with several boundary conditions can be found in the literature but because of the complexities of analytical results, a discussion only will be presented. It is important to mention some characteristics of this type of damping mechanism. Firstly, the damper resonant frequency must coincide with the structure resonant frequency of interest in order to achieve optimum performance. The structural resonance peak is split into two smaller peaks. One corresponding to the mass m and the structure moving essentially in phase, and the

other with them moving in opposite directions. In most cases, two resonance peaks are observed. However, if the damper is not properly tuned, one of the peaks will be greater than the other and actual damper effects reduced.

This system is ideal for structures having basically one dominant resonant frequency or a group of frequencies very close together. Usually the dampers effectiveness is limited to resonant frequencies concentrated in a band less than one octave. This type of spectrum is not, however, very common in machine structures. Impulsive forces and the high modal densities, lead to a uniform distribution of the vibratory energy throughout the audio spectrum. In a few cases, for example the fundamental mode of a C-framed punch press, a distinct resonant frequency is observed and vibration absorbers could be useful.

2.4.6 Damping by "air pumping"

Damping provided by air trapped in gaps between plates and between beam/plate joints has been shown to produce reasonably high loss factors[23,24]. The damping effect is due to the viscous energy dissipation as the air is forced to move from one region to another as the structure vibrates. The viscous nature of the dissipation makes this mechanism frequency dependent. At low frequencies, velocity gradients are low and so is the energy dissipation. At high frequencies the air has no time to move, and behaves as a stiff spring, resulting in little dissipation. At intermediate frequencies, however, velocity profiles are capable of maximising the damping(Fig. 2.9). In practical cases, such optimum frequencies are of the order of 100 Hz, so that in the audio frequency range damping tends to decrease with frequency.

There are two important parameters directly related to the damping levels. The first is the air gap thickness. Experiments suggest that small gaps lead to the highest loss factors, i.e., plates bolted directly together or with spaces of less than about 0.5 mm. For spaces of 1 mm η_s is reduced by a factor of 2 to 3. Spacing between fixing bolts does not seem to affect damping levels to any great extent (bolt spacing was varied from 10 cm to 20 cm, fig. 2.10).

The second important parameter is the plate thickness ratio. Equal thickness plates may vibrate in phase producing little relative displacement

with minimal "air pumping". It is thus desirable to mismatch the plate thickness.

Ratios can vary from 1 (for equal plates) to a minimum when one of the plates is much thinner than the other. Ratios of about $\frac{1}{4}$ can already provide high damping levels (fig. 2.11).

The attachment of thin plates (e.g., 1 mm thick) to typical machine components would then produce the maximum damping possible from this damping mechanism. Ideal applications for this technique are casings or any other plate-like components.

2.5 Total Damping Prediction

The damping of the various types of joints and their interface conditions, the material damping and the use of spectral damping treatments, all contribute to the overall damping of each individual component.

Due to the bulky characteristics of typical machine components, their mode shapes are little affected by the addition of structural damping, with the exception of vibration absorbers when applied to slender beam-like and plate-like components. In this case, modes of vibration can be modified by the large forces exerted by the damper. Since the use of vibration absorbers is only efficient if the noise radiated is concentrated in a narrow frequency band, they are rarely employed in the reduction of machinery noise.

The prediction of the overall amount of energy dissipated (per cycle) in components in which several damping mechanisms are present, can then be approximated by the summation of dissipations provided by individual mechanisms, so that,

$$E_{diss_{total}} = E_{diss_{hysteresis}} + E_{diss_{joints}} + E_{diss_{visc.\ layers}} + \ldots$$

and if expressed in terms of loss factors, one obtains,

$$\eta_{s_{total}} = \eta_{s_{hysteresis}} + \eta_{s_{joints}} + \eta_{s_{visc.\ layers}} + \ldots$$

i.e., the overall loss factor represents the summation of loss factors produced by individual mechanisms.

2.6 Damping of Some Machine Structures

Several projects involved with noise control of machines such as presses, drop forges, rock drills, etc., have necessitated a review of all the parameters related to the noise radiation, of which the loss factors had to be experimentally determined.

A discussion of some of the measurements is presented in this section.

Figure 2.12 shows loss factor results of a third-scale drop hammer model (by the decay rate method). Anvil and column show identical loss factors, damping decreasing with frequency at a range of 10 dB/dec. Loss factors of the anvil and columns were measured before assembly, giving values of the order of $\eta = 10^{-3}$, i.e., considerably less than when assembled. Friction within the joints is responsible for the higher levels of damping.

Measurements on a full-scale drop hammer were compared to results from the model, to test the frequency effect. No significant variation was detected which suggests that damping decreases with frequency due to amplitude dependent mechanisms only. Figure 2.13 also shows several attempts to increase the damping of structural components by inserts - without much success. The best results achieved were loss factors of about 3 dB higher when columns were filled with dry sand compared to empty columns.

As column internal cavity dimensions are of 4" to 6", optimum damping provided by sand was expected to occur in the frequency range of 300 to 500 Hz.

If damping improvements at frequencies around 2 kHz is sought, column cavities should have cavities with a typical dimension of about 1".

Similar levels of damping observed in a C-framed punch press (figure 2.14). Punch press joints are characterised by having bolted (dry friction) joints and lubricated sliding bearings.

Corrosion, lubrication oils, grease and moisture are impurities being deposited during use which greatly modify conditions from an ideal dry friction joint.

It is interesting to note the high damping levels ($\simeq 5 \times 10^{-2}$) already existent in machines at low frequencies. To further increase

these damping levels is a difficult task. Bulky components such as solid drop hammer components could perhaps be made from a number of parts or laminated to deliberately introduce frictional damping at joints.

Dry frictional damping decays rapidly as amplitude is reduced, making it very much a low frequency damping technique. Modern viscoelastic materials with a high elasticity modulus could possibly be introduced into joints without creating serious structural stiffness problems to improve damping at higher frequencies. Such joints however act as isolators and could lead to increased sound radiation.

Figure 2.15 shows loss factors of various panels tested as part of a program to quieten a stillage (container for transporting pieces inside factories). A 10 gauge perforated steel panel had very little inherent damping, resulting mainly from the plate boundaries (welded). Loss factors were around 10^{-3}. A sandwich construction with viscoelastic material between two steel sheets (sound deadened steel - SDS) marketed by British Steel, showed loss factors of the order of 10^{-2}, as would be expected from a constrained configuration. Reasonably high damping was also shown by the three layered panel in which air pumping was the predominant mechanism. No spacers between plates were used. A rapid decay of damping with frequency is apparent but average values were of 10^{-2}. The woven construction proved to be very successful from an acoustic point of view despite its relatively low damping level. Friction between strips is the main source of energy dissipation.

Rock drills have two major sources of noise, the pneumatic noise of the exhaust system and the noise radiated from the rod vibrating in flexural modes. Damping is the most important noise control parameter. One damping technique tested on drill rods consisted of winding around the rods, metal springs with various degrees of tightness. Best results were achieved for a loosely fitted spring, perhaps because contact forces approach optimum conditions for dry friction and energy dissipation (fig. 2.16).

2.7 Conclusions

The actual damping of machine structures is of the order of 1×10^{-2} to 5×10^{-2}, and it is attributed almost entirely to dissipation at joints. Damping levels of machine structures show a distinct decrease with frequency. This is thought to be by amplitude-dependent rather than frequency-dependent mechanisms. The actual mechanisms of energy dissipation at joints, particularly at higher frequencies, is at present to some extent unknown. In fact it could be said that the whole area of damping of industrial machinery is still in its infancy. Further work is required to promote better understanding of damping in joints under various conditions (oil films, viscoelastic inserts and dry friction). There is a need for improvements at medium frequencies (500 Hz to 3000 Hz) where most of the industrial noise energy lies. Applications of conventional and new techniques to machine components should also be encouraged.

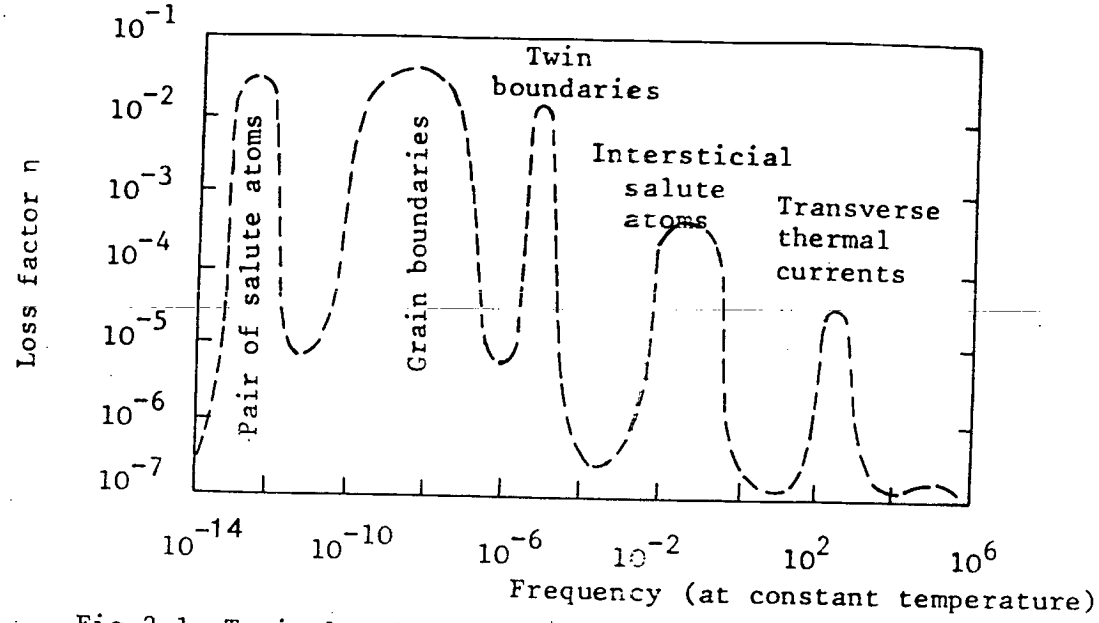

Fig 2.1 Typical relaxation spectrum as suggested by Zener for a "hypothetical" material, showing the several mechanisms of damping and their relative levels

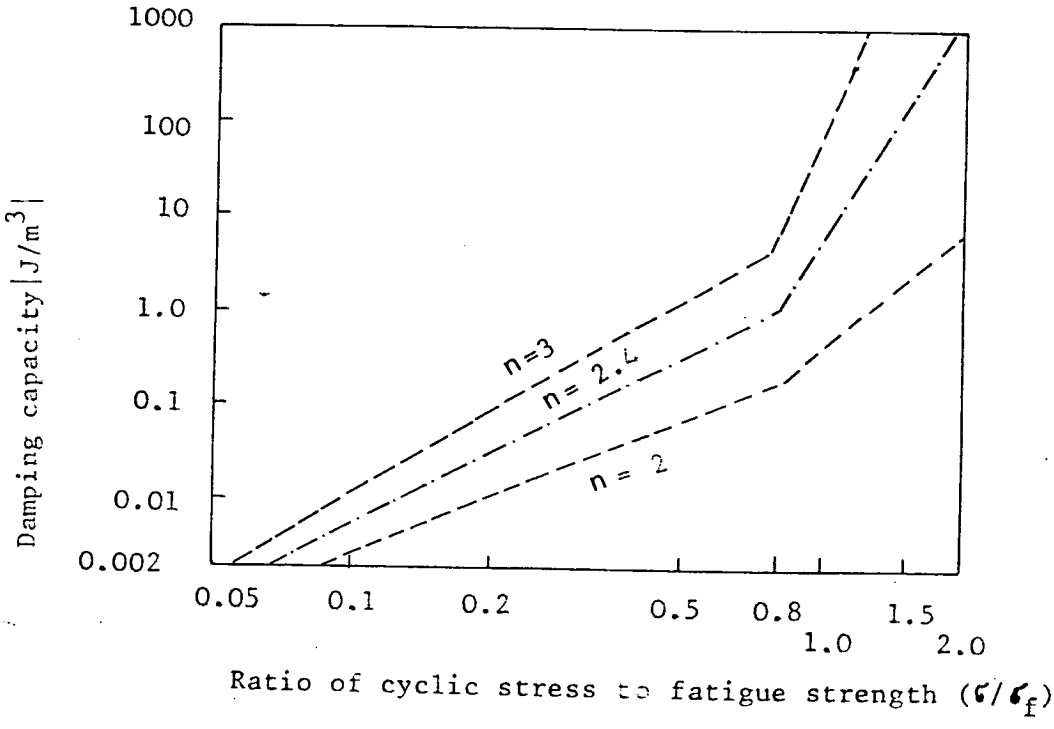

Fig 2.2 Dependence of unit damping energy of various anelasto-plastic materials upon ratio of cyclic stress to fatigue strength, as observed by Lazan (5). (Materials: sanvik steel, glass laminate, titanium alloys, SAE 1020 steel, aluminium, magnesium alloy, grey iron).

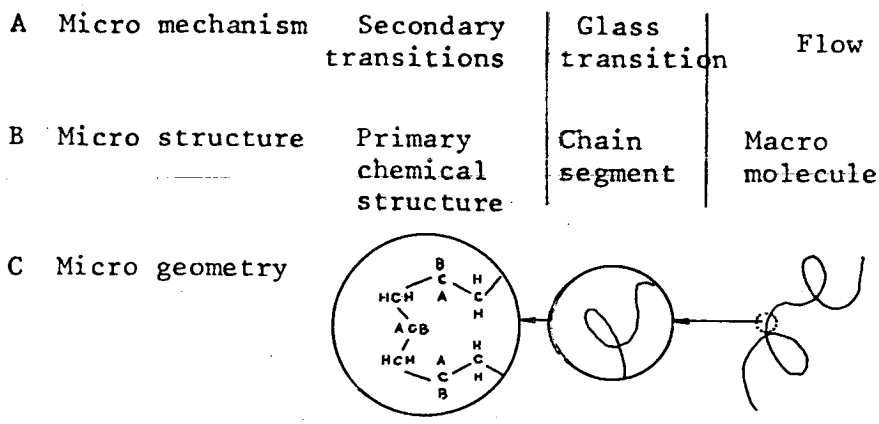

Fig 2.3 Micro-mechanisms in damping of polymers

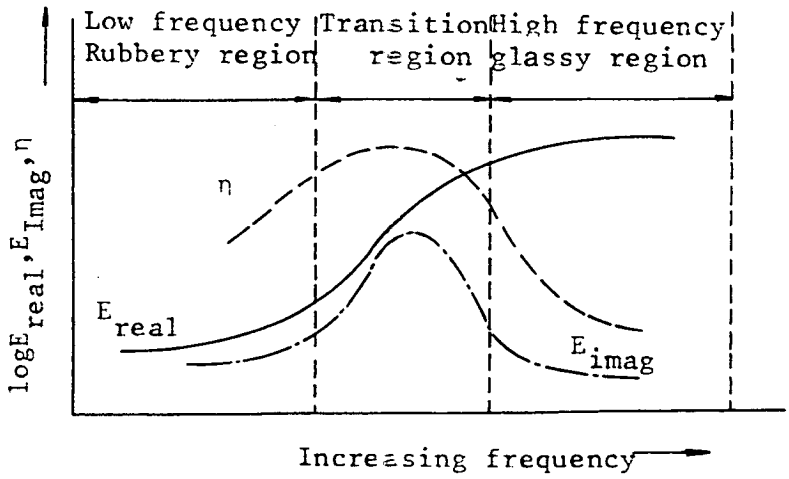

Fig 2.4 Effect of frequency on the real and imaginary parts of a typical polimer and on its loss factor

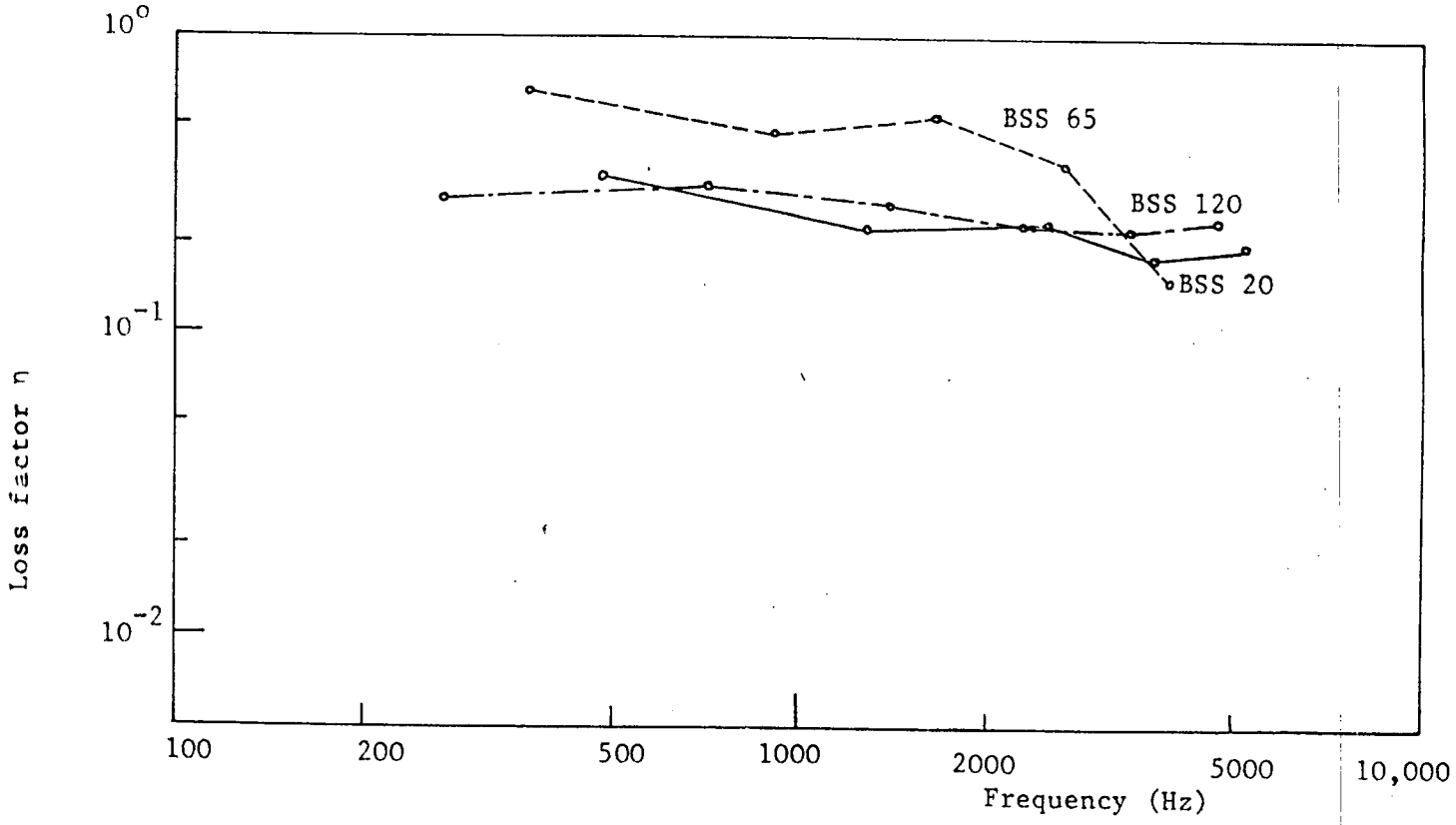

Fig 2.5 Damping results for PVC samples (ICI)

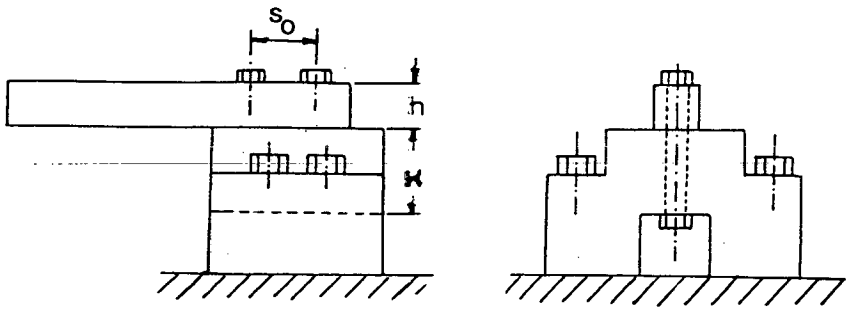

Fig 2.6A Test rig as used by ITO and MASUKO[15] for dry friction damping studies of bolted joints

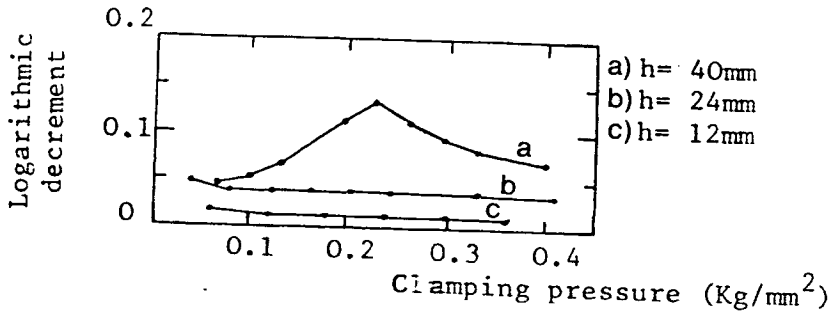

Fig 2.6B Effect of thickness of the bar upon damping (H=100mm, S_o=60mm), from reference (15).

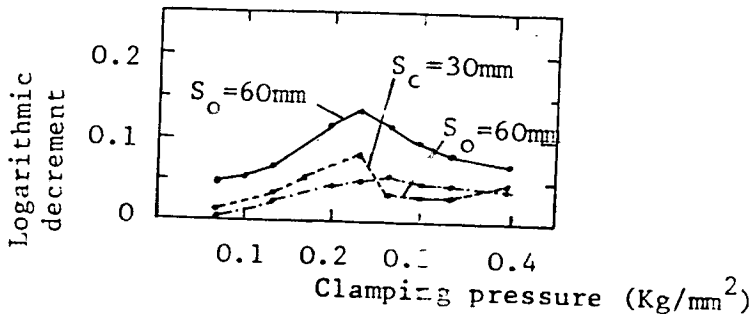

Fig 2.6C Effect of bolt spacing upon damping (H=100mm, h=40mm), from reference (15).

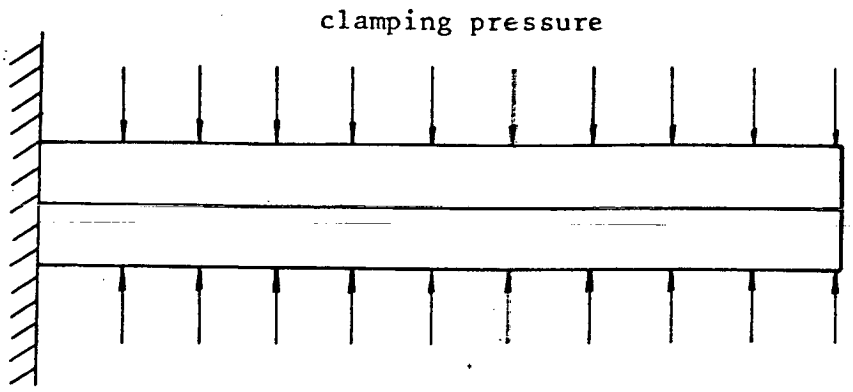

Fig 2.7A Test Rig for dry frictional damping analysis of a double-leaf cantilever, as studied by Goodman and Klumpp (16).

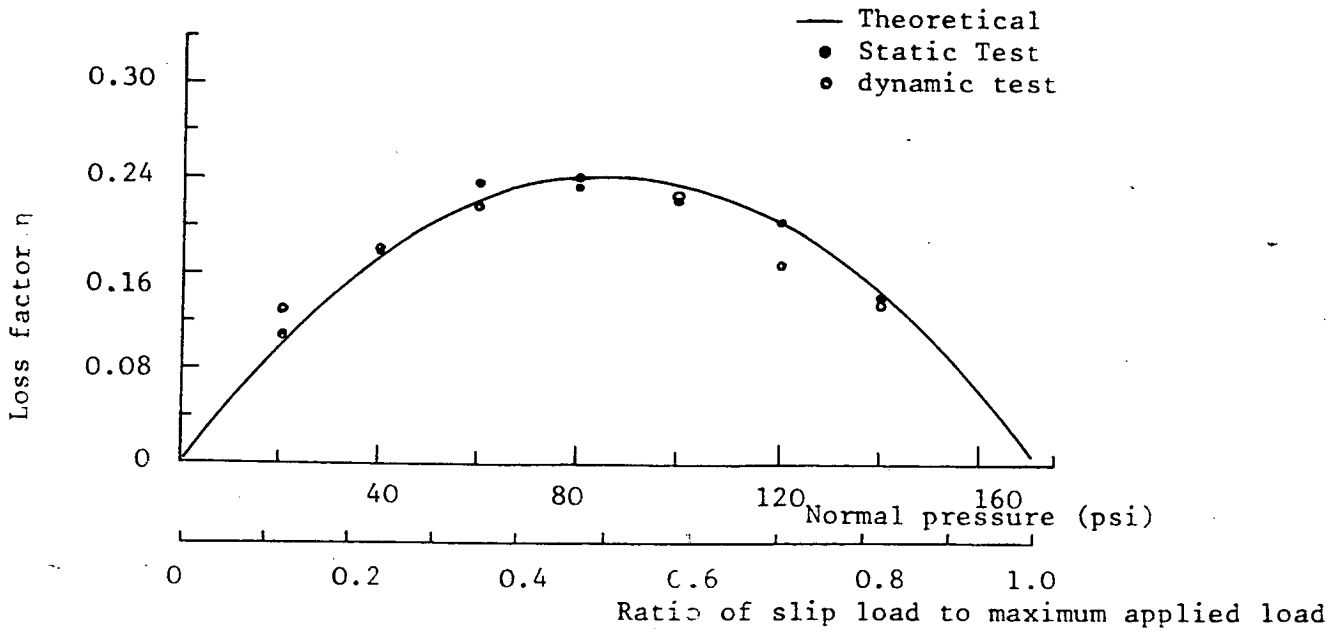

Fig 2.7B Comparison between theoretical and experimental results for a double-leaf cantilever, from reference (16)

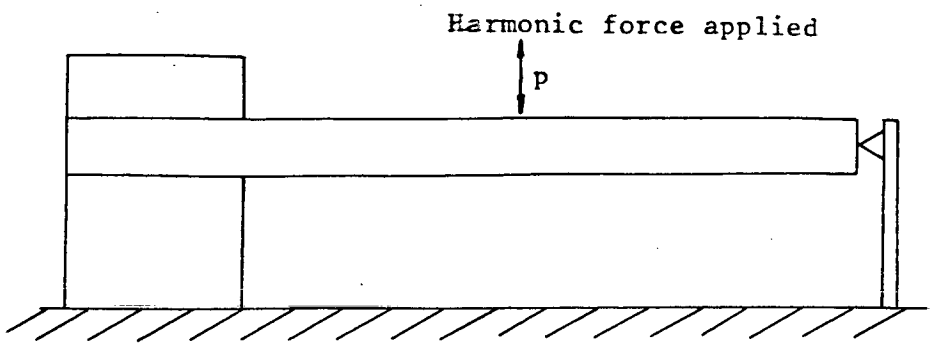

Fig 2.8A Diagramatic representation of the system showed by Earls and Beards (17).

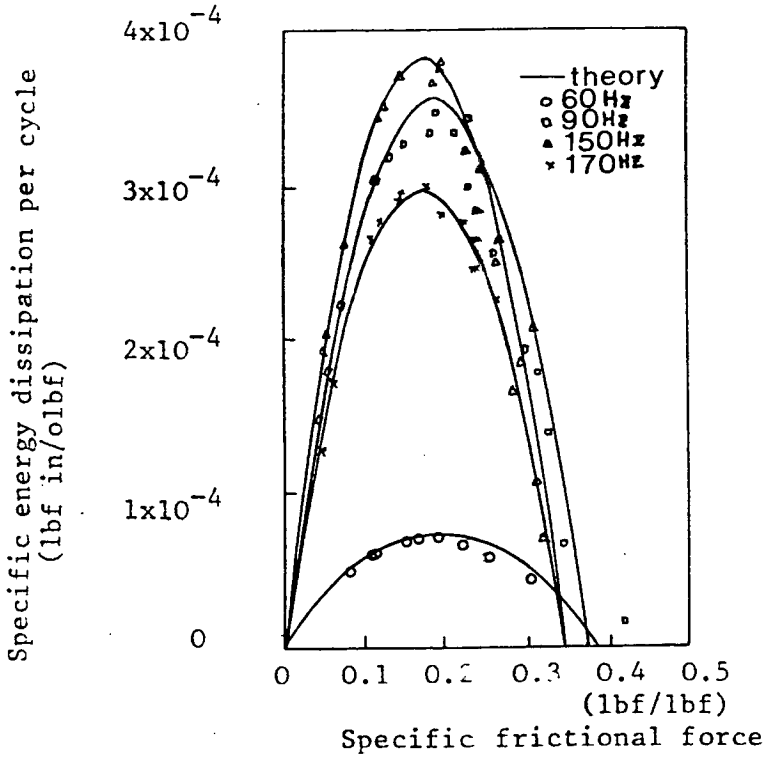

Fig 2.8B Comparison between theoretical and experimental results of a cantilever beam having a dry friction damper at the free end, from Ref (17)

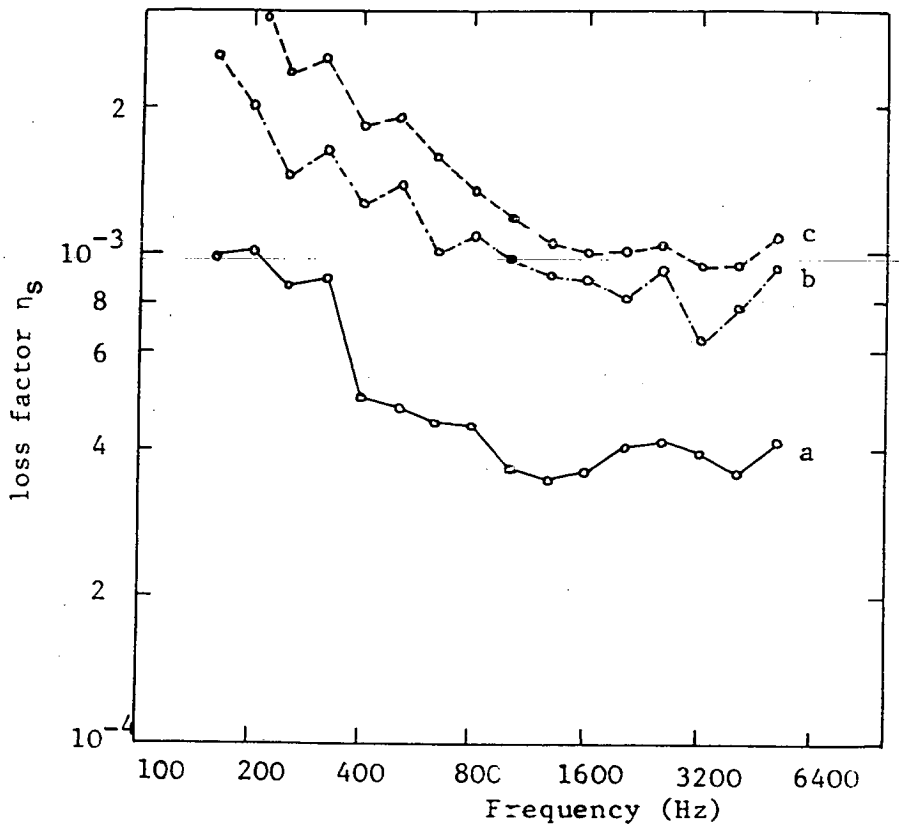

Fig 2.9 Effects of gap thickness between plates (from ref (23)). All plates are 2mm thick.

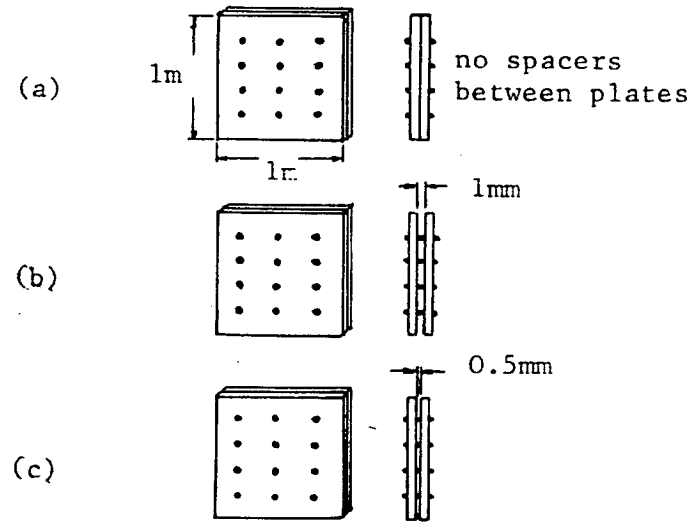

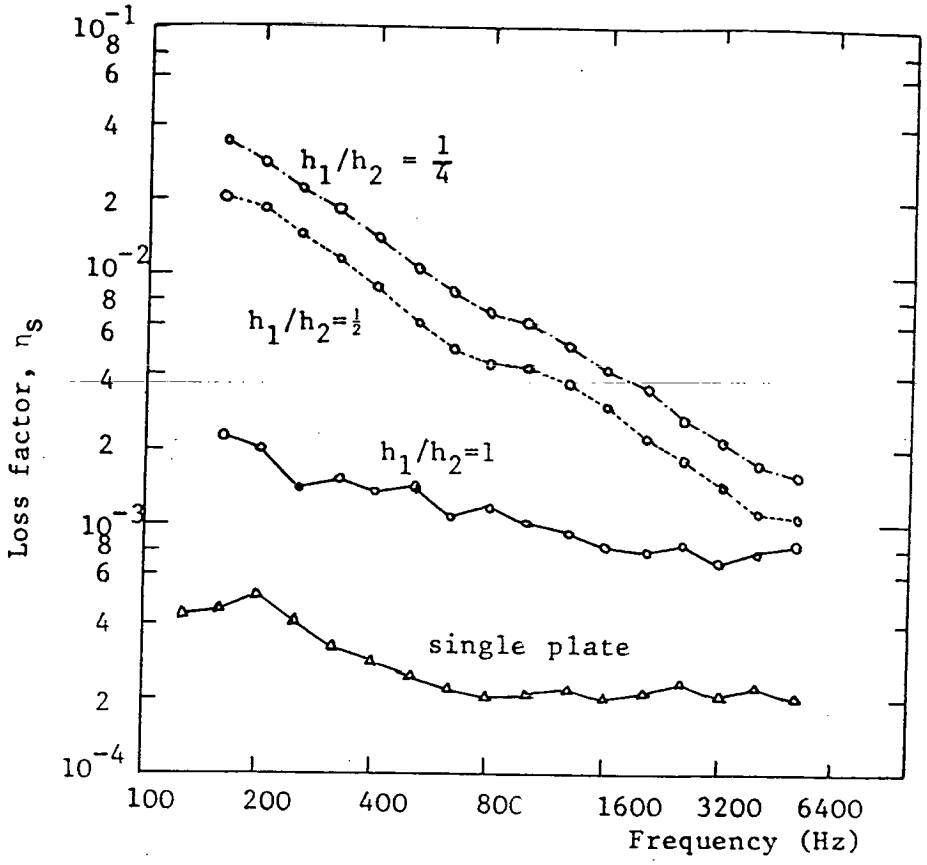

Fig 2.11 Effect of plate thicknesses (Ref (23))

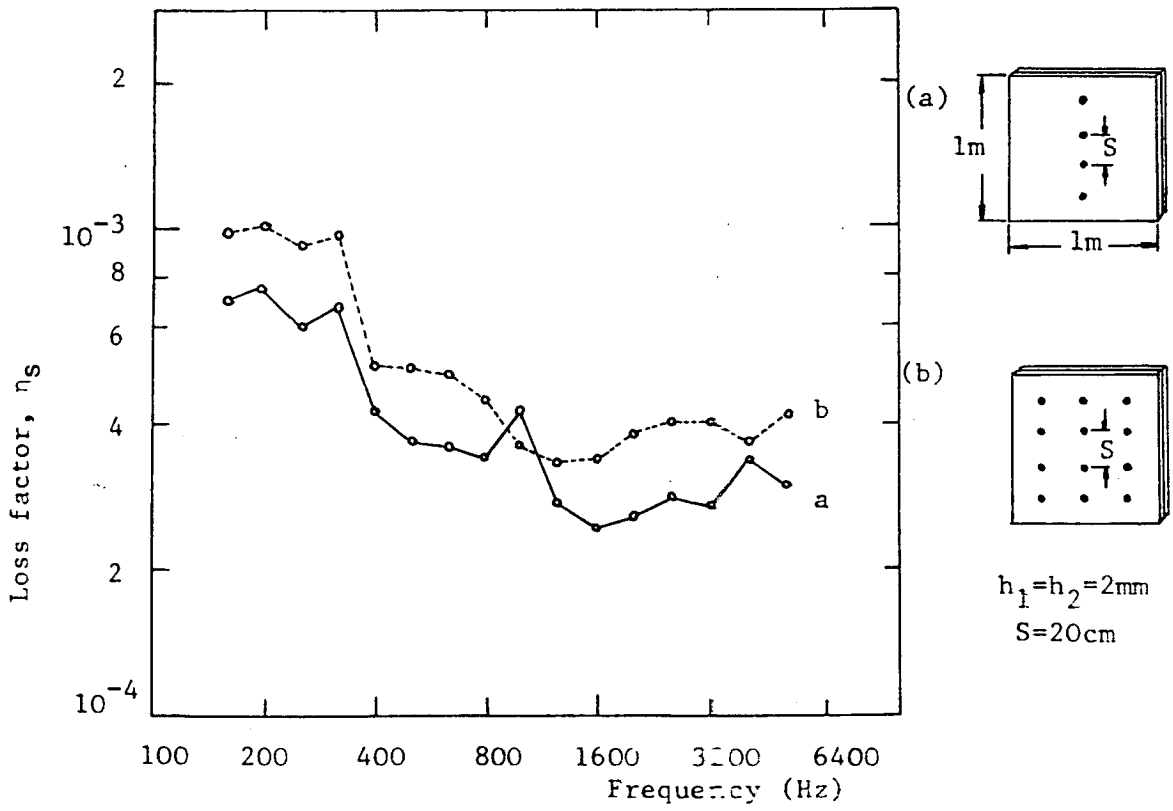

Fig 2.10 Effect of number of bolts (Ref (23))

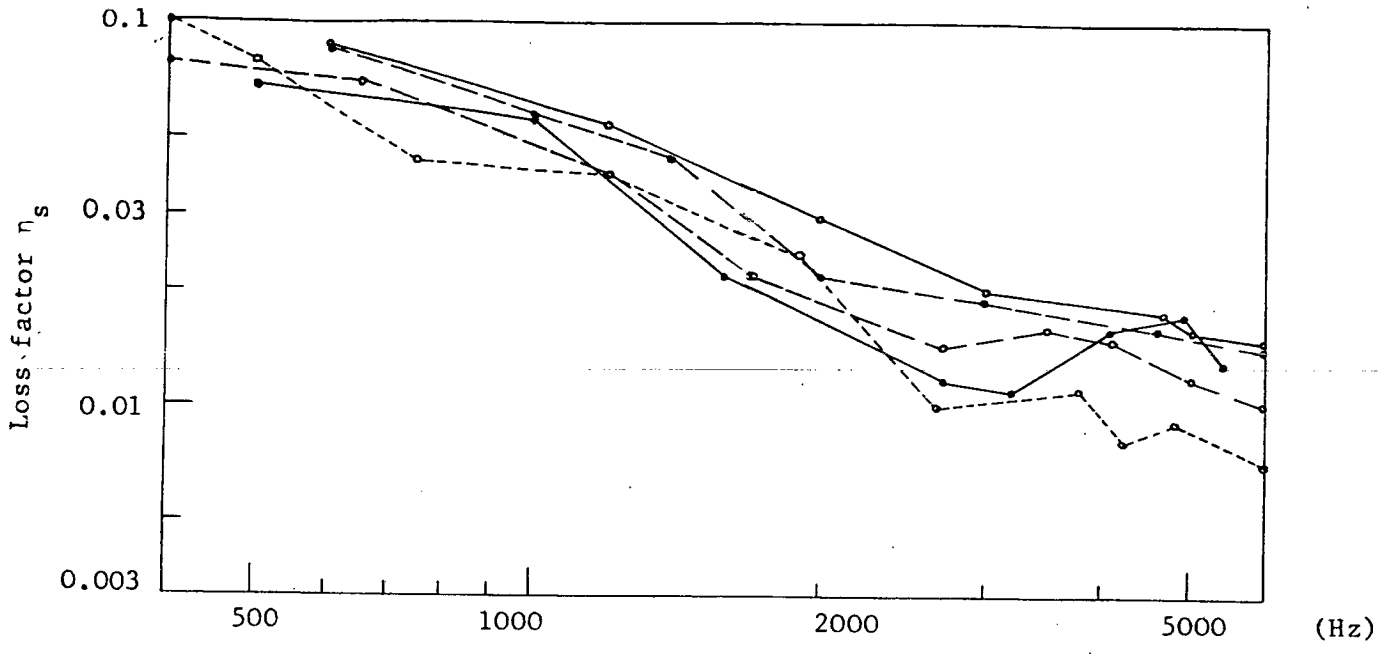

Fig 2.12 Loss factor measurements results on a Drop Forge Model

Anvil
Column
Column with rubber insert between anvil and column guides
Column with rubber inserts between anvil/column and column/tup
Column with both rubber inserts and filled with sand

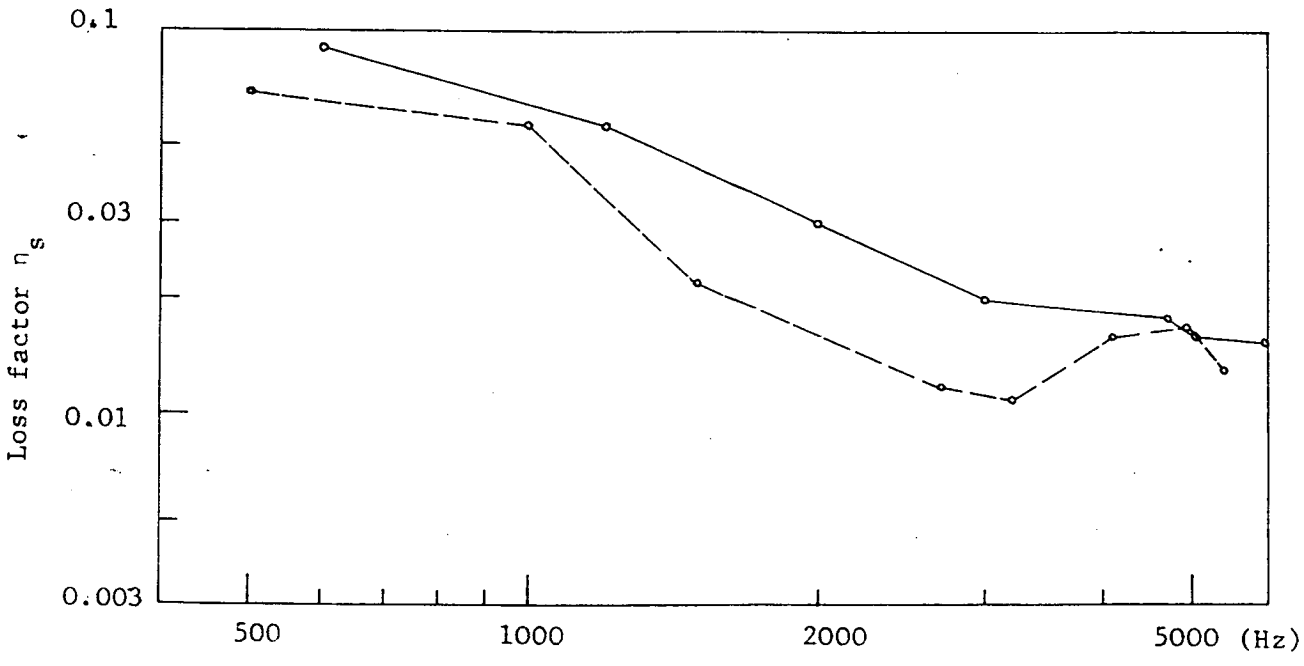

Fig 2.13 Loss Factors comparision measured on a column of a drop forge

Column - no damping treatment

Column - full of sand and rubber inserts at anvil/column and column/tup guides joints

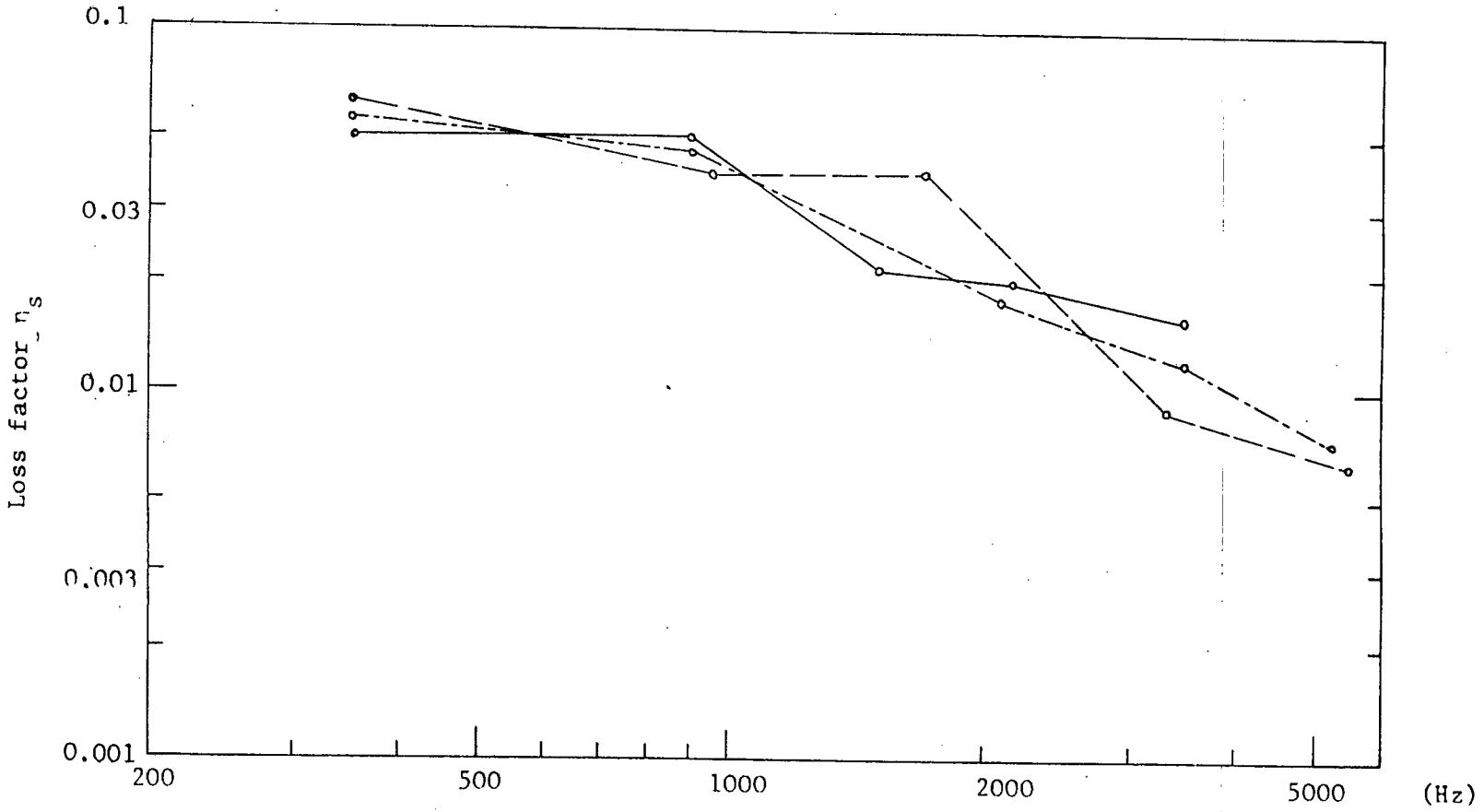

Fig 2.14 Loss factors measurements results on a punch press

Top of C-Frame

Side of C-Frame

Bed Plate

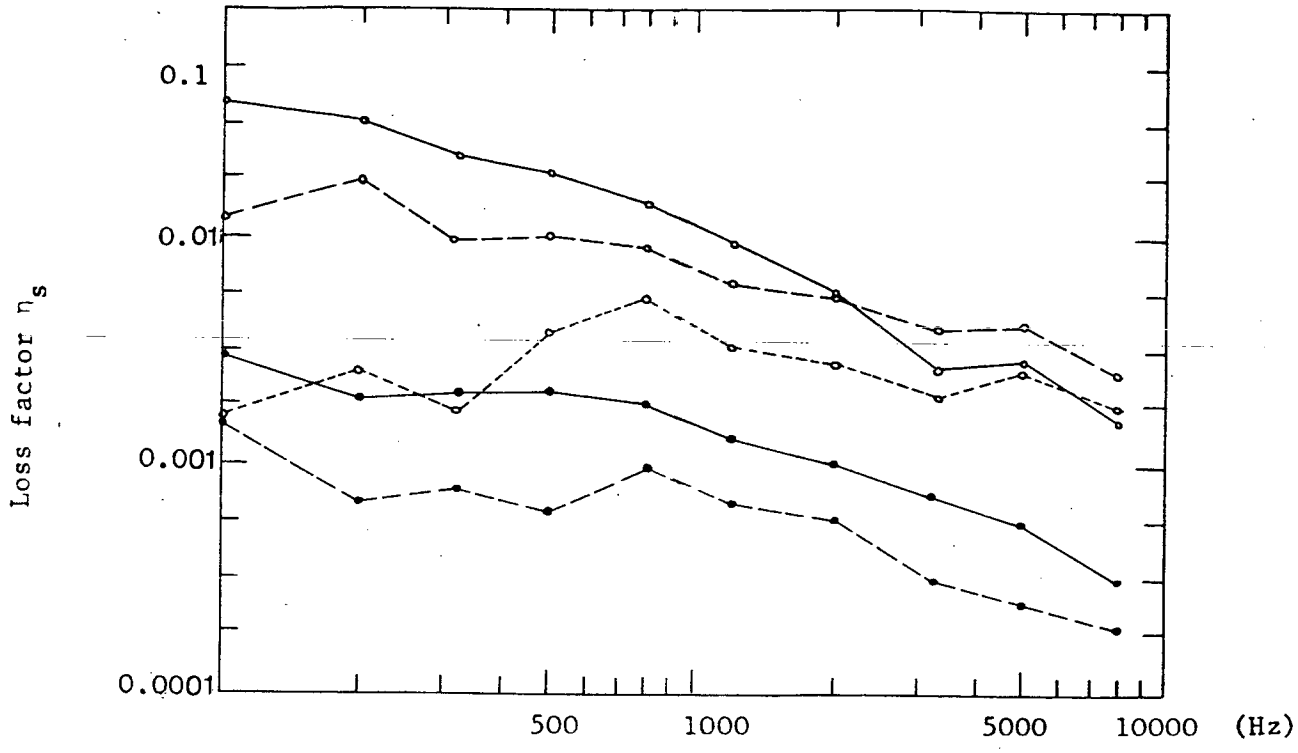

Fig 2.15 Loss Factors of several panels

- Three layers spot welded panel
- SDS panel
- woven panel
- 10 gauge sheet panel
- 10 gauge perforated sheet panel

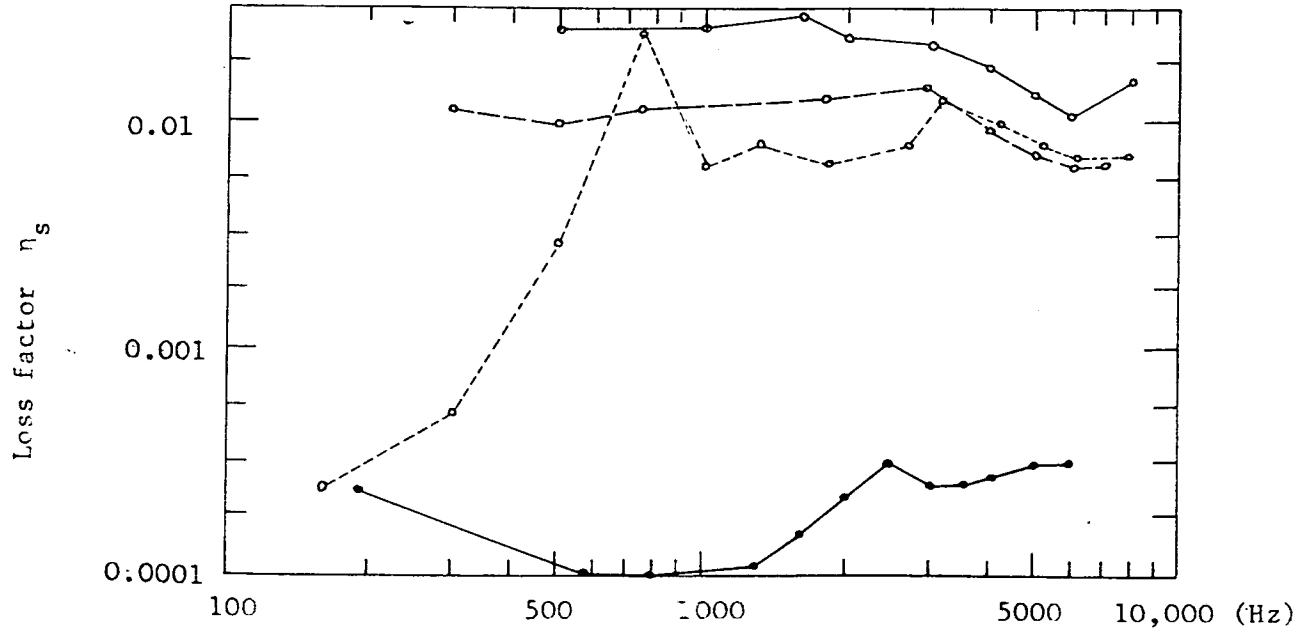

Fig 2.16 Loss Factors of a rock drill rod, having various damping treatments

- Rock with long spring loosely fitted
- Rod with long spring welded ends
- Rod with long spring as reed.
- Standard rod - untreated

CHAPTER 3

BASIC EXPERIMENTS ON DAMPING OF GRANULAR MATERIALS

3.1 Introduction

The broad survey undertaken of the several damping mechanisms existent in machine structures (presented in Chapter 2) has lead to the conclusion that the loss factors of machine structures exhibit a distinct decay with frequency (approaching 10 dB per decade). It has not been possible from the present work to conclude confidently whether this decay is caused by amplitude or frequency dependent processes of energy dissipation, although the former is more likely. Damping levels of machine tools such as power presses, drop forges, etc., are typically 5×10^{-2} at low frequencies (around 300 Hz), and 10^{-2} at higher frequencies (around 5000 Hz).

For noise control it is important to maximise the damping, particularly in the medium frequency range to achieve significant reductions in L_{eq}. Hence, one of the main objectives of this thesis has been the study of a damping technique capable of producing additional loss factors of at least 10^{-2}, especially at medium frequencies.

The reason for choosing granular materials, and specifically sand, was based on two major factors which showed some of their potential as damping material. The first one is the internal damping which can be very high. According to published data, for instance, internal loss factor of sand is about 0.1. The second, and perhaps most convincing, has been the work reported by Wolf[27] in which steel boxes filled with sand were attached to a large I-beam raising loss factors from 10^{-4} to between 0.01 and 0.2, depending upon the amplitude of vibration. Considering that sand is cheap and can be applied into cavities of machine components without altering their external dimensions, and because of its high temperature resistance, sand could be used as an effective damping material.

3.2 Review of Previous Work on the Damping of Sand-filled Structures

Although very little work has so far been done in this field, the results have led to important indications about the dynamic characteristics and damping of sand. Wolf[27] carried out experiments to determine the damping efficiency of gravel and sand, particularly at low frequencies. Steel boxes filled with gravel were attached to an I-beam (0.15m high, 0.10m wide and 3.0m long) and damping was measured at the three first resonances (40 Hz, 110 Hz and 220 Hz) for several acceleration levels (from 1 to 6g). Loss factors tended to increase for higher order modes (0.05 for the first mode and 0.1 for the second and third modes). Beams positioned horizontally produced somewhat higher loss factors than in vertical positions.

In a second experiment, Wolf measured the damping of a large concrete panel (1.25 m squared, 0.10m thick) whose cavities (4.5 x 15 x 15 cm^3) were filled with sand. The ratio mass of sand to mass of concrete was 1:4. Loss factors varied from 0.015 (at 170 Hz) to 0.078 (at 880 Hz) for measurements at acceleration levels of 0.1g. As acceleration increased to 1g, low frequency loss factors increased to 0.075.

It was generally observed in Wolf's work that the strong damping dependence upon amplitude of vibration occurred especially at low frequencies. The amplitude dependence was observed for beams either positioned horizontally or vertically.

Based on Wolf's results, Kerwin[28] presented an empirical relationship between loss factor and the amplitude of vibration, as follows:

$$\eta \doteq 0.013\alpha^{1.5}$$

where $\alpha = \ddot{x}/g$, the maximum vibratory acceleration of the beam relative to g, the acceleration of gravity. This result is valid for the range $2 \lesssim \alpha \lesssim 6$, for the three first modes of vibration of the beam in the horizontal position.

Similar acceleration amplitude dependence was reported by Kuhl and Kaiser[29] on their damping studies of short concrete bars and aluminium tubes filled with sand. Relative motion between grains of sand and between sand and the bar (at higher acceleration levels) increases the damping by up to three times its previous value.

Two sands of quite different grain size were also tested; the results showed damping level variations of less than 2 dB.

A concrete bar vibrating in flexural modes and loaded with granular material showed a maximum damping region at about 1000 Hz (the dimension of the cavity was 4 cm). Different sand grain sizes showed very little effect upon frequency curve and damping level.

Kuhl and Kaiser also showed that a mixture of sand and soft granular substance such as sawdust, resulted in a reduction of the sound velocity and the frequency associated with the maximum damping value for the case of equal cavity volumes. The total amount of maximum damping was also reduced. Cremer and Heckl refer to this work in reference (21), and explain the maximum damping being due to resonance in the granular material, i.e., for cavities whose dimensions are equal to two thirds the wavelength of longitudinal waves reaction forces are produced by the standing waves, opposing free vibrations of the structure.

The damping dependence upon the direction of the vibrations was also investigated by Kuhl and Kaiser. Flexural waves normal to the plane which carries the sand was noticed to produce damping up to ten times higher than for flexural vibrations in this plane or for longitudinal vibrations. Rougher surfaces would reduce such differences. The energy dissipated in the granular material is then predominant compared with the energy dissipated at contacts between cavity surfaces and grains.

The precise mechanisms of energy dissipation in granular materials is still very much unknown. Kerwin[28] summarises three most likely mechanisms as being friction between grains, local nonlinear deformations at sharp points of contact between grains and resonances in the granular material.

A possible but controversial dissipation mechanism that caused concern amongst workers in the field was the inelastic nature of impacts between particles and the structure to be damped. In such cases, particles could be spread loosely over a vibrating surface or trapped in cavities. Kerwin reports that preliminary theoretical analysis has lead to conclusions contradictory to observations made in experiments.

It is obvious from the limited results described in the literature that there is great uncertainty concerning the exact mechanisms of damping

of granular materials, the related parameters, the structural damping levels capable of being produced, as well as other dynamic characteristics, including the speed of waves. One concern of the present thesis has therefore been to investigate the physics involved in the damping of granular materials to allow future mathematical modelling and applications to the quietening of industrial machinery.

3.3 Project Objectives

The complexity of the dynamic behaviour of granular materials is quite obvious. It was felt necessary to start the investigation with experiments seeking first of all the determination of the important parameters and their relative effects upon the energy dissipation. The parameters referred to here are amplitude of vibration, pressure, grain sizes, dimension of cavities and frequency of vibration.

3.4 The Choice of a Damping Measurement Method

The method used for making damping measurements on hollow beams filled with sand was the input power measurement method. The main reasons for such a choice were the previous knowledge that sand had relatively high internal loss factors and also the high levels of structural damping which may be produced when sand is used as a damping treatment. These factors, and others, made the alternative methods of decay rate and the half power bandwidth measurement unsuitable for the experiments. Structures with cavities filled with sand can have loss factors of the order of 0.1 or even higher in some cases; such high damping levels cause a rapid decay of free vibrations so that the reading of the slope in the decay rate method is very imprecise. A fact that has been observed in Wolf's experiments where the decay rate method consistently indicated lower values (loss factors were always less than 0.1) than those measured by other methods. Another disadvantage of the use of the decay rate method is the damping dependence upon the amplitude of vibration which produces a decay of

reducing slope instead of a straight line as expected from linear systems. This effect has been observed by Kuhl and Kaiser. This method therefore does not allow an appropriate amplitude control during measurements.

The half power bandwidth method is only applicable to well defined and separated spectral peaks. Its use is therefore limited to the first few structural resonances as modal density (for flexural modes) increases with frequency and bandwidth reading 3 dB down from the peak becomes impossible for higher order modes.

Damping determination by measurement of the decay of amplitude of waves travelling along a beam has also been considered inadequate because it would require excessively long beams especially for low frequency measurements.

Despite some disadvantages, i.e., time-consuming and requiring careful measurement of the input power to structures, the input power method was found the most suitable method because of the high damping levels under investigation, and for ease of control of amplitude of vibrations. An important feature of this method that also influenced the choice was that the measurement of power dissipated by the structure, after conversion into energy dissipated per cycle, can provide valuable information with regard to the damping mechanisms under investigation.

3.5 Damping Measurement Description

The measurement consisted of exciting flexural vibrations with an electrodynamic shaker in sand-filled beams by a pure sinusoidal force. The RMS force (F_{rms}) and RMS velocity (V_{rms}), at the excitation point were measured by a force transducer (B & K 8200), an accelerometer (B & K 4344) and an RMS electronic voltmeter (B & K 2417). The phase difference, ϕ, between force and response was measured using a phase meter with accuracy of one degree. A two-channel phase matched filter eliminated spurious signals from force and response (fig. 3.1). The power input was determined by the product

$$W_{in} = F_{rms} \times V_{rms} \times \cos \phi .$$

The space averaged velocity squared was determined by measuring the velocity at points uniformly spaced along the beam length. The distance

between the points was maintained at one third of the beam standing wavelength (measurements at discrete points lead to exact estimation of $\langle \overline{v^2} \rangle$ whenever n points per wavelength are taken, n being equal to or greater than 3). The least possible number of points was chosen to save time. Loss factor values were then determined from the relationship:

$$\eta_s = \frac{W_{in}}{2\pi f M \langle \overline{v^2} \rangle}$$

where M is the total mass (including the mass of sand which was about 70% that of the beam) and f, the excitation frequency.

Phase mismatch errors between transducer pre-amplifiers (B & K 2635) were compensated for by a correction table previously made to cover the frequencies of interest. The table was produced from measurements made by attaching two accelerometers to a shaker, passing their signals through the pre-amplifiers and the phase difference read on a phase meter. Errors were of the order of 5 to 7° except at frequencies around 2 kHz where the error was of 11°.

3.6 The Structure

The structures chosen for the experiments were hollow commercial beams of several cross sections, i.e., square 2" x 2"; rectangular 3" x 2"; 2" x 1" and round 2½" diameter, all with wall thicknesses of ⅛". Rectangular cross section beams were chosen to allow comparison of the damping produced by the granular material when vibrations were excited in the different directions of the cross section. A circular cross section beam was also included to investigate the shape of cavity effect by comparing results to the square cross sectional beam.

All beams were made 1.5m long so that their first natural frequencies would be low - around 100 Hz. Shorter beams would increase their natural frequencies and information with regard to sand behaviour at this low frequency region would be missed.

The exciting force was applied at one end of the beam which is always an antinode for all bending resonances, as the beam was suspended it vibrates in free-free modes.

Because these beams have quite thin walls, the excitation was applied via a 10 mm thick plate welded to one end of the beam to excite bending modes (figure 3.2). The direct application of the force at the beam walls could excite circumferential modes which was not of interest in this experiment. As power input was measured by use of accelerometers and force transducer, local deformations would produce false phase readings between force and velocity signals. In fact, in a preliminary test in which the force was applied to the wall of the beam, significant variations were noticed when the accelerometer was positioned at several points around the excitation point. These variations were eliminated by the plate welded at the end of the beam. An impedance head was not used because it is very sensitive to lateral deflections which could not be controlled in the experiment.

3.7 The Suspension

Although beams were suspended by thin wires and despite being thin and flexible, some energy flow to the rig, increasing the apparent damping, was unavoidable.

Loss factor measurements for empty beams were carried out to estimate how much 'damping' the suspension was providing. Values not greater than 10^{-3} were observed, so that the energy escaping through the supports is at least 10 dB lower than the energy being dissipated on the beams when full of sand (whose loss factors were always greater than 10^{-2}). The suspension was thus considered adequate for the experiment. It should be mentioned that suspensions and supports offer measurement difficulties only when the structure under test is lightly damped (for instance, in material damping measurement), or in the absence of any damping treatment.

3.8 The Sand

Dry sands with various grain sizes were employed to investigate the size effect of granules upon the damping. Sand was chosen for being a typical and cheap granular material, whose dynamic properties had already been the subject of some attention. Very little of the previous work,

however, is directly comparable with results obtained in this work. The sand was dried before use in the experiments to reduce the effects of water content. Four different gradings were used, the actual grains diameters were as follows: 0.3 mm to 0.6 mm; 0.6 mm to 1.18 mm; 1.18 mm to 2.36 mm and 2.36 mm to 4.75 mm.

3.9 Results and Discussion

Measurements were made at discrete frequencies corresponding to beam bending resonances. As damping is amplitude dependent, measurements were also made at four or five different vibration levels and each point then represents the amplitude averaged damping, for the cases where the parameter amplitude is not being analysed.

3.9.1 Quantity of sand

An experiment was first carried out to investigate the loss factor variation with the amount of sand in a vertical beam. Beams half full of sand have loss factor values about 3 dB higher than beams one-quarter full, as shown in figure 3.3, and the damping of a beam full of sand is also about 3 dB higher than for half full. One notices the approximately linear relationship between damping and mass of the granular material, which is an important parameter to be considered in the damping prediction of sand-filled structures.

It was noticed that the location of the granular material in relation to the beam mode shape had some effect on damping levels. This is because displacements are greater if the granular material is located around the antinodal regions. Damping variation with modes of vibration is particularly noticeable at low frequencies, and for smaller proportions of sand variations are less than 3 dB.

3.9.2 The grain size effect

Results obtained for beams filled with sand of different grain sizes are shown in figure 3.4. It can be seen that loss factors do not differ much except at 1 kHz where a 5 dB difference is observed. It suggests then

that some sort of compensation must be taking place. Although the number of contacts per unit volume is less for larger grains, tangential and normal forces at contacts must be higher when stresses propagate through the material. The nonlinearities between forces and relative displacements at contacts makes difficult any a priori prediction with regard to wave propagation and damping of granular materials. Theoretical work which is described in the next chapter indicate that the diameter of grains has no influence on damping or the speed of waves which agrees with observations made experimentally.

3.9.3 The effect of the cavity dimensions

The effect that the cavity's dimension may have upon the damping of structures was investigated by measuring the loss factor of sand-filled rectangular cross section beams for vibrations excited at different directions of the cross section. Figure 3.5 shows results for beams positioned vertically and Figure 3.6 for beams in horizontal positions. The dimension effect is better shown in figures 3.7-3.10 where the same results are repeated.

The first observation of the damping curves is the already familiar maximum region appearing at frequencies around 1 kHz. One can also see that vibrations excited in the direction of the larger dimension of the cavity shifts the maximum damping frequencies to lower values, and vice-versa. Such experimental observation that cavity dimension and maximum damping frequency are inversely proportional to each other, indicates some sort of resonance in the sand caused by the presence of elastic waves.

Published values for the speed of longitudinal waves in sand vary considerably, 50 to 100 m/s by Kuhl and Kaiser, and 150 m/s by Heckl for example; assuming an average value of 100 m/s, it is evident that a cavity 5 cm wide will accommodate a full standing wavelength at the frequency of 2 kHz. Sand particles near both walls (of the cavity) have antiphase motion which minimises sand impedance at these regions, and consequently the energy transfers from the structure to the sand. This also explains the minimum damping that follows the region of maximum damping.

Halving the frequency, the cavity would accommodate half a standing wavelength only, so that sand impedance is maximum at the walls which maximises the energy transfer.

3.9.4 The effect of cavity shape

In order to determine the effect of cavity shape upon damping, a circular cross section beam was selected and results compared to those of a square cross section beam (2") the choice of the diameter was based on cross sections of equal areas, and it was estimated a diameter of $2^1/4$". As at the time of the experiment such beam was not readily available, a bean with $2^1/2$" in internal diameter was selected. Such dimensions, deliberately chosen to be as close as possible, made the cavity dimension variable to have little influence, and any deviation on the results should therefore be attributed to variation in the shape of cavity only. The square and circular shapes were considered two possible extremes found in usual machine components and their influence upon damping was the objective of the experiment.

Similar results were obtained from both beams for damping levels as well as for frequencies of maximum damping, as shown in figures 3.11 and 3.12. The results strengthen the above explanation that maximum damping is due to resonances in sand, since both beams present identical loss factor spectra. It can then be concluded that the shape of cavities is not important. The important factor is their typical dimensions.

3.9.5 The pressure effect

Static pressure on sand restricts the movement of the grains and reduces the internal damping and the damping of sand-filled structures. This effect was studied on beams suspended in horizontal and in vertical positions so that the sand was subjected to differente pressures caused by gravitational forces. It is noticeable from figures 3.13-3.18 that frequencies of maximum damping have been slightly shifted towards lower values and that horizontal beams present higher damping at lower frequencies.

It would be expected that sand under lower pressure will dissipate extra amounts of energy due to the increased freedom that loose grains have to slide relative to each other. Horizontal beams were, however, found to have higher loss factors (by 3-4 dB) at low frequencies only, below about

500 Hz. As displacements at high frequencies drop considerably, the invariance observed in damping with pressure above 500 Hz indicates that sand damping mechanisms at high frequencies are independent of amplitude of vibration.

The maximum damping frequency shift towards lower values is attributed to variation in the speed of waves with pressure. The irregular shape of grains may cause the nonlinear relationship between speed of waves and pressure, especially in the low pressure range where the experiments were conducted. In such a range, any variation in pressure may well change the dynamic characteristics of the granular material.

It can be concluded from the experiment that pressure has also some influence upon the frequency of maximum damping, but this is small compared to the influence of the cavity dimensions.

The pressure range tested varied from a minimum, when sand is simply resting inside a horizontally positioned beam, to about 5×10^4 N/m^2 (0.5 atm.). This corresponds to approximately the maximum pressure existent in typical machine structures when sand is under the pressure of its own weight. Higher pressure effects were not investigated because previous damping measurements on sand samples under pressures up to 2×10^5 N/m^2 indicated a decrease in loss factor with pressure and that was against the interests of this project.

A perspex beam of 2" x 2" was specially constructed in an attempt to observe the sand behaviour inside structures. In the vertical position the beam showed movement of sand particles on the upper 10 cm of the beam for the first few resonances only. Grains ascended in the middle, along the beam axis, and descended near the walls. Such near field effects were observed along the whole of the beam length when positioned horizontally. Sand tended to localise itself at antinodes, leaving little mass at nodes. Above about 500 Hz particle movement ceased to occur. At low frequencies it was possible to see through the beam walls, the relative motion of some of the grains.

3.9.6 The amplitude of vibration effect

Loss factor values as presented so far represent, for each frequency, an average value for four or five different vibration amplitude levels. Damping was found to be amplitude dependent for a certain frequency range (figure 3.19). At frequencies below about 1 kHz, loss factors were noticed to vary linearly with amplitude, while that dependence was not observed at higher frequencies.

In order to determine loss factor, the power dissipated by the granular material was measured. This was latter converted into energy dissipated (Ediss) per cycle (Wdiss = Ediss/cycle), and plotted against beam amplitude of vibration, seeking a better insight into the actual damping mechanism.

Figures 3.20 - 3.23 show a few examples of Ediss variation with beam displacement.

For large displacements, E_{diss} varies linearly with displacement at a rate of 30 dB/dec., i.e., loss factors are linearly dependent upon the amplitude, as it is also shown in figures 3.20-3.23. For smaller displacements, a 20 dB/dec. variation is observed, showing the damping independence of the damping mechanism. Another important observation in these results is also the frequency independence which suggests dry friction damping mechanisms as expected from dry sand.

E_{diss}/cycle of maximum frequencies follow the same pattern as other frequencies indicating that the energy supplied to the beam is dissipated at all frequencies depending directly upon the amplitude. The damping maximisation is then concluded to be caused by reaction forces of the granular material acting against the walls of the beam. Sand therefore behaves as a tuned damping device.

The variable displacement as can be seen in Figs. 3.20 - 3.23, represent beam displacement, since sand particle displacements, once trapped inside cavities are difficult to measure. Although it is not necessarily equal to the seam displacement, it is expected not to be very much different though, and considering that it extends itself for over four orders of magnitude, they are here assumed to be identical.

3.9.7 The effect of air pumping between grain interstices

Air trapped at interstices is forced to move from one region to another

as the structure vibrates, dissipating energy by viscous forces related to the velocity gradiants of the air. The objective of this particular experiment was to determine the contribution of this mechanism to the overall damping.

The square cross section beam was specially sealed for vacuum, and damping measurements were carried out for two air pressures inside the beam, atmospheric and for an absolute pressure of 3 cm Hg. At 3 cm Hg the density of air is reduced by a factor of 11.

Damping variations of less than 1.5 dB were observed between the two cases which leads to the conclusion that viscous damping by air flow through interstices is insignificant compared to frictional damping.

3.10 Conclusions

The series of experiments here described have permitted the identification of the important parameters involved in the dissipations of energy in granular materials and the damping of sand-filled structures. The maximum damping has been attributed to resonances in the granular material and the possibility of tuning is an important factor, since it can be matched to frequencies where the reduction of sound radiation is desirable. The internal dimension of cavities and the quantity of granular material are the two most important parameters to be considered in the estimation of the damping.

Pressure has little effect on the speed of waves, to an extent that it can be ignored provided it does not exceed levels caused by the material's own weight, as applied to typical components. Higher damping is, however, achieved when the granular material is loosely placed in cavities, but that is the limit one can reach. If even higher damping is sought, new materials should then be studied.

From the experiments it was also possible to observe a double mechanism of damping in sand, which depends upon the amplitude of vibration. The energy dissipation is thought to be caused by friction between grains or internally inside grains. Possibilities of other mechanisms such as air pumping at interstices and friction between cavity walls and sand particles have been shown to contribute insignificantly to damping levels.

Further work aiming at a deeper understanding of internal damping and of the speed of waves in granular materials, was carried out as described in the following chapters.

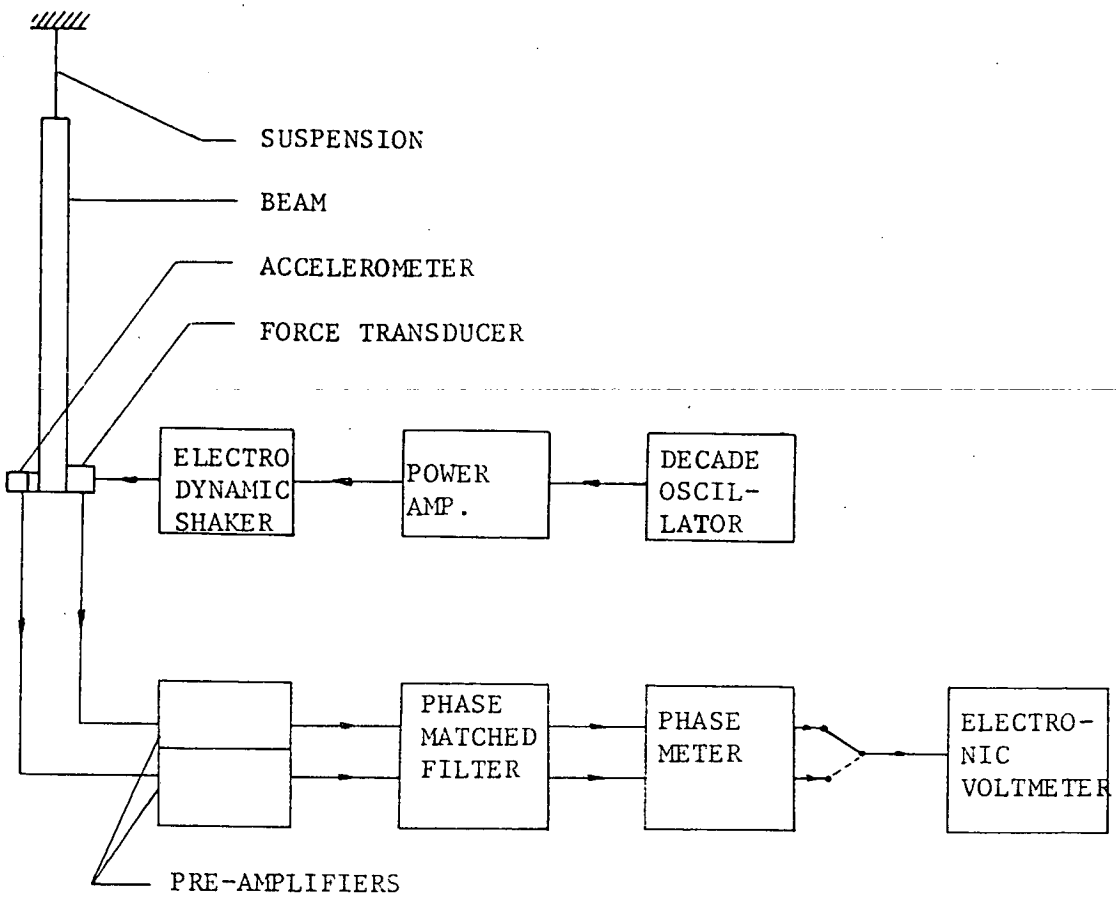

Fig. 3.1. Experiment equipment lay-out.

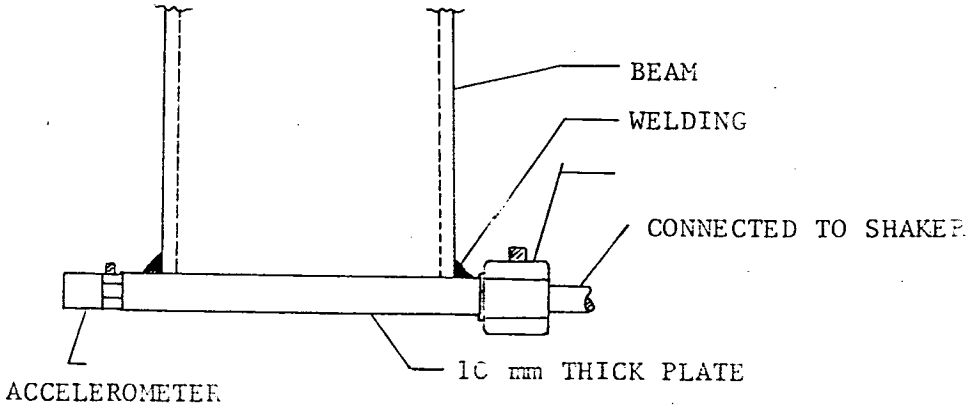

Fig. 3.2. Detail showing accelerometer and force transducer set-up for power input measurement.

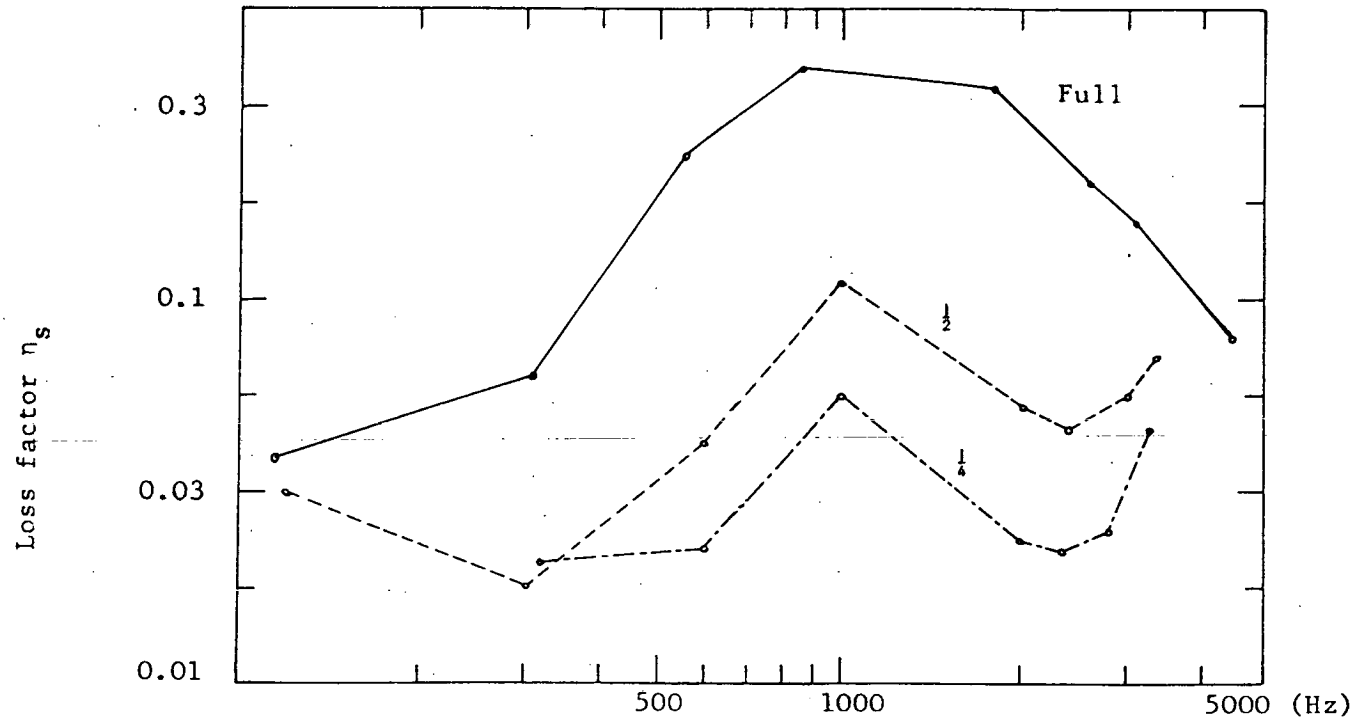

Fig. 3.3 Loss Factors comparison for a 2" x 2" x 1.5m long beam vertically suspended and filled to various degrees with sand 0.6 to 1.18mm.

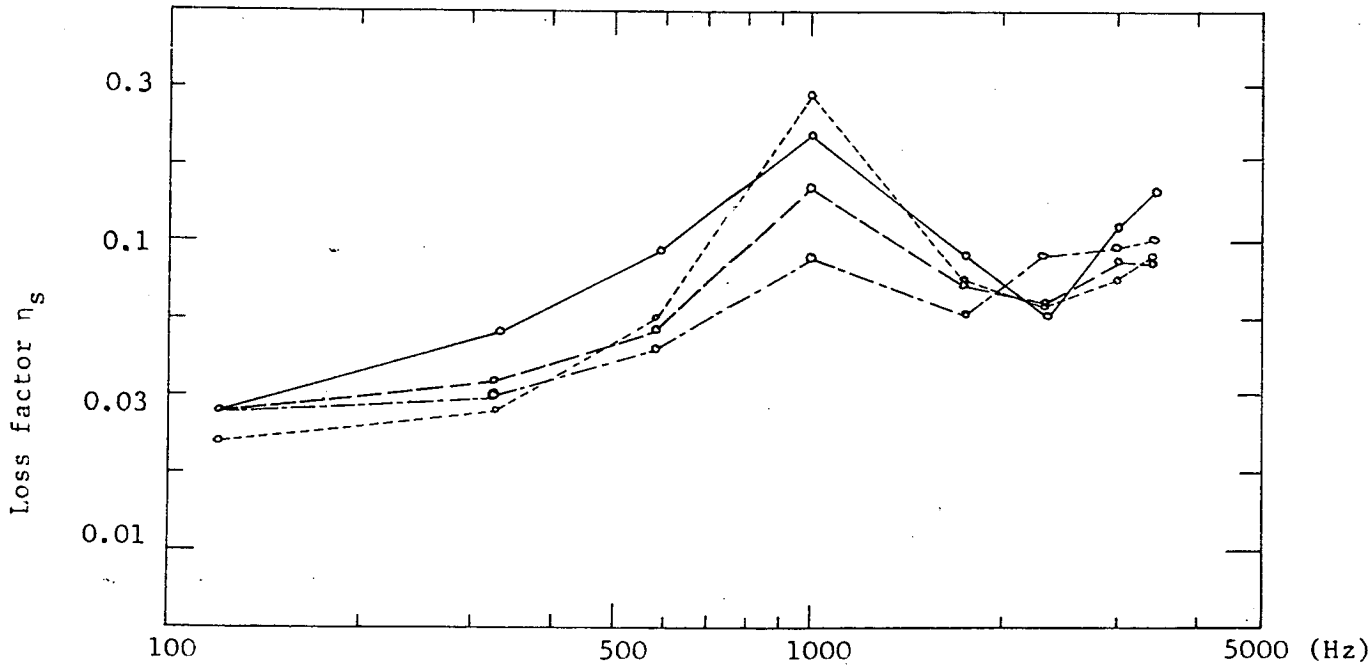

Fig. 3.4 Loss factors of a vertical beam (2" x 2" x 1,5mm long) full of sand of various types

sand 0.3 to 0.6mm
sand 0.6 to 1.18mm
sand 1.18 to 2.36mm
sand 2.36 to 4.75mm

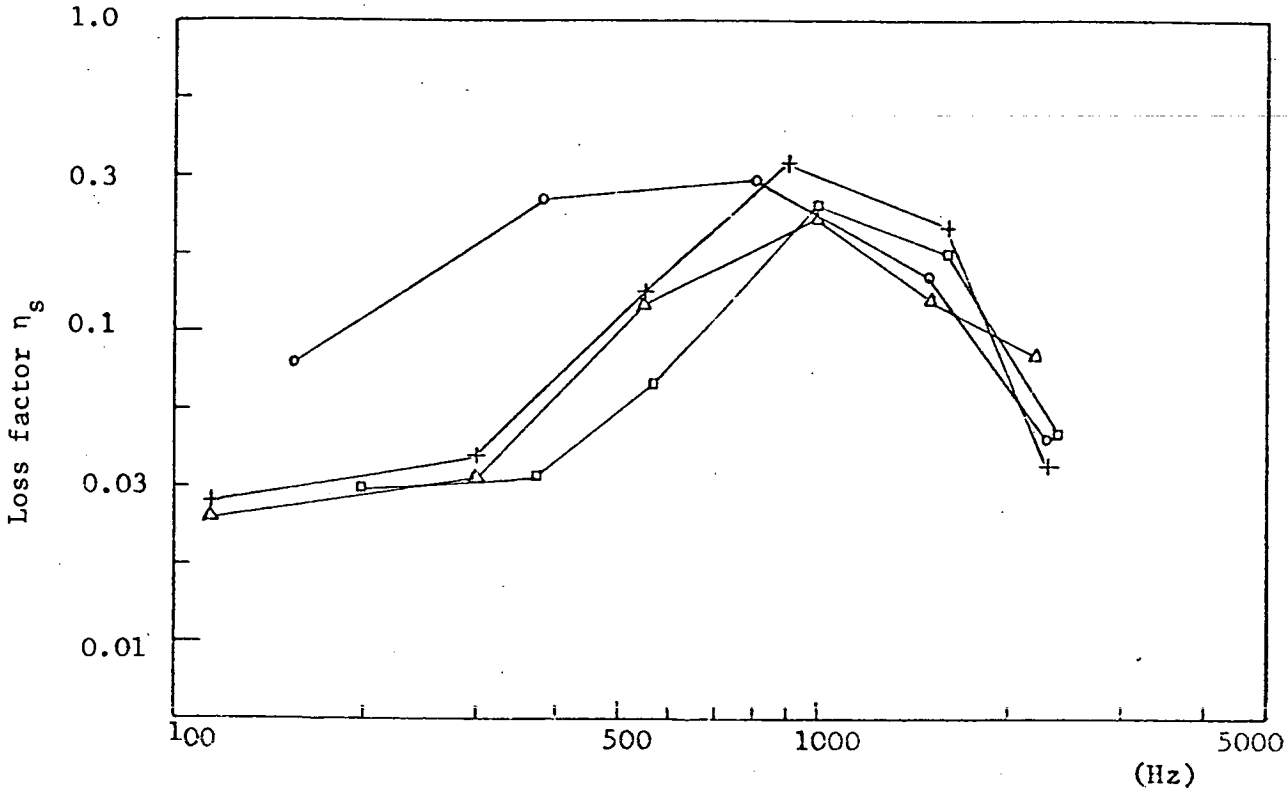

FIG. 3.5. LOSS FACTOR VALUES COMPARISON FOR RECTANGULAR BEAMS WITH DIFFERENT DIRECTIONS OF EXCITATIONS. BEAMS ON VERTICAL POSITION, FULL OF SAND (0.6 TO 1.18mm).

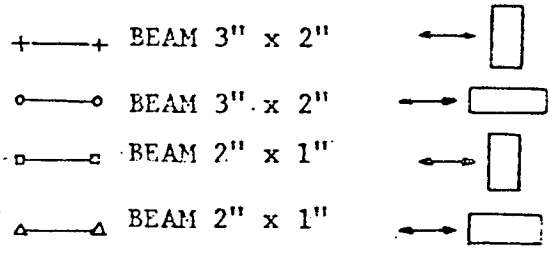

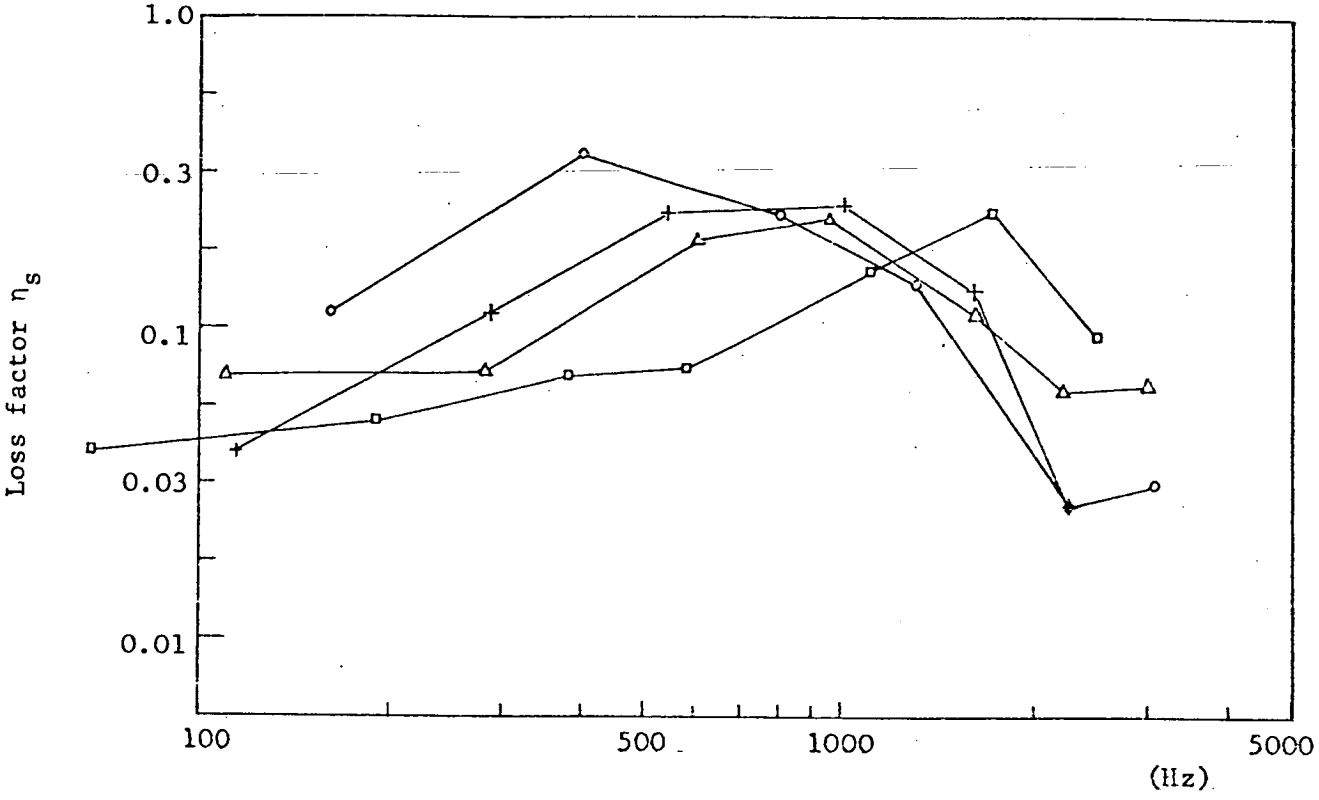

FIG. 3.6. LOSS FACTOR VALUES COMPARISON FOR RECTANGULAR BEAMS WITH DIFFERENT DIRECTION OF EXCITATION. BEAMS IN HORIZONTAL POSITION, FULL OF SAND (0.6 to 1.18mm)

+——+ BEAM 3" x 2" ⟷ ▯

o——o BEAM 3" x 2" ⟷ ▭

□——□ BEAM 2" x 1" ⟷ ▯

△——△ BEAM 2" x 1" ⟷ ▭

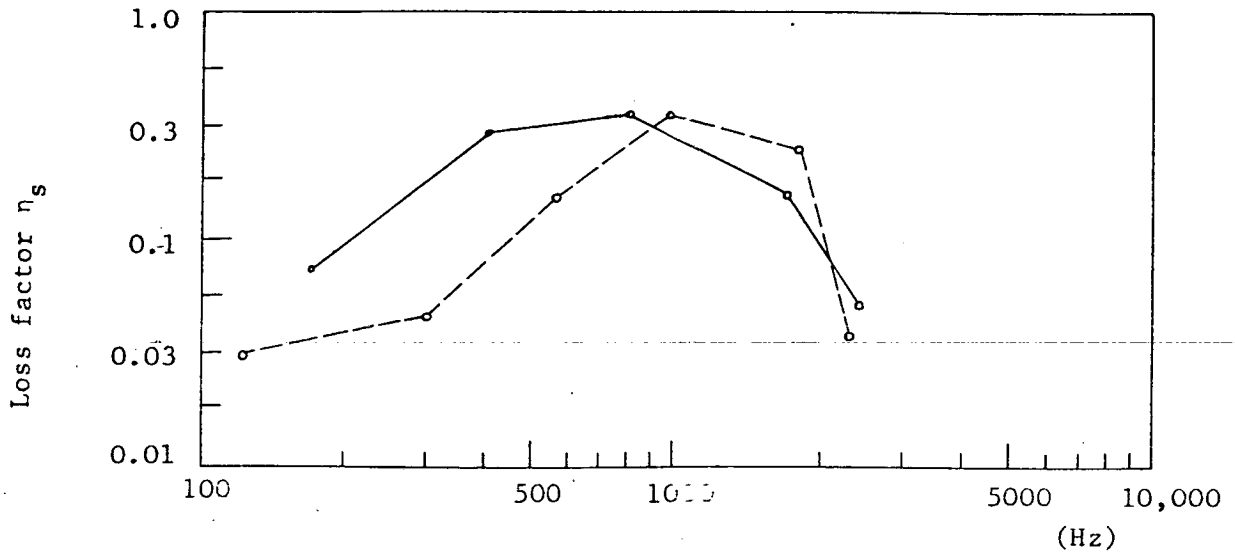

Fig. 3.7. Beam 3" x 2" in vertical position, full of sand 0.6 mm to 1.18 mm

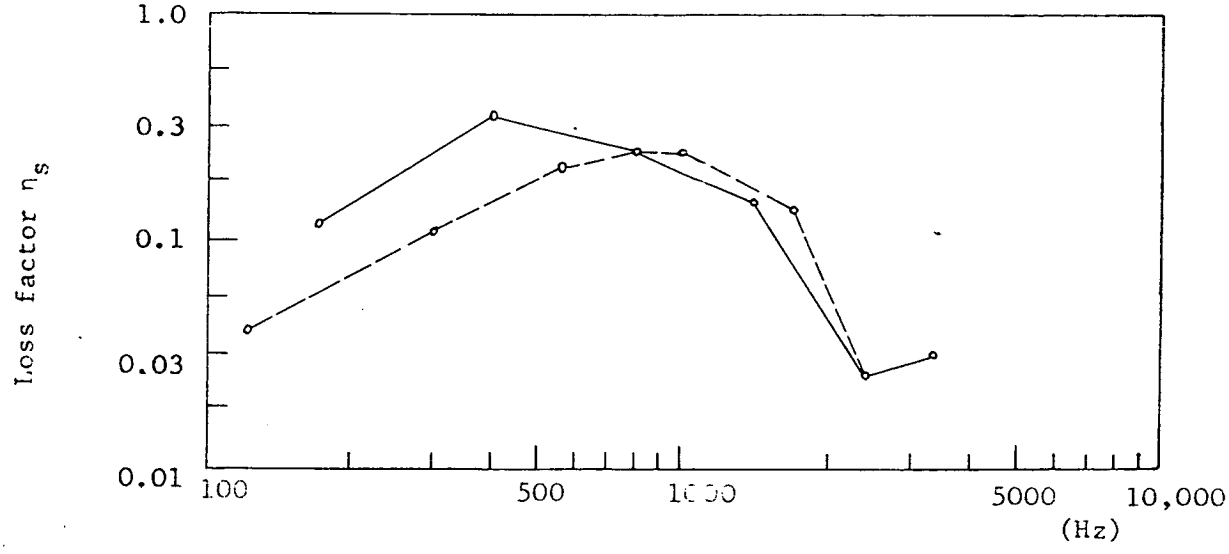

Fig. 3.8. Beam 3" x 2", in horizontal position, full of sand 0.6 mm to 1.18 mm.

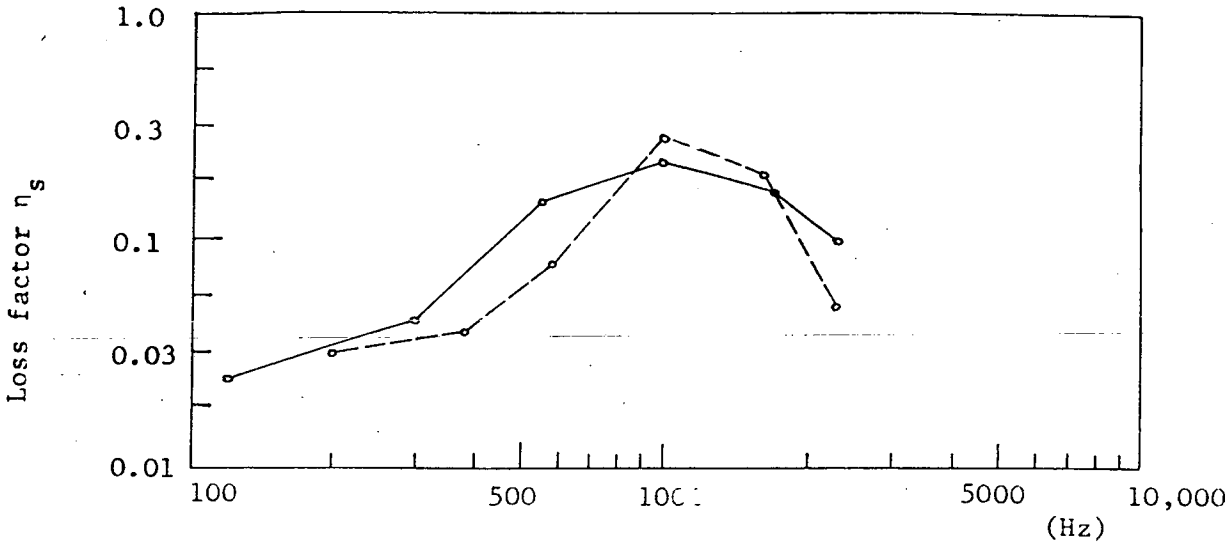

Fig. 3.9. Beam 2" x 1" in vertical position, full of sand 0.6mm to 1.18mm

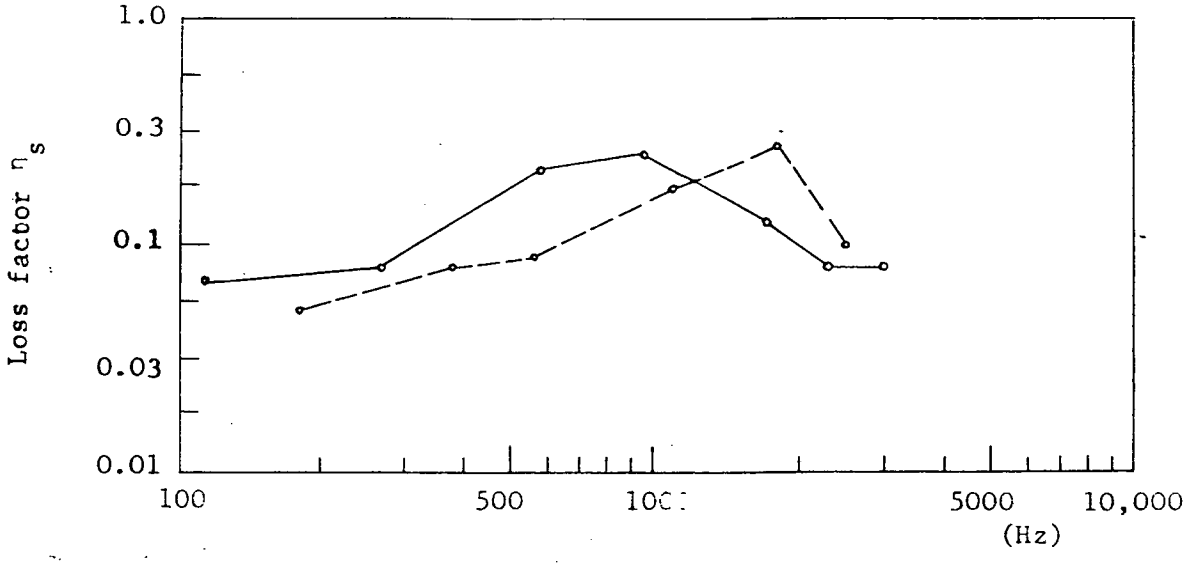

Fig. 3.10. Beam 2" x 1" in horizontal position, full of sand 0.6 mm to 1.18 mm

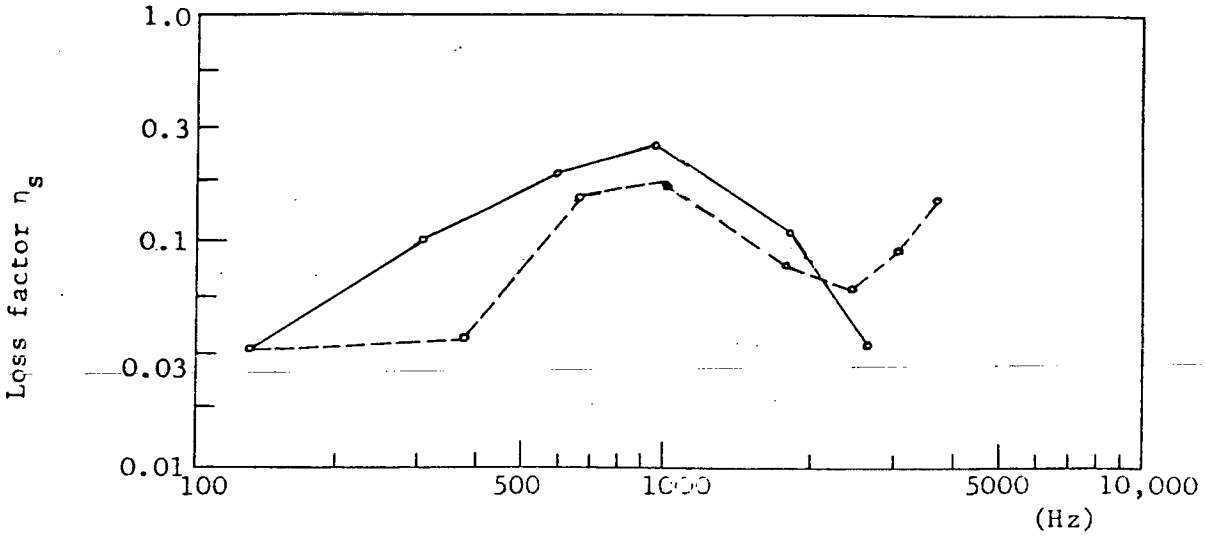

Fig. 3.11. Loss factors comparison for beams of different cross section shapes. Beams suspended vertically and full of sand 0.6 mm to 1.18 mm.

Ø2½"
2" x 2"

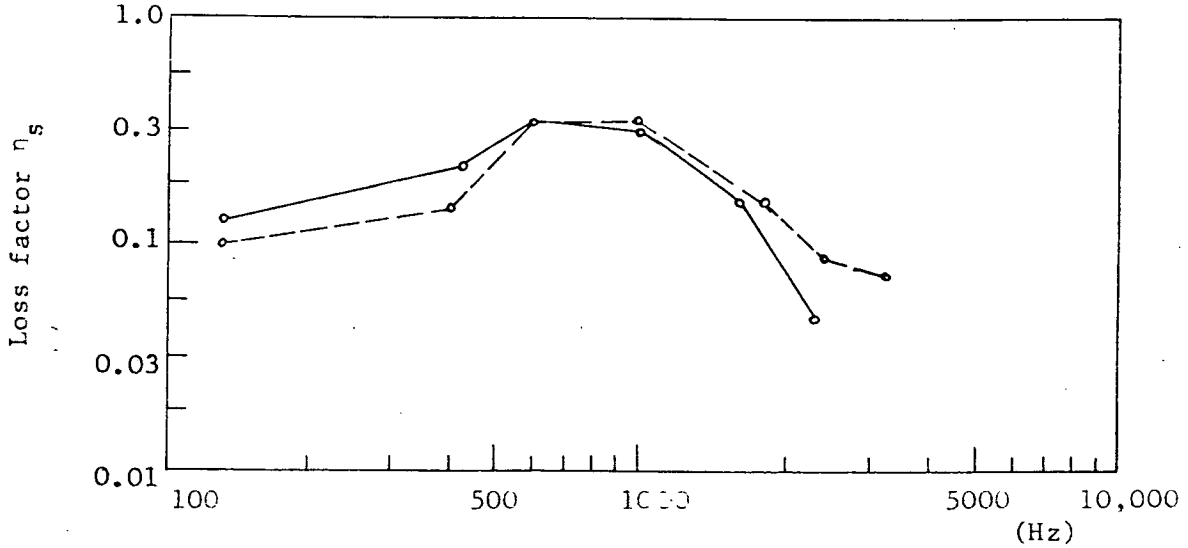

Fig. 3.12. Loss factors comparison for beams of different cross section shapes. Beams suspended horizontally and full of sand, 0.6 mm to 1.18 mm.

Ø2½"
2" x 2"

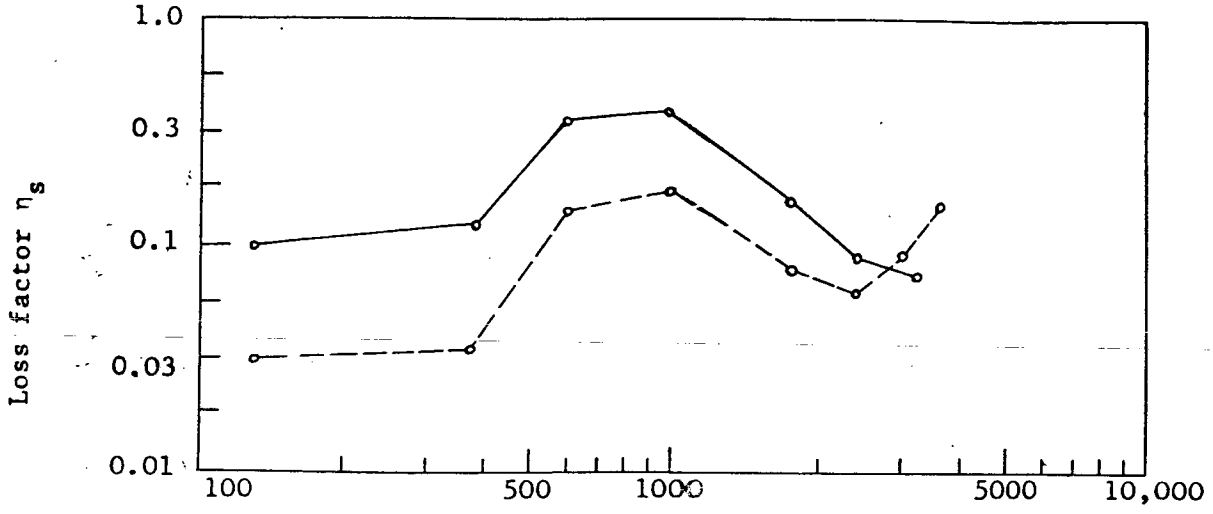

Fig. 3.13. Loss factors comparison for beams positioned horizontal and vertically; full of sand 0.6 mm to 1.18 mm; cross-section: 2" x 2"

Horizontal position

Vertical position

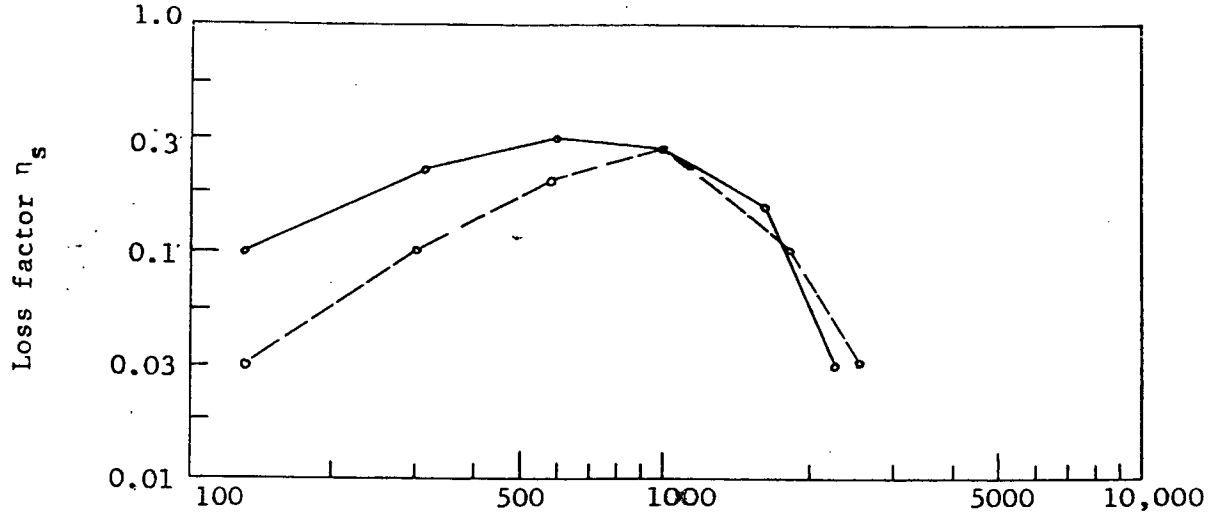

Fig. 3.14. Loss factor comparison for beams positioned horizontal and vertically; full of sand 0.6 mm to 1.18 mm; cross-section: Ø $2\frac{1}{2}$".

Horizontal position

Vertical position

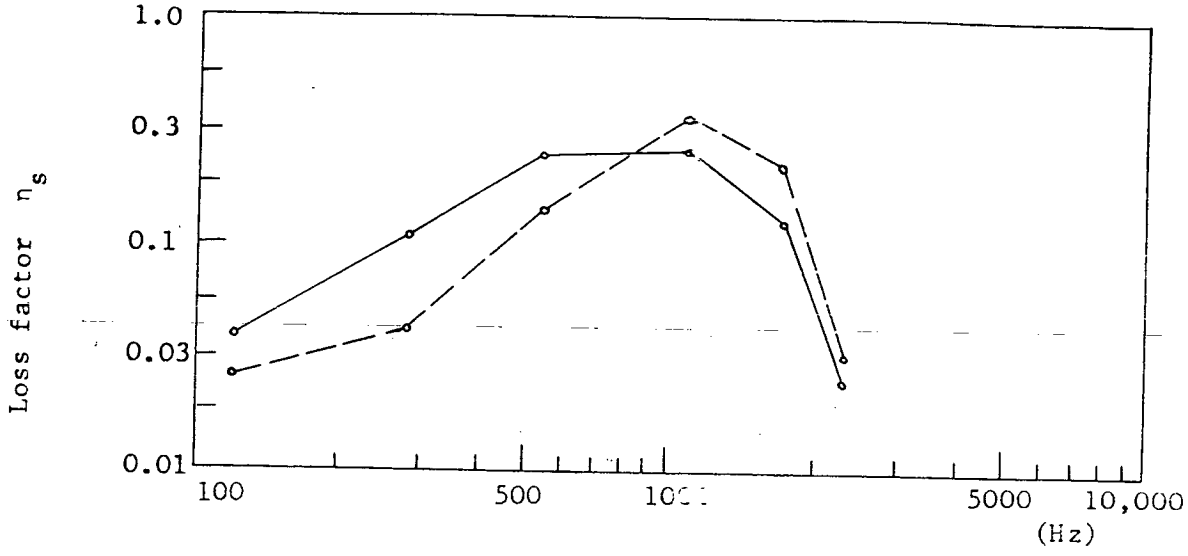

Fig. 3.15. Loss factor comparison for beam positioned horizontal and vertically. Beam cross section: 3" x 2"; full of sand 0.6 mm to 1.18 mm.

Horizontal position

Vertical position

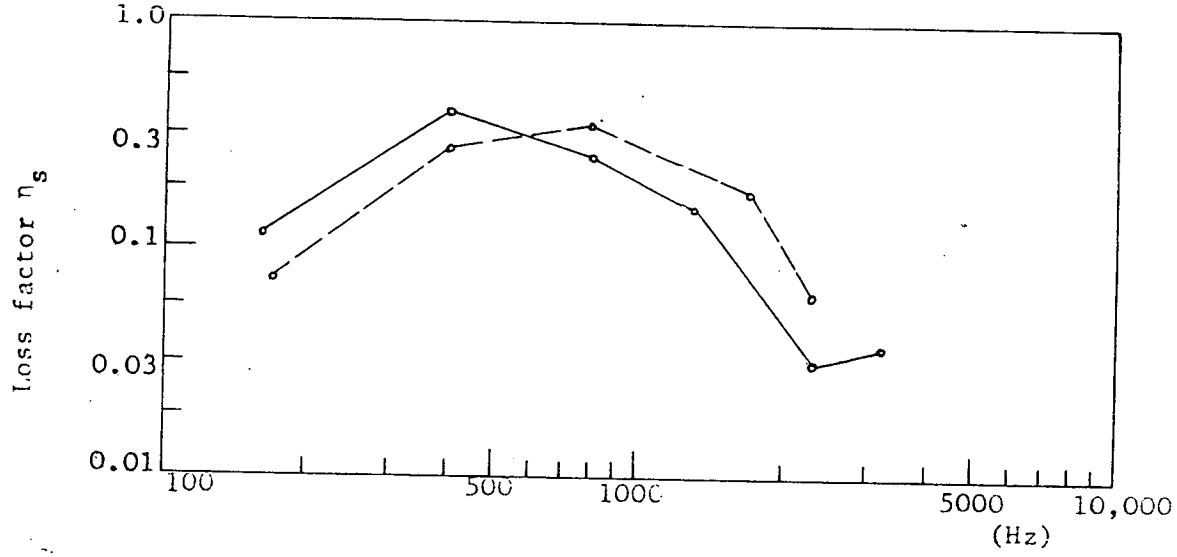

Fig. 3.16. Loss factors comparison for beam positioned horizontally and vertically. Beam cross section 3" x 2"; full of sand 0.6 mm to 1.18 mm

Horizontal position

Vertical position

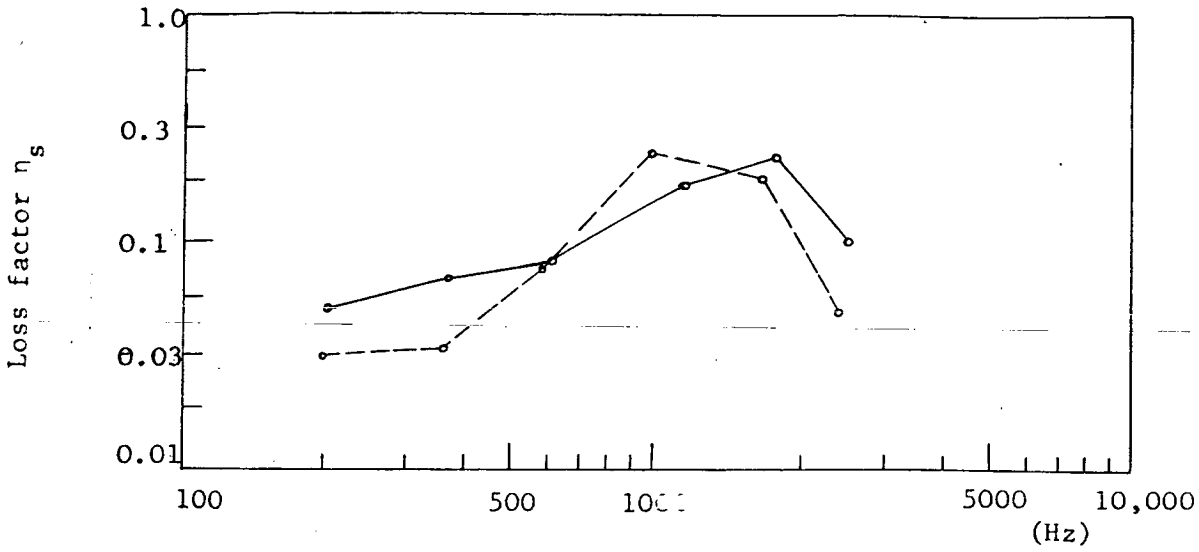

Fig. 3.17. Loss factor comparison for beam positioned horizontally and vertically. Beam cross section: 2" x 1"; full of sand, 0.6 mm to 1.18 mm.

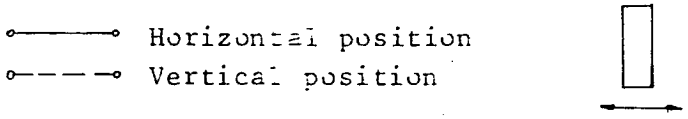

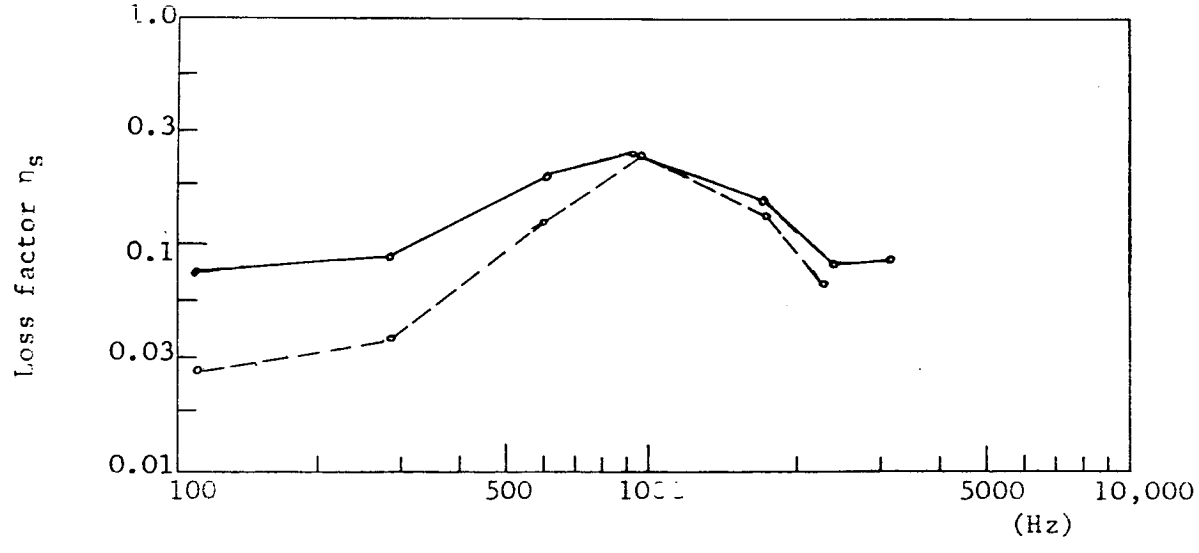

Fig. 3.18. Loss factor comparison for beam positioned horizontally and vertically. Beam cross-section: 2" x 1"; full of sand 0.6 mm to 1.18 mm.

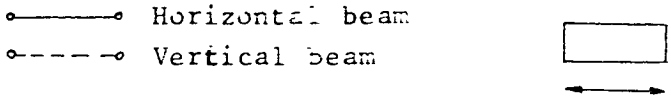

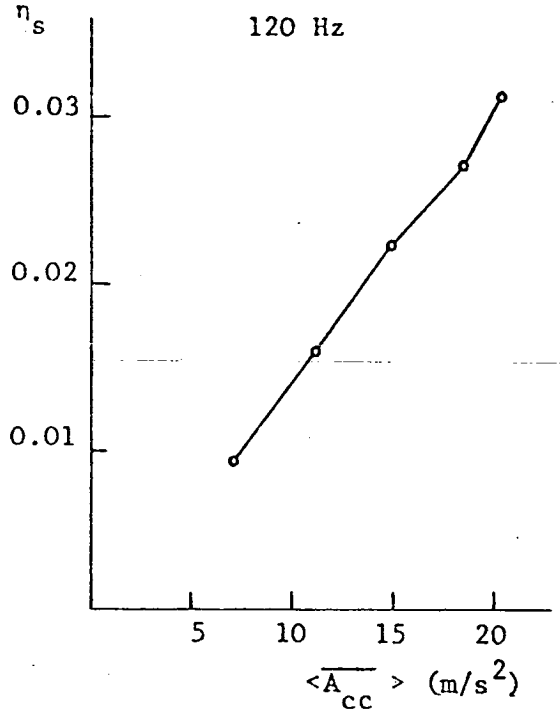

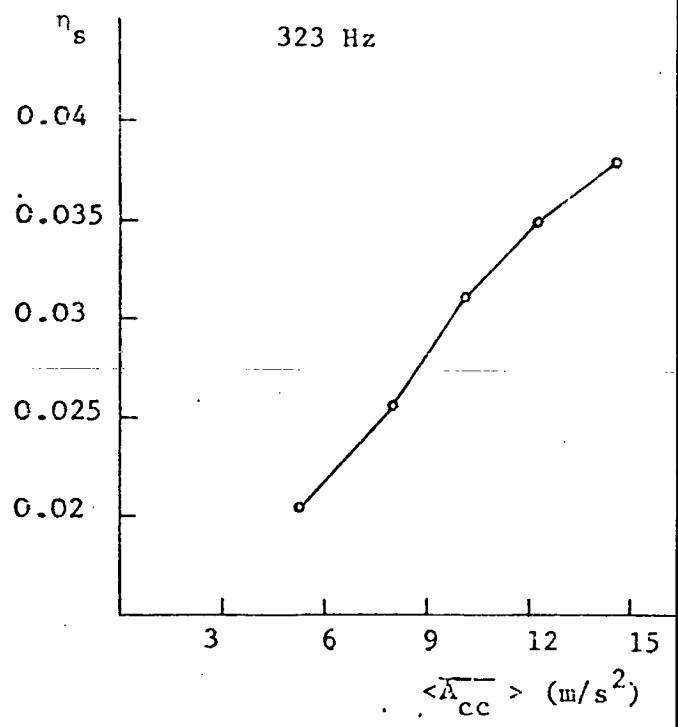

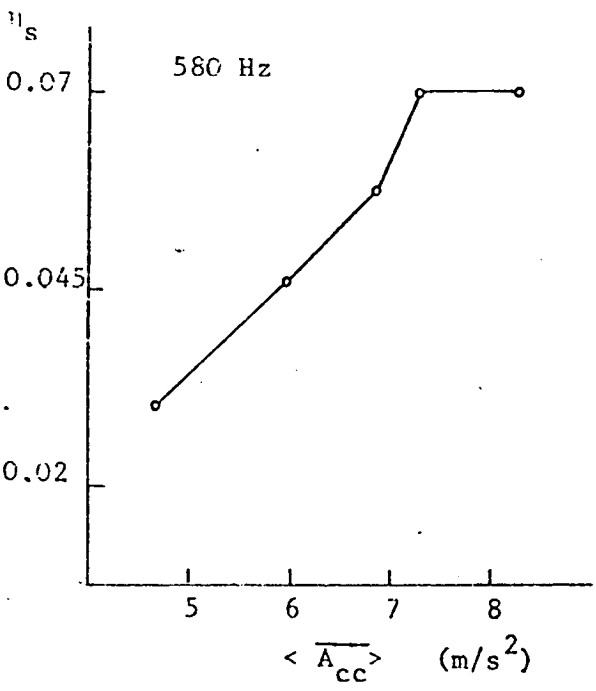

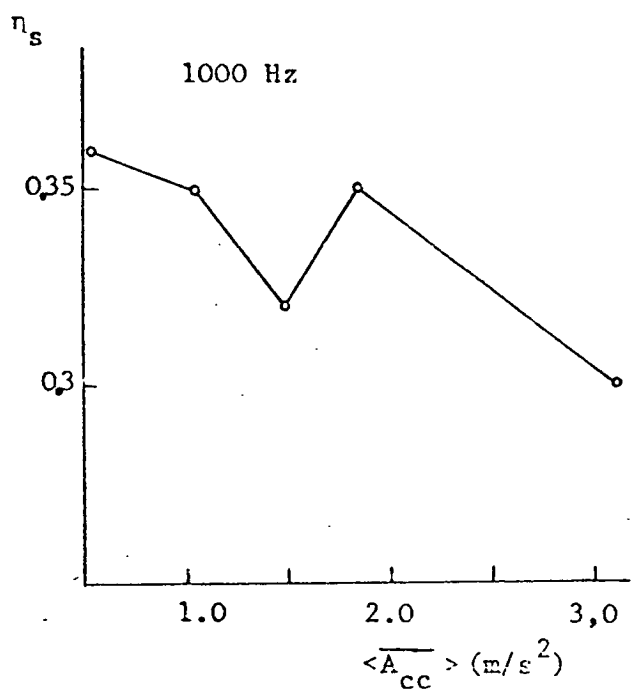

Fig. 3.19a. BEAM 2" x 2", VERTICAL FULL OF SAND 2.36 TO 4.75 mm

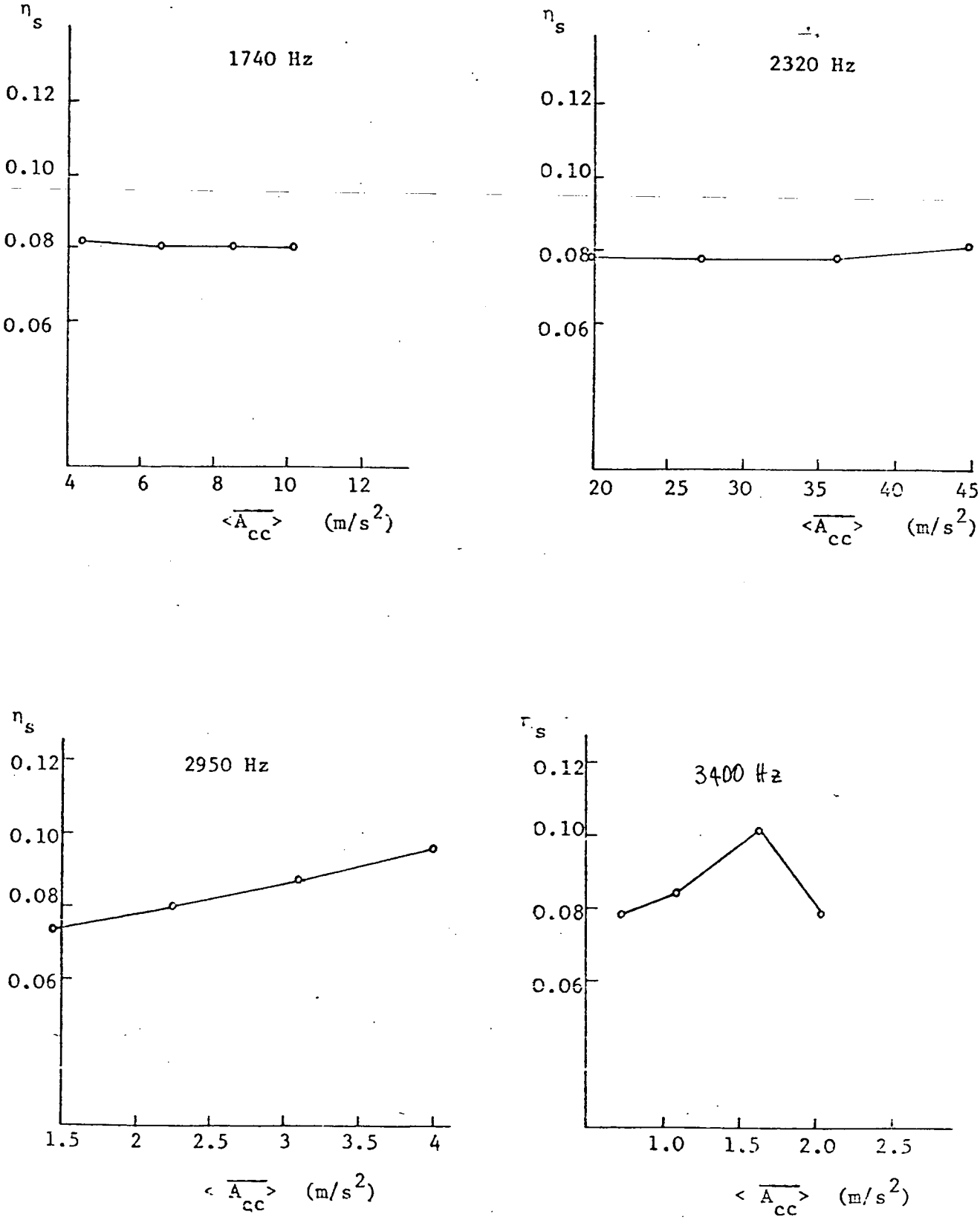

Fig. 3.19b. BEAM 2" x 2", VERTICAL, FULL OF SAND 2.36 TO 4.75mm

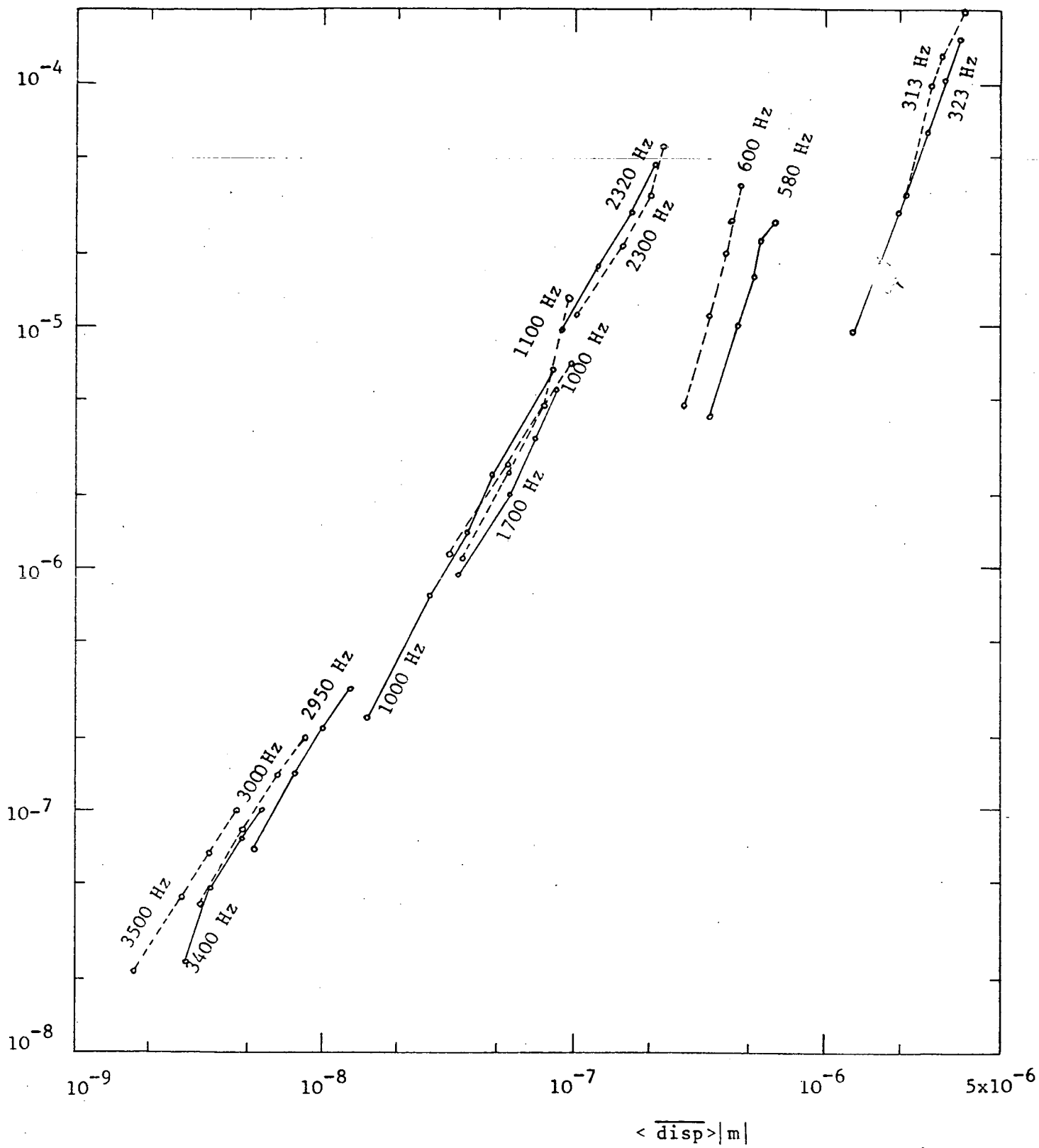

Fig. 3.20. Comparison of energy dissipated per cycle for two different sand grain types. Beam 2"x2"x1.5m long ($\frac{1}{8}$" wall)

——— sand 2.36 to 4.35mm

- - - - sand 0.3 to 0.6mm

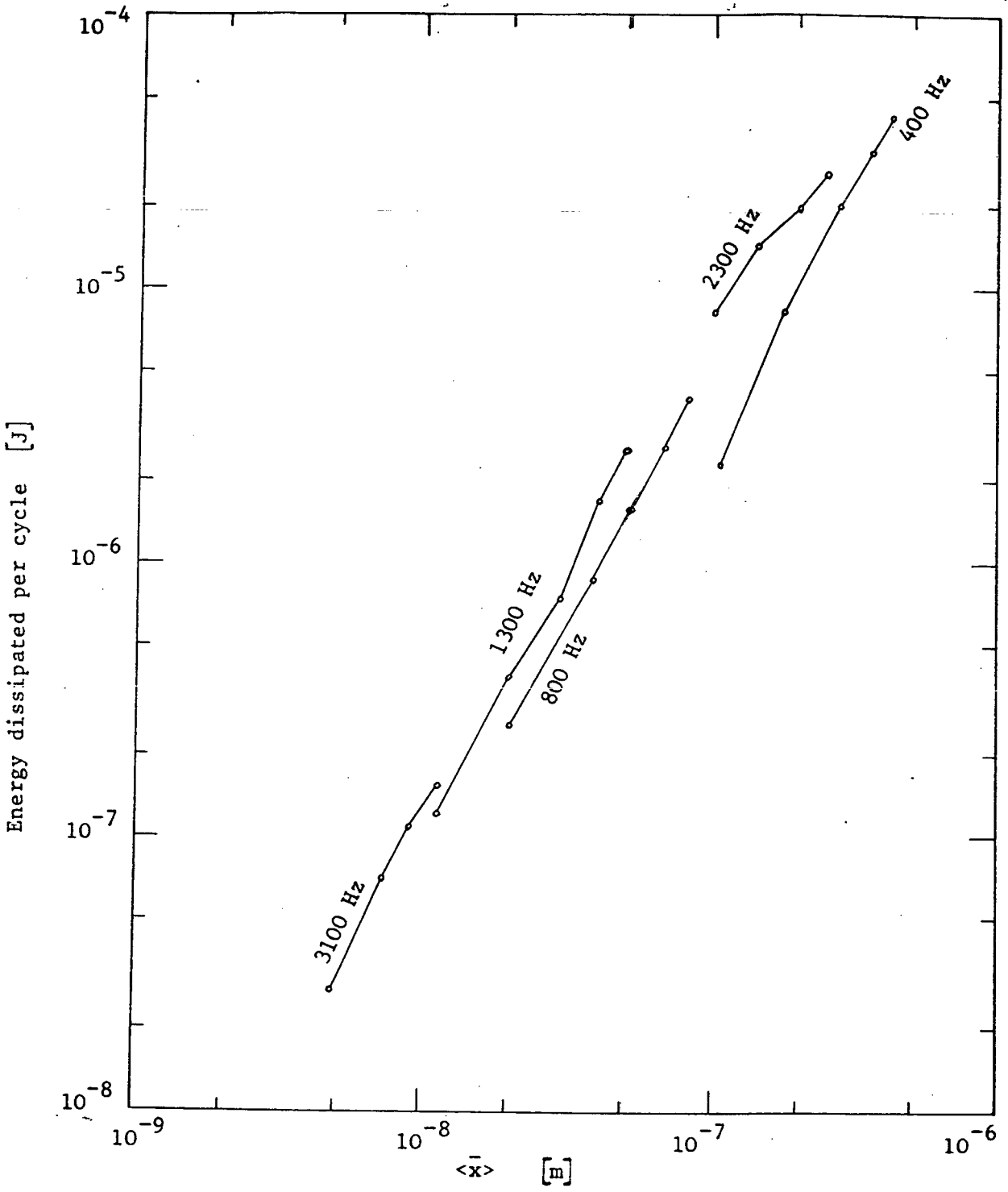

Fig. 3.21. Energy dissipated per cycle by the sand against beam amplitude of vibration. Beam 3" x 2", horizontal position; full of sand. 0.6 mm to 1.18 mm.

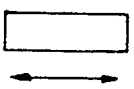

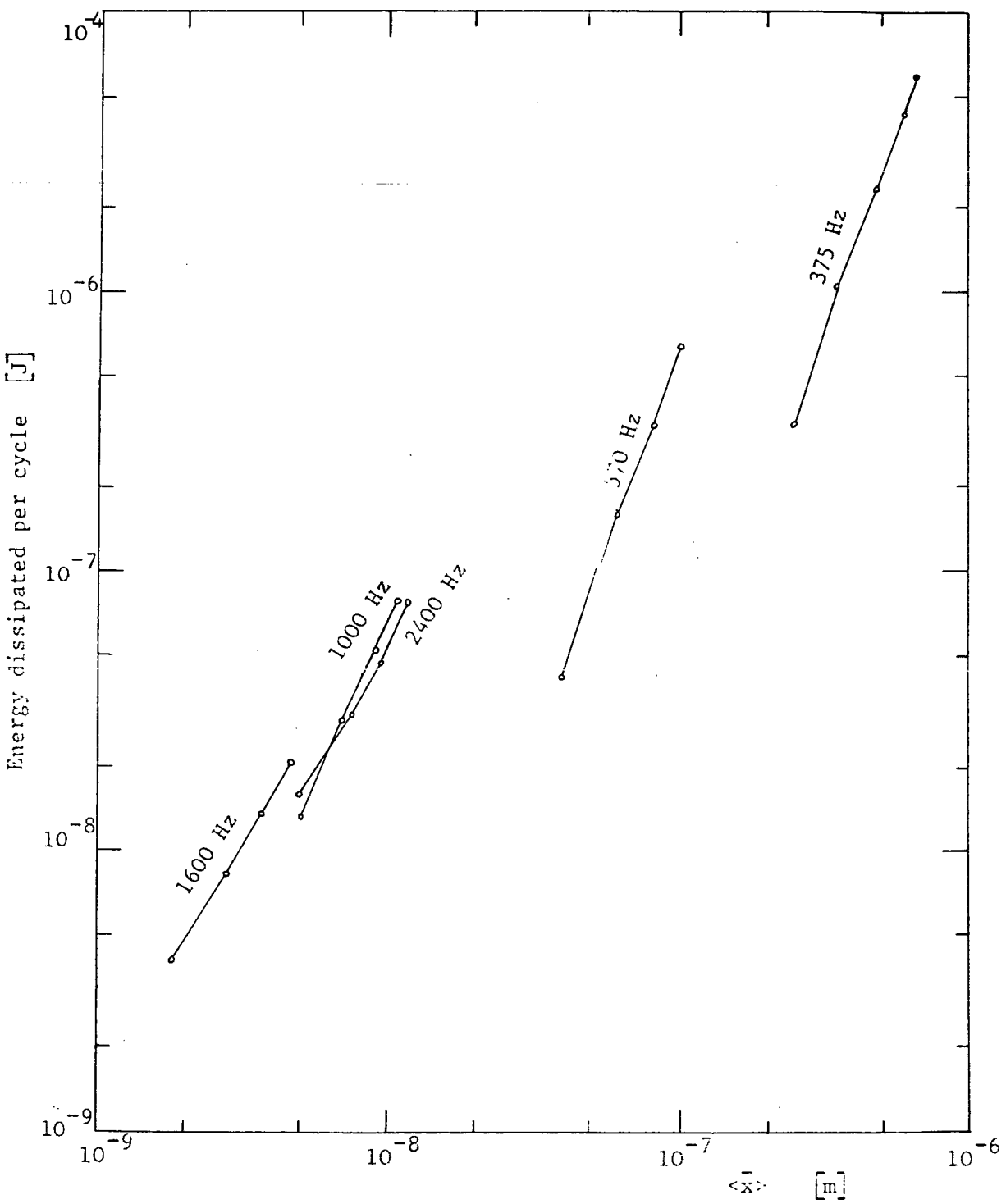

Fig. 3.22. Energy dissipated per cycle by the sand against beam amplitude of vibration. Beam 2" x 1" in vertical position. Full of sand, 0.6 mm to 1.18 mm.

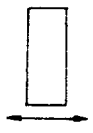

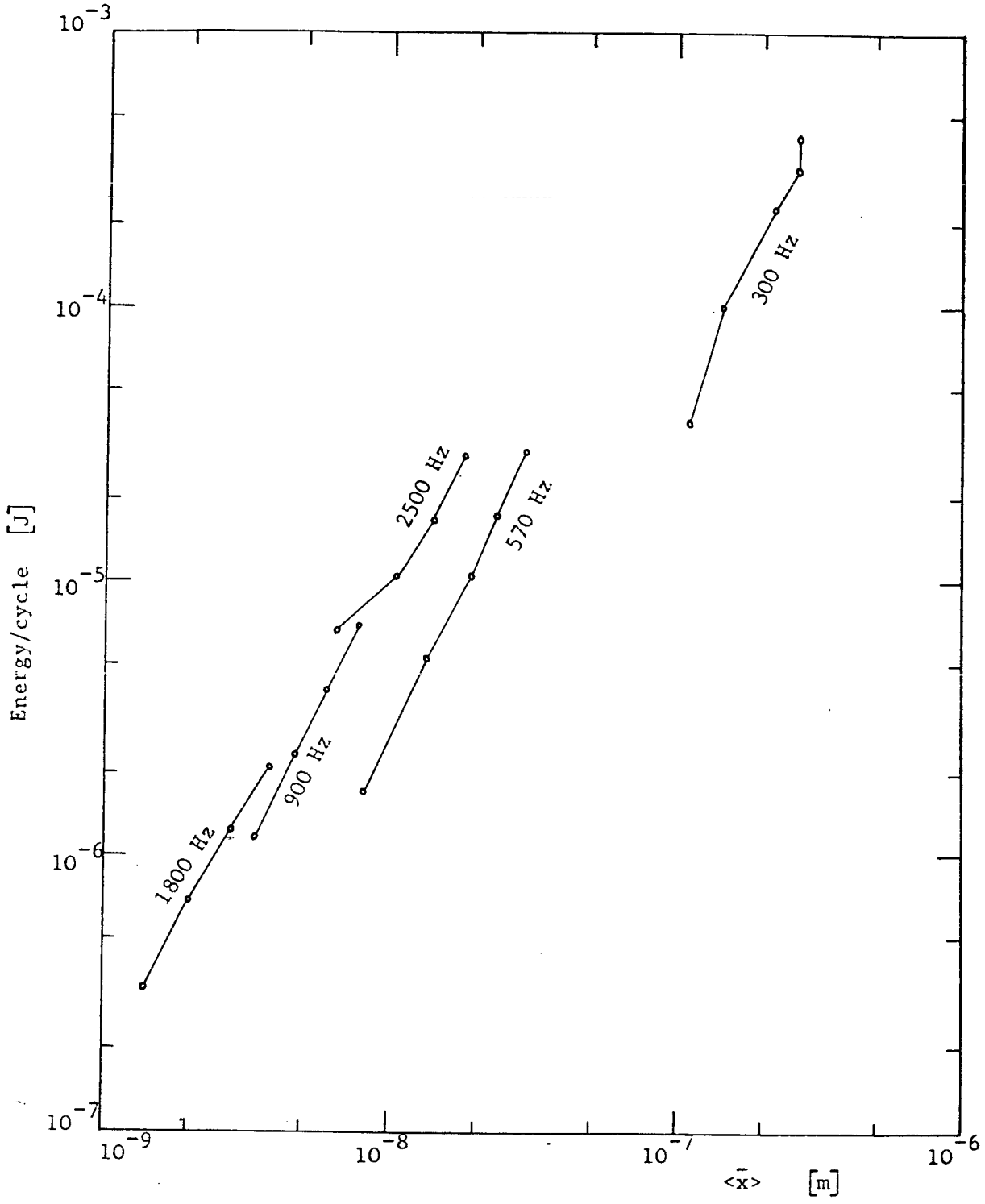

Fig. 3.23. Energy dissipated per cycle by the sand, against beam amplitude of vibration. Beam Ø 2½", in vertical position, full of sand 0.6 mm to 1.18 mm.

CHAPTER 4

DAMPING IN GRANULAR MATERIALS

4.1 Introduction

The experimental work (described in Chapter 3) has shown that sand filled beams exhibit a two regime damping characteristic related to the level of beam displacement. Damping was observed to be proportional to amplitude of vibration for large displacements ($> 10^{-7}$m) and independent of amplitude for small displacements ($< 10^{-7}$m). The experiments have also shown that the amount of energy dissipated per cycle of vibration is independent of frequency, particularly for small displacements.

The actual mechanisms of energy dissipation in granular materials are to some extent still unknown and those described in the literature only supply a vague description of the physical phenomena involved. Experimental work has been carried out with the object of seeking answers to many uncertainties, especially as to whether energy is dissipated by friction at contacts between grains or internally within the grains themselves. The determination of parameters and laws dictating the amount of energy dissipation in granular materials are discussed in this chapter.

Several materials found both naturally and man made are basically granular (e.g., rocks, bricks, concrete, cast iron, etc) as their microstructure is composed of granules. The difference between this type of granular material and others such as sand, lies in the freedom that grains have to move relative to each other. The damping of some of the granular materials mentioned above have already been the subject of studies, particularly internal damping of rocks by geophysicists. This work is reviewed in this chapter and the relationships developed for the damping of rocks extended to sand.

4.2 Internal Damping of Rocks

Most of the work prior to this present study on the damping of sand and rocks has been aimed towards seismic waves which are characterised by low amplitude and frequency. Strains are normally of the order of 10^{-9} and frequencies range from 1 mHz to 10 Hz. Damping measurements at such low strain levels can present a very difficult practical problem as conventional measurement techniques may no longer be applicable. The stress-strain relationship for example cannot be used because only a small hysteresis area is produced which is greatly affected by external factors such as the deformation of supports.

The measurement technique usually adopted, as reported in the literature[30], consists of determining the internal damping at high frequencies (ultrasonic frequencies) by driven resonance methods. This covers a strain range from 10^{-10} to 10^{-5}. A piezoelectric resonator made exactly one wavelength long for the frequency to be used is cemented to the specimen to be studied. The length of the specimen is made half the excitation wavelength. The resonator is then forced to vibrate by applying a harmonic voltage (up to 1000 Volts) to its end. The resultant amplitude of vibration is measured by the voltage generated in a smaller second piezoelectric component cemented between specimen and resonator.

Although frequencies associated with this technique are of the order of 100 kHz, it can be used for damping studies of seismic waves because, as will be discussed in a later section, damping of rocks is independent of frequency.

4.2.1 Damping level of some types of rocks

Several experimental results can be found in the literature, one of which is reproduced in figure 4.1. The significant characteristics of the results are that internal damping of all rocks is much greater than that of the single crystals that constitute the rocks (such as quartz) and that internal damping is also quite insensitive to the strain amplitude lower than about 10^{-6}. It is also noticeable from the results of Gordon and Davis[30] that damping of rocks is related to the details of the microstructure of the particular sample studied. This conclusion results from the observation that the highest and lowest damping observed in their

measurements both occur in quartzite. The observed damping must then be related to interfaces and cracks present in the rock.

Internal loss factors of the various types of rocks vary from 10^{-3} to 3×10^{-2} (for dry rocks), and it is interesting to compare with loss factors of steel, about 3×10^{-4} and cast iron, 10^{-3}.

4.2.2 The effect of frequency on the internal damping of rocks

Damping measurements at various frequencies, differing by a factor of more than 10^6 (14 mHz and 90 kHz), have been made by a number of researchers using stress-strain and driven resonance methods. The results obtained are remarkably close, supporting the idea that interface (frictional) damping is, to a very good approximation, frequency independent. Attewell and Ramana[31] have catalogued and analysed results from twenty five reports on the frequency effects of damping in rocks (in a wide range, 0.001 Hz to 10^8 Hz) and their work strengthens the conclusion that damping is independent of frequency.

4.2.3 The effect of amplitude of vibration

It has been generally observed from experimental results[30] that damping of rocks varies with the amplitude of waves travelling through the specimen. For very low strains ($< 10^{-6}$) damping is amplitude independent while that for larger strains ($> 10^{-6}$) damping is proportional to amplitude. Loss factors are noticed to increase about 10 dB per decade increase in strain (in the large amplitude region). It is clear that a double damping mechanism is occurring in rocks.

4.2.4 The damping mechanism of rocks

One of the most intuitively accepted and widely discussed mechanisms proposed for seismic energy loss is based on simple Coulomb friction, because it commonly occurs on macroscopic sliding surfaces and is also frequency independent.

Frictional sliding at crack surfaces and grain boundaries has been suggested as an important if not dominant mechanism of wave attenuation in rocks, at low confining pressure (a few atmospheres), and particularly in the absence of fluids.

An examination of the microstructure of rocks reveals the existence of cracks typically[33] 0.1 mm to 1 mm long. Relative slips caused by the passage of a wave will obviously be of "partial slip" nature, where, as discussed in Chapter 2, the amount of energy dissipation by frictional forces is proportional to the amplitude cubed, and consequently, the loss factor is proportional to amplitude. Such amplitude dependence is in fact observed experimentally leading to the conclusion that friction at cracks may dominate for large strains but must be secondary to linear mechanisms at low strains (seismic waves). It is observed experimentally[32,33] that the transition region occurs at strains of about 10^{-6}.

If crack lengths are of about 1 mm, the actual amount of slip at strains of 10^{-6} is 10^{-8} m (100 Å), which is comparable to atomic spacings. At small strains then (less than 10^{-6} or so), dry friction probably cannot be the mechanism responsible for the damping.

Unfortunately, the actual linear mechanisms observed at low strains are not yet known. Some suggestions have been put forward, for instance, grain boundary relaxation as described by Jackson and Anderson[34] or dislocation mechanisms similar to those discussed by Mason[35] where layers of atoms or molecules are forced to slide relative to others which are restrained by tiny impurities acting as pins. This is the general Granato-Lucke[5] theory of dislocation which closely describes the internal damping of metals. Mavko[36] also pointed out that the presence of even minute quantities of fluid can easily increase loss factors of rocks to 10^{-2}. Whatever the cause may be, however, it is almost certain that the mechanism does not involve any concept of macroscopic friction as it does at large strains, herein now considered larger than 10^{-6}.

4.2.5 The effect of external pressure

It is thought that wave attenuation in rocks at large strains requires cracks barely closed to allow relative slip. As external pressure is applied, such loose contact interfaces in the rock would begin to disappear due to the compression of the solid.

The effect of a large contact pressure is to clamp interfaces responsible for the internal friction. Large contact pressure prevents relative slips taking place at the interfaces and also restricts microstructural dislocations which occur at low strains. As a consequence of the increased pressure, the internal loss factor of rocks is decreased to about 10^{-3} for hydrostatic pressures in the order of 1000 bar, compared to about 10^{-2} in the absence of external pressure[30].

4.2.6 The effect of fluid

Since perfectly dry rocks, such as those used in many laboratory experiments, are not expected to be found in the earth because of the presence of ground water or air humidity, the contribution of small amounts of water on the overall internal damping of the rock has been studied by geophysicists. The process of drying a rock sample consists of soaking it in volatile liquids (such as alcohol) and leaving it to dry in a vacuum oven. The damping of the sample is measured at regular periods and it is assumed to be dry when the damping level does not change after two successive dryings. On the other hand, a sample is saturated in water by soaking for several weeks.

The most noticeable feature of the results is that the addition of water greatly increases the damping[30] (by about one full order of magnitude). This is associated with fluid flow inside pores and cracks which dissipates energy by the viscous forces produced by the velocity gradients.

It is noticed that internal damping of saturated samples varies with frequency, i.e., in the milliHertz region, damping is frequency independent, whereas the presence of water in the kiloHertz region increases damping by almost an order of magnitude.

4.3 Experimental Studies of Damping of Some Granular Materials

Some work can be found reported in the literature on damping and other dynamic characteristics of sand in reference to the speed of elastic waves in soils and their attenuation. It is these parameters which are necessary for the calculation of vibrations emanating from earthquakes and ground vibrations transmitted from roads to residences built nearby.

Laboratory damping measurements were performed by Hall and Richart[39] on a column of sand enclosed in a thin plastic layer. Longitudinal vibrations were excited along the axis of the column by a magnetic shaker. A short metal cylinder was placed on the top of the column to simulate a single degree of freedom system to facilitate damping measurement. The system was driven at its first resonant frequency and damping was measured by cutting off the power and recording the rate of decay of the amplitudes. Air was removed from the inside of the column to subject sand to different hydrostatic pressures from the atmosphere. Hall and Richart present their results plotted against the amplitude of vibration level immediately before the power was cut off. Loss factors vary between 10^{-2} and 8×10^{-2}, depending upon pressure and amplitude. In general, they found that the loss factor for dry sand increased with amplitude at an approximate rate of 5 dB per decade and decrase with pressure at a rate of about 3 dB per decade.

Although Hardin[40] and Hall and Richart[39] describe in detail every precaution taken to ensure accurate measurements, the method employed is perhaps not adequate for wide amplitude ranges, since it extends for one order of magnitude only and measurements at higher frequencies are virtually impossible due to the very rapid decay of vibrations. The method is therefore of limited use.

The major disadvantage of this method is the limited amplitude range over which measurements can be made, because as was observed in damping measurements on rocks, changing the strain by several orders of magnitudes permitted the detection of a double damping mechanism which could also occur for sand.

The frequency range over which experiments have so far been carried out is very much limited to the lower part of the audio spectrum (up to a few hundred Hertz). Such a range should be extended to a few kiloHertz in order to test the frequency dependence upon damping.

Richart et al[41] concluded from his experimental studies that some viscous-type mechanism of damping is apparent in sand based on the observation that the rate of decay of free vibrations in a column of sand followed a straight line when the logarithm of amplitude was plotted against time in linear scale. The conclusion is, however, incorrect because all quadratic damping mechanisms present such behaviour and viscous damping is only one type of such a mechanism.

In view of so many contradictions, it has been felt necessary to carry out a series of experiments to investigate in more detail the effects of the various parameters upon damping, including other materials such as lead shot, which had not been studied yet. These are described in the following paragraphs.

4.3.1 Experiment description

Based on the experience learned from published works dealing with damping measurements of sand, it soon became clear that the method employed (the decay rate method) has serious amplitude and frequency range disadvantages and limitations which excluded its use in the present research.

The experiment consisted of making a column of the sand specimen to be studied, contained by a thin-walled plastic and flexible tube of 5 cm diameter, just thick enough to contain the material to avoid the propagation of energy through the walls. Any applied force or movement had thus to be transmitted through the material only. The lower end of the tube was bonded to a metal cylinder which served a double function: firstly, to permit the column to be fixed on a large mass and, secondly to allow its connection to a vacuum pump for air removal, as shown in figure 4.2. The internal vacuum caused an external hydrostatic pressure to be applied by the atmosphere. The attachment of the column to the large mass held the lower end firm and it was assumed to have zero displacement (tests confirmed this). At the top of the column, a metal disc 5 mm thick was placed and connected to an electrodynamic shaker. Dynamic

weaknesses associated with threads in the connector caused the combination mass-connector to behave as a single degree of freedom system. Its resonant frequency originally was 2000 Hz, but after reducing its thickness to 5 mm and changing the material to aluminium, the frequency was shifted to 5 kHz. Resonances in the lower connecting bolt of the lower end of the column were also found to be higher than 5 kHz so that the system allowed measurements up to 5 kHz before problems of spurious signals associated with such resonances were observed.

4.3.2 Equipment lay-out

A harmonic signal generated by a decade oscillator (Muirhead D-890-A) was used to drive an electrodynamic shaker (Goodman 380), through a power amplifier (Power Amplifier Beam Echo DL7-35) as shown in figure 4.3. Force and response signals were measured by means of an impedance head (B & K 8201) placed between the aluminium disc and the connector. The impedance head signals were passed through a pair of charge amplifiers (B & K 2635) and a band pass filter. The filter had adjustable central frequency and bandwidth. The phase mismatch error of the charge amplifiers and filter is around 1^{o}, which was considered satisfactory for the experiments. An oscilloscope was used to monitor the signals. Phase between signals was measured by a phase meter (AD-YU 406L) and their amplitudes by a voltmeter.

4.3.3 Damping calculation

Loss factor determination was by the power input method. This required measurement of the power supplied to the sand specimen and of its maximum vibratory energy. The impedance head provided force and velocity signals at the point of application of the force, which give the power supplied to the column:

$$W_{supp} = F_{rms} \times V_{rms} \times \cos \phi$$

where ϕ is the phase angle between the two signals. It is assumed here that the power is entirely dissipated by the sand column. As measurements

were always made at resonances of the column, the phase angle was 90^{o}, and was constantly monitored by the phase meter.

Column resonant modes are such that at the lower end, particle displacements are always zero (node) and are a maximum at the top (antinode) where the force is applied. The first resonant mode consists of a standing wave of one quarter of a complete wavelength in the column, the second three-quarters of a wavelength, the third one and a quarter wavelengths. The maximum vibratory energy of the column is given by

$$E_{max} = \tfrac{1}{2} M \, V_{rms}^2$$

where M is the mass of the column and loss factor is given by

$$\eta = \frac{W_{supp}}{2\pi f \, E_{max}}$$

4.4 Damping Measurement Results

Damping results presented in this chapter are plotted against strain so that better comparisons could be made with data on internal damping of rocks which is usually presented in this form. Strains indicated in the figures represent maximum values which occur at the top of the column (the strain follows a sinusoidal distribution along the column). The strain was then computed as the ratio maximum displacement to one quarter of the wavelength.

Three hydrostatic pressure values were used in the experiment: 1.3×10^4 N/m^2; 6×10^3 N/m^2 and 3×10^3 N/m^2, corresponding to maximum pressures existing in columns of sand of 1 m, 0.5 m and 0.25 m high, respectively, which are regarded as typical dimensions for machine components. The effects of higher pressures were not investigated because, as already mentioned, damping levels of granular materials are reduced.

Frequencies indicated in the figures correspond to resonances of longitudinal vibrations in the column.

4.4.1 Sand loss factor results

Figure 4.4 shows loss factors of sand with grain diameters 0.6 mm to 1.18 mm, subjected to the highest pressure applied. The major feature of the results is the damping variation with strain which is similar to that of rocks, i.e., independent of amplitude at low strains but increasing with strain at a rate of about 3 dB/decade at higher strains. Results for three different frequencies show remarkably good agreement which confirms the conclusion that damping of sand is not influenced significantly by frequency; the small deviation being attributed to experimental accuracies only.

The transition region between the two regimes occurs at strains around 10^{-7}, unlike rocks for which transition occurs at somewhat higher strains, 10^{-6}. This is attributed to the loose and independent nature of grains in sand whose energy dissipation at contacts may amount to larger quantities, compared to the limited energy dissipated at cracks in rocks.

Damping at low strains agrees very well with results obtained from rock samples, which leads to the conclusion that at low strains damping of sand is entirely due to energy dissipated inside grains, and the damping contribution provided by dry friction at contacts is negligible. The contribution of individual minerals to the overall damping of a particular type of sand should be considered since their damping can vary by factors of up to ten. Granite, pheldspar and mica commonly occur in rocks, and if present in large proportions, as is often the case for granite, the overall damping of the rock can be greatly affected.

Damping loss factors at large strains show good agreement with values of sand found in the literature (typically, η = 0.06 to 0.2), i.e., for measurements carried out at low frequencies, which are associated with large amplitudes of vibration.

Hydrostatic pressure was found to have little influence upon damping, in accordance with theoretical predictions based on energy dissipation at contacts of spheres, as described in section 4.5.3, where damping due to friction at contacts under partial slip is inversely proportional to pressure to the power 1/6 (figure 4.7).

Damping of sand of a different grain size (2.36 mm to 4.75 mm) was also tested for analysis of the grain size effect (figures 4.8, 4.9 and 4.10). No significant variation of damping with grain size was found, as is shown in figure 4.11.

4.4.2 Lead shot loss factor results

Most of the work in this project has been performed with sand because it is easily accessible and absorbs high energy. Sand, however, lacks high internal damping and density, which enables the material to generate larger reaction forces against vibrations of structures. With these two characteristics in mind, lead shot was tested and results are presented in figures 4.12, 4.13 and 4.14.

The major observation was that damping variation with strains followed a reverse pattern to that of sand, constant damping for small strain and decreasing with amplitude at larger strains. The oxide layer covering the tiny lead spheres is thought to form a lubricant, reducing the ability of the material to dissipate energy by friction at contacts as is the case in sand.

Internal damping of lead predominates at small strains because displacements are so small that they make friction unlikely to contribute to the overall damping in this region. At large amplitudes, granules are forced to slip relative to each other without being able to dissipate energy.

The experiment was also used to test the accuracy of the measuring system since internal loss factor of lead is known (from 0.05 to 0.3 according to various sources[5,21]) and good agreement was achieved.

Pressure was noticed to have no significant effect upon damping.

The damping variation with amplitude, as shown in figures 4.12, 4.13 and 4.14, is an important feature for machinery noise control purposes. High damping levels exist at the middle and high frequencies (low vibrational amplitudes) usually associated with noise radiation. As density is also about

four times higher than sand, the filling of cavities with lead shot permits high mass of granular material to mass of structure ratios; important for increasing structural damping.

4.4.3 Loss factor results from spheres of glass

Results obtained from measurements carried out on sand showed a double damping behaviour, according to the amplitude of waves excited at the sample under study. The damping increase with strain observed for large amplitude waves has been attributed to friction taking place at grain contacts, in the form of gross and partial slips. The actual configuration of the contacts existing throughout the sample may vary significantly from sharp edges to almost flat surfaces, due to irregularities in the shape of sand grains. Experiments were therefore carried out on a sample composed of spheres of glass (whose diameters vary from 1 mm to 2 mm), seeking observation of the damping variation in a material where all contacts are of spherical shape. The objective was to compare results from both materials. As can be seen from figures 4.15 and 4.16, damping of glass spheres follows an identical pattern to that observed in sand. It is concluded that as long as granules are not perfectly spherical, occurrence of both forms of slip (partial and gross) is inevitable, yielding to identical damping as obtained from irregularly shaped granular material.

4.5 Theoretical Analysis of the Parameters Associated with Energy Dissipation at Contacts of Spheres

Theoretical models involving description of granular materials, assume as a first approximation, that granules can be represented by spheres, i.e., neglecting the irregularities in the actual shape of grains which, if taken into account, could make theoretical analysis very complex. Despite this approximation, theoretical results discussed in this section accurately represent the mechanisms of energy dissipation at grain contacts in sand and other granular materials. Use is made of the Hertzian contact theory of elastic bodies for the determination of stress and deformation relations as the basis for the damping analysis.

Hertz theory of contact applied to spheres has been dealt with in detail in many publications including textbooks of elasticity[43] and specialised books[42]. Thus, only the essential expressions, enough to support an understanding of the physical phenomena involved, will be presented, rather than deriving them in a step-by-step procedure.

4.5.1 Stress distribution and contact area

If two elastic spheres are pressed together with a force N, the direction of which passes through the centre points of the spheres (normal to the contact plane), the normal stress distribution over the contact area, as shown by Goldsmith[42], is of quadratic (parabolic) form, given by the expression

$$\sigma(r) = \frac{3N}{2\pi r_o^2}\left[1 - \left[\frac{r}{r_o}\right]^2\right]^{\frac{1}{2}} \qquad (4.1)$$

where r is the distance from the centre of the contact surface and r_o is the radius of the contact area, which is given by

$$r_o = \left[\frac{3(1-\gamma)RN}{8G}\right]^{1/3} \qquad (4.2)$$

R is the radius of the spheres, γ is Poisson's ratio and G the shear modulus of the material of the spheres. It is assumed that both spheres have equal radius

4.5.2 Shear Stress and Annular Slip Area when Tangential Forces are Added

As shown in section 4.5.1, normal stresses are of parabolic form with the maximum value at the centre of the contact area and decreasing to zero at its circumference. Analysis carried out for elastic spheres where relative displacements of opposing points on the contact area are taken into account show that the application of a tangential force produces shear stresses over the contact area as shown in figure 4.15.

In an annular region close to the circumference of the contact area, shear stress is greater than the friction resistance which causes relative slip to occur, dissipating energy. It is assumed that Coulomb's law of friction holds at each point on the slip area. As the tangential force T is increased, the inner radius of the annulus of slip diminishes according to the expression[44]

$$r_i = r_o\left(1 - \frac{T}{\mu_f N}\right)^{1/3} \tag{4.3}$$

As long as relative displacement is allowed to occur over part of the contact area only, the "joint" is said to be of the "partial slip" type. If the tangential force is increased to values greater than the total frictional resistance caused by normal stresses, a "gross slip" type of friction is obtained.

4.5.3 Energy dissipation per cycle by an oscillating tangential force

As long as the tangential force is kept smaller than the frictional resistance provided by the normal force ($T \leq \mu_f N$), slip is confined to an annulus and the energy dissipated per cycle is given by the following expression

$$E_{diss}/\text{cycle} = \frac{9(2-\gamma)\mu_f^2 N^2}{5Gr_o}\left[1 - \left(1 - \frac{T}{\mu_f N}\right)^{5/3} - \frac{5}{6}\frac{T}{\mu_f N}\left[1 + \left(1 - \frac{T}{\mu_f N}\right)^{2/3}\right]\right] \tag{4.4}$$

For very small values of T ($\ll \mu_f N$), the above expression reduces to

$$E_{diss}/\text{cycle} \simeq \frac{(2-\gamma)T^3}{18G\, r_o\, \mu_f N} \tag{4.4a}$$

which corresponds to the limiting case when forces at contacts caused by the passage of elastic waves are small compared to those caused by the hydrostatic pressure applied to the granular material. Equation (4.4a) therefore represents the case of waves of very small amplitude.

The equation is also limited to maximum values of T $(= \mu_f N)$ which is the limit before gross slip starts to occur. It is difficult to determine an exact expression for the gross slip case because contact area and especially the associated normal stresses, may assume values which are difficult to predict, but it is expected, however, that parameters involved in E_{diss}/cycle will follow closely those for simple lap joints under gross slip.

Maximum values for E_{diss}/cycle, prior to gross slip taking place, are given by

$$E_{diss}/\text{cycle} = \frac{9(2 - \gamma)\mu_f^2 N^2}{30Gr_o} .$$

The variation of E_{diss}/cycle with T follows a cubic law (30 dB per decade), as would be expected from partial slip conditions.

Several experiments have been carried out in the past to test the validity of this theory. Mindlin et al[45] used a pile of three polished glass lenses, pressed together with a normal force, and an oscillating transverse force (60 Hz) was applied to the central lens. As expected, relative displacements at the contact surface occur only in an annulus, the dimensions of which were compared with the theory by measurements of wear patterns. Measurements of energy dissipation have shown good agreement with theory at large amplitudes, but at small amplitudes energy dissipation varied as the square of the tangential force rather than the cube as the theory predicts.

Johnson[46] reports a careful series of experiments in which hardened steel spheres were subjected to cyclic tangential loading. Also, by means of wear patterns, it was possible to verify the dimensions of the slip annulus given by the theory. His energy dissipation results did not at first follow the expected theory since they appeared to indicate the presence of a geometrical factor not accounted for, but later it was found to be due to a variation in the friction coefficient over the contact area caused by an oxide layer not removed prior to the experiment.

Goodman and Brown[47] have carried out the most complete series of experiments in this particular area. Experimental results were observed to follow very closely predictions made by the theory so that it can be assumed accurate enough for engineering applications. Reported in this

reference is an attempt to measure the internal material damping of the spheres. However, this attempt failed because the amplitude range of the experiments was such that the damping provided by friction at contacts predominated.

Material damping at low amplitudes has been measured by Johnson[48] with only an oscillation normal force. Although shear at the contact did not exist, measurements at very small amplitudes indicate damping did not fall to zero as anticipated by the theory, but to a small constant value, indicating the presence of material damping.

Duffy and Mindlin[49] carried out measurements on a granular bar 10 cm long and 1.5 cm wide, constructed of steel ball bearings held in place by an externally applied hydrostatic pressure. Ball diameters were 3 mm and within $.25 \times 10^{-6}$ m of tolerance. Damping was determined by observation of the decay of free vibrations from an initial vibration amplitude of about 10^{-8} m. Results indicated that the logarithmic decrement is amplitude independent in this range, suggesting therefore that the damping mechanism is linear. Considering strains in the bar were always lower than 10^{-7}, Duffy and Mindlin's results confirm the conclusion that at very small amplitudes internal damping of granules predominates and provides linear damping, rather than the direct amplitude dependence which occurs at high amplitudes, due to the friction at contacts.

In the analyses of the several parameters involved in equation (4.4), it was observed that E_{diss}/cycle per unit volume is inversely proportional to the hydrostatic pressure to the power 1/3, independent of granule diameter, proportional to the cube of the amplitude and inversely proportional to the friction coefficient, as shown below

$$E_{diss}/\text{cycle} \propto \frac{x^3}{\sigma_{hyd}^{1/3}\mu}$$

The theoretical analysis discussed above shows that partial slip at contacts provides damping directly proportional to amplitude, which is equivalent to an increase of 10 dB per decade increase in strain. However, the irregular shape of grains allows gross slip to take place at some of the contacts so that the resultant damping variation with strain is expected to be less than that caused by partial slip alone.

4.5.4 The friction coefficient of brittle materials

The mechanism of friction in metals is characterised by plastic deformations of the asperities when two surfaces are brought together, cold welded junctions are formed at the contact points, and the frictional resistance represents the summation of forces required to shear the junctions (or close to the junctions).

Rocks, however, are characterised by their brittle nature, i.e., they are fragile materials in which fracture occurs soon after the elastic limit, and therefore do not exhibit any plastic deformation. If the surfaces of two brittle materials are brought into contact and caused to slip relative to each other, asperities are thought to fracture at their base, where bending moments are higher. Byerlee[37] analysed theoretically this situation assuming the "frictional" energy loss is entirely due to the work required to fracture the triangular shaped asperities at their base by tangential forces applied at their top. This model predicts friction coefficients of the order of 0.4 - 0.5. Experiments carried out by Byerlee[37] agree very closely with such prediction, but for very few oscillations, after which measured values drop to about 0.1 - 0.2. This is thought to be due to residues of fractures being formed between the surfaces.

4.6 Conclusions

The experimental work on damping of granular materials, particularly sand, described in this chapter, shows that granular materials exhibit a double damping characteristic according to the strain level. At small amplitudes loss factors were found to be independent of amplitude and similar to those of rocks, suggesting that damping of sand at this strain range is entirely concentrated at the interior of grains and evidence has also been presented supporting this conclusion, based on reports available in the literature where similar conclusions were reached. At larger strains, energy dissipation by friction at contacts between grains predominates, showing amplitude dependence characteristics attributed to a combination of partial and gross slips. Amplitude of vibration is therefore an important parameter related to internal damping of granular materials. Hydrostatic pressure has less influence since damping is proportional to the cube root of pressure, according to the theory, while the present experiments suggest it is proportional to the power 1/6.

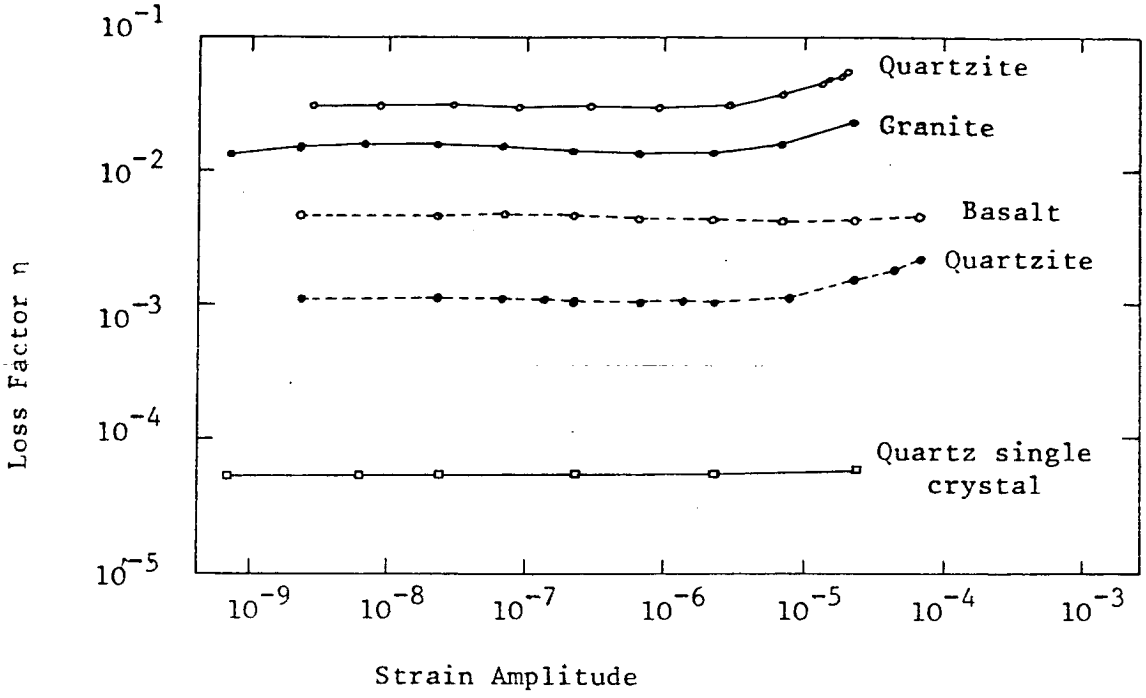

Fig 4.1 Loss Factor of Some Rock Samples, measured in long. oscillations at 90 kHz

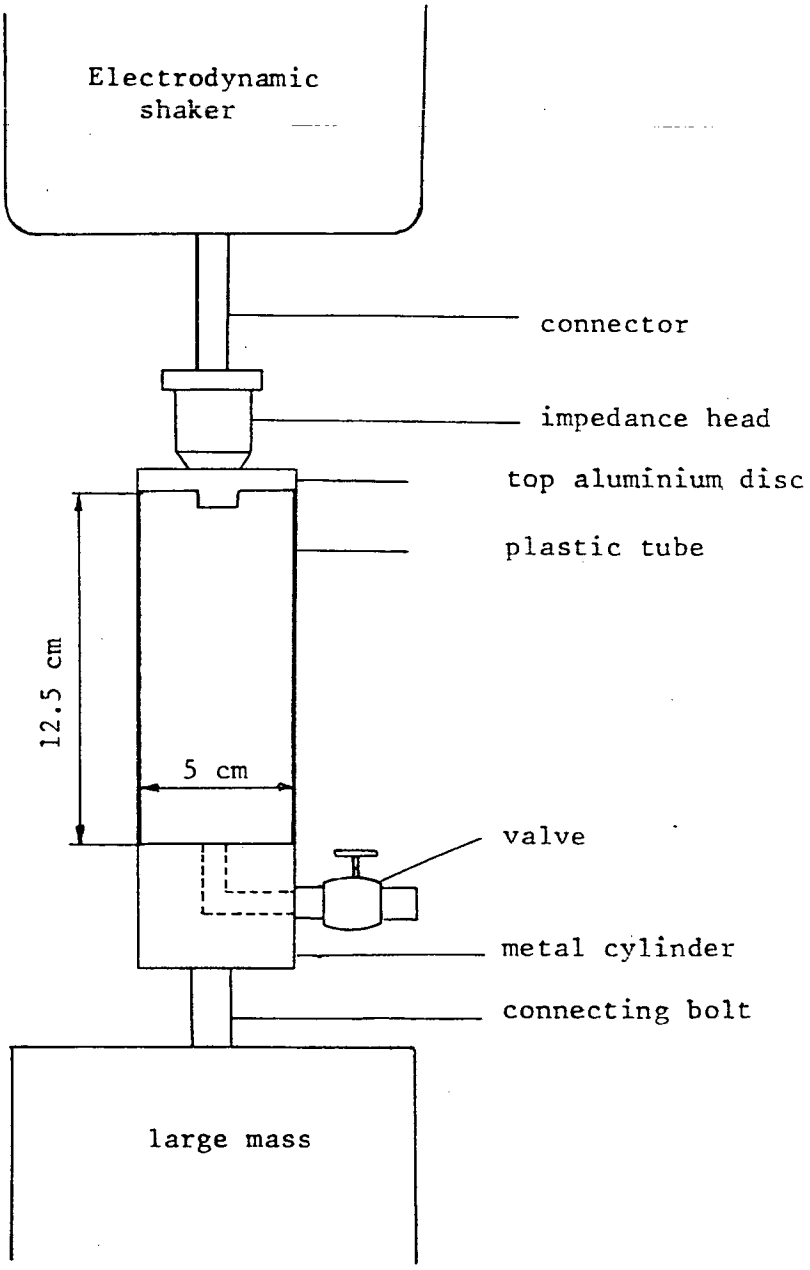

Fig 4.2 Experiment Set Up

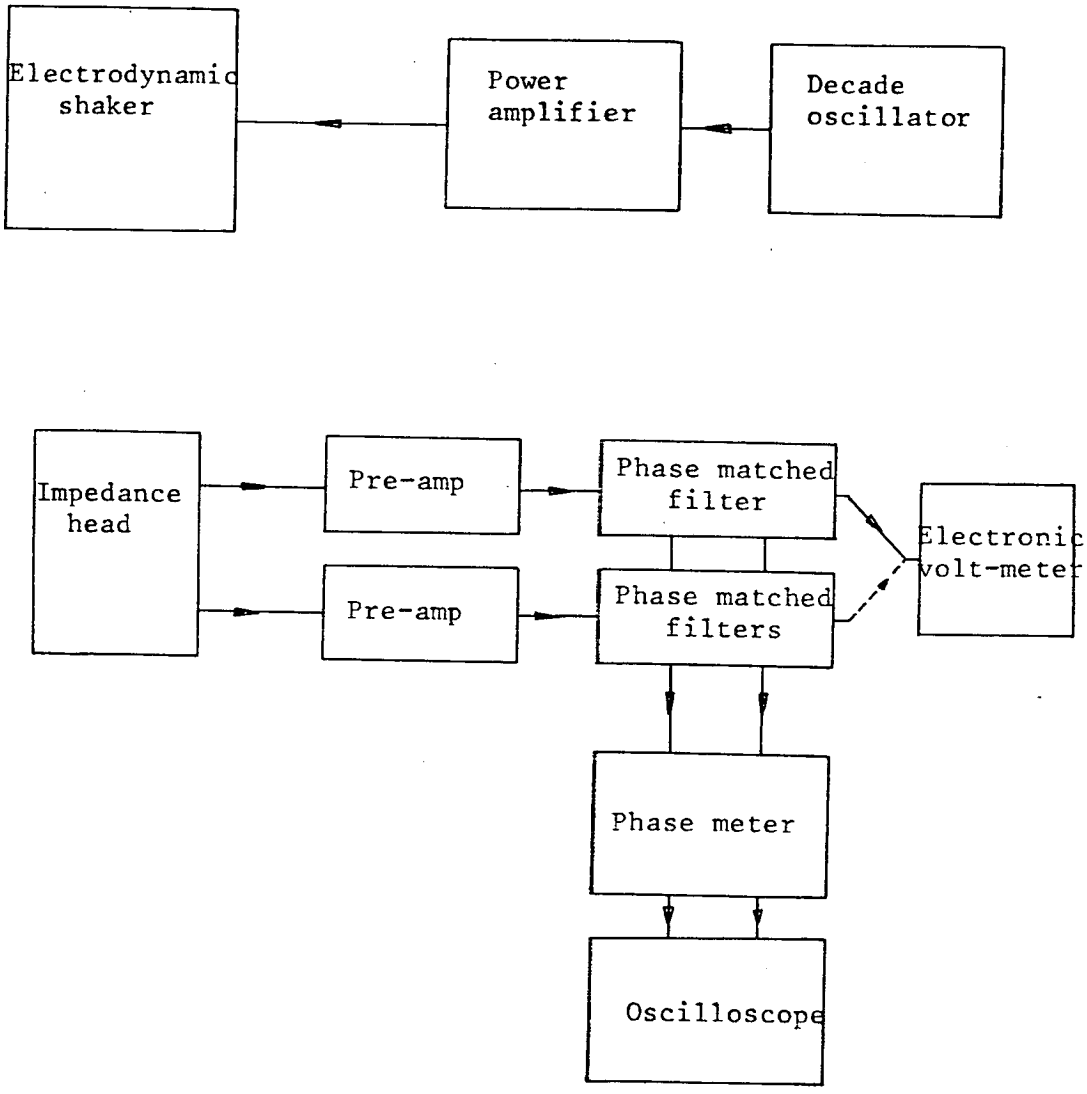

Figure 4.3 Equipment Lay-out

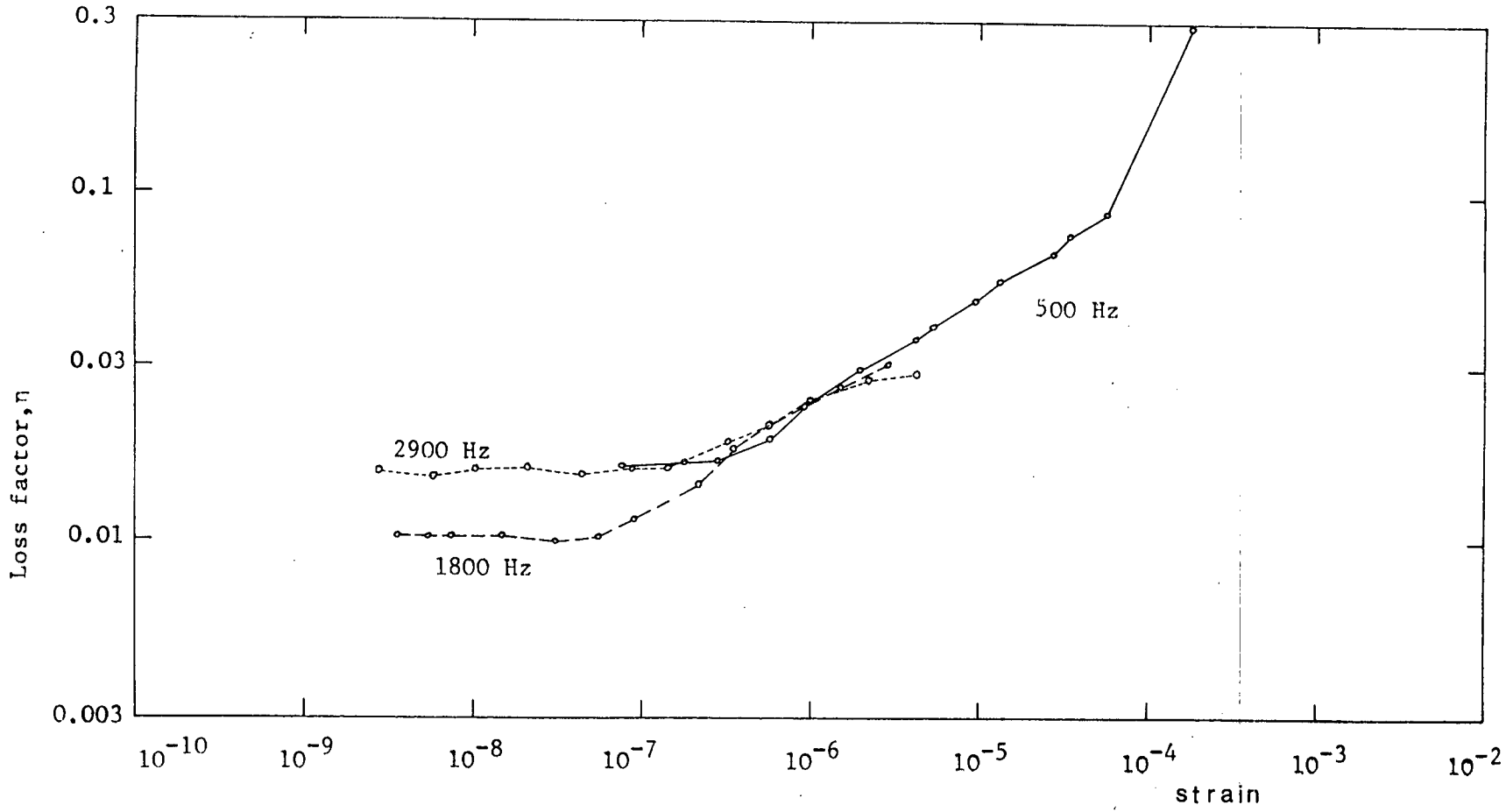

Fug 4.4 Internal loss factor of dry sand (grown type: 0.6mm to 0.18mm)
Hydrostatic pressure: 1.3×10^4 N/m^2

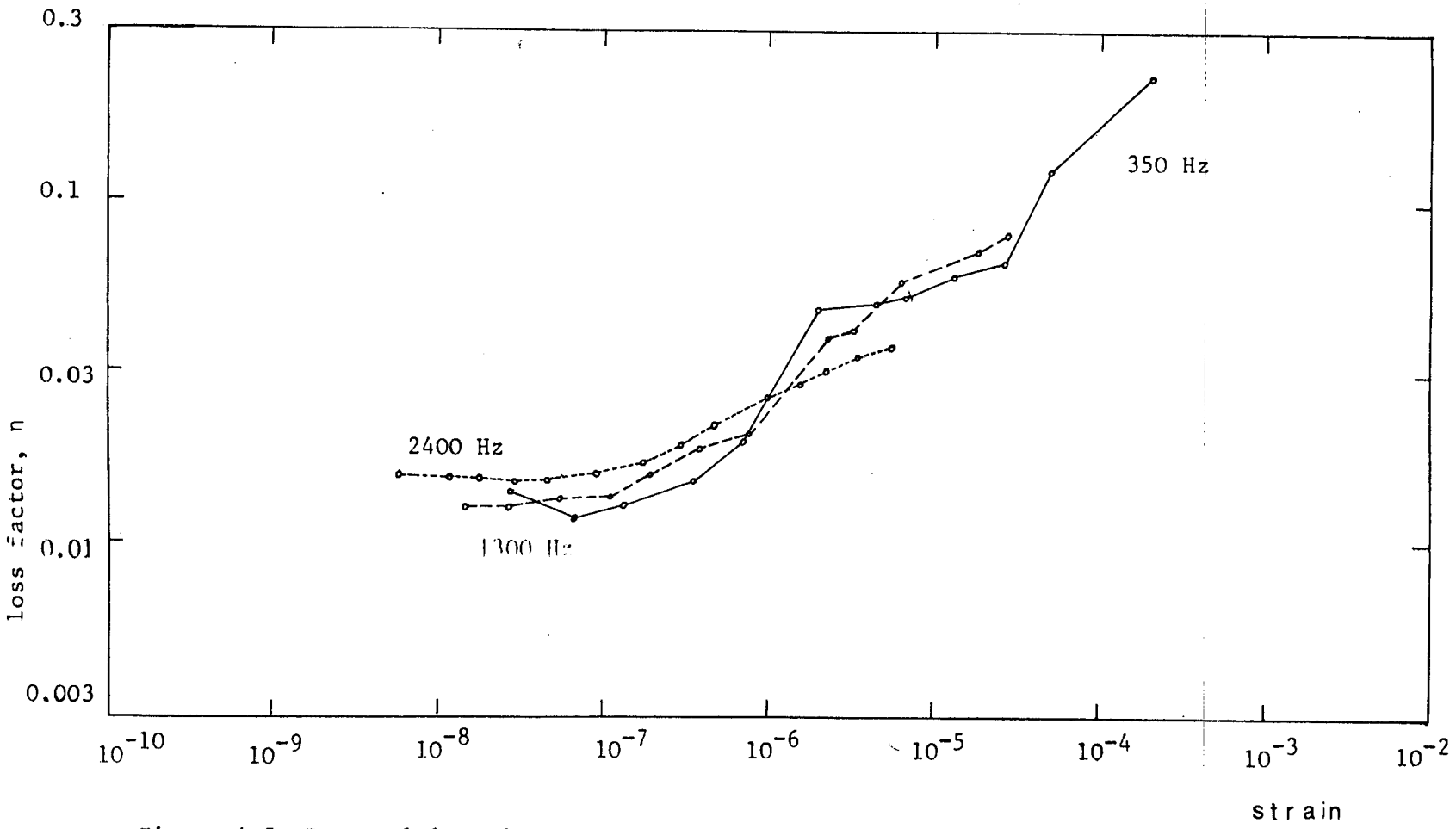

Figure 4.5 Internal loss factor of dry sand (0.6mm to 1.18mm) Hydrostatic pressure: 3.0×10^3 μ/m^2

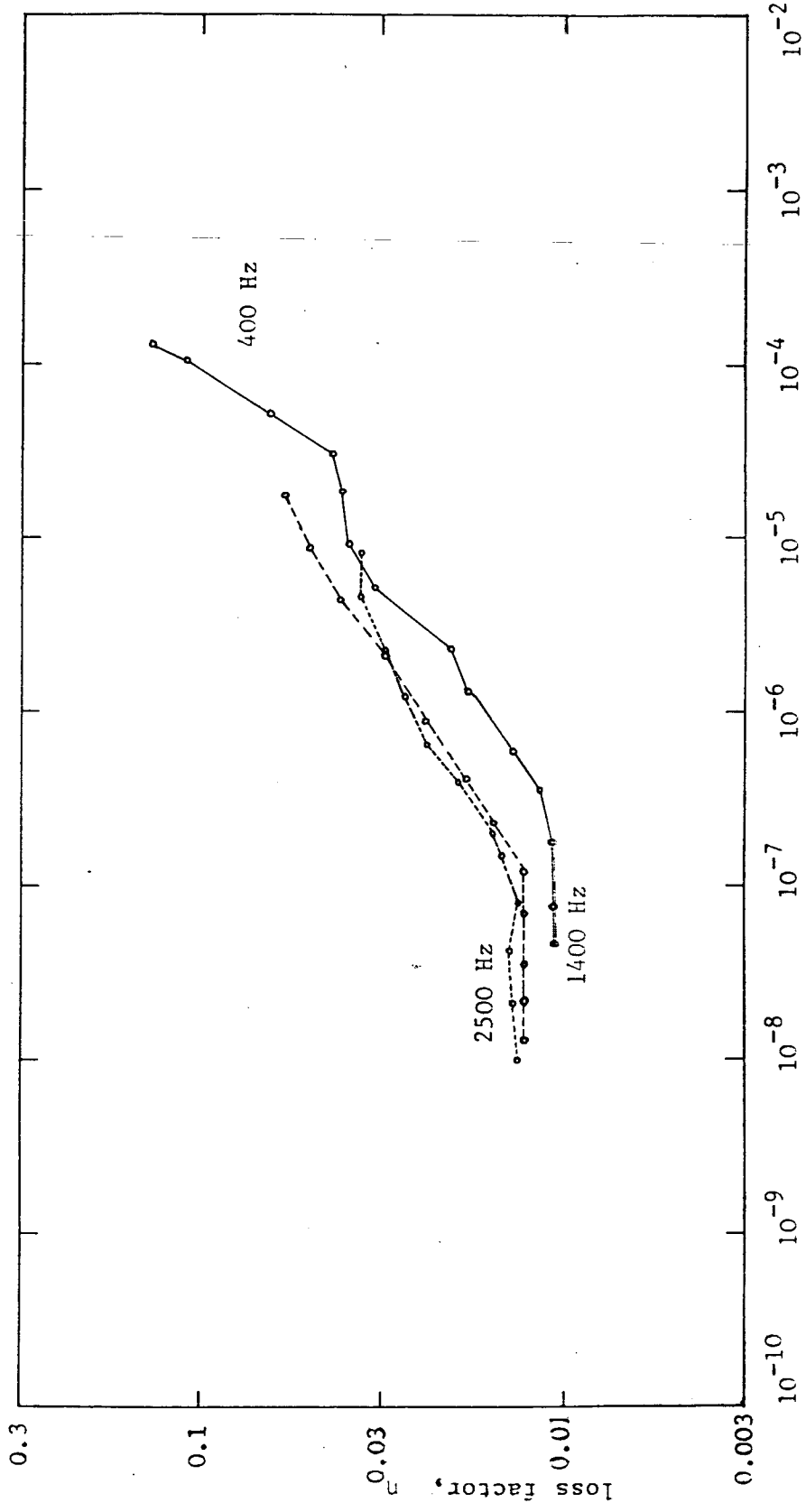

Fig 4.6 Internal loss factor of dry sand (0.6mm to 1.18mm) Hydrostatic pressure: 6.5×10^3 N/m^2

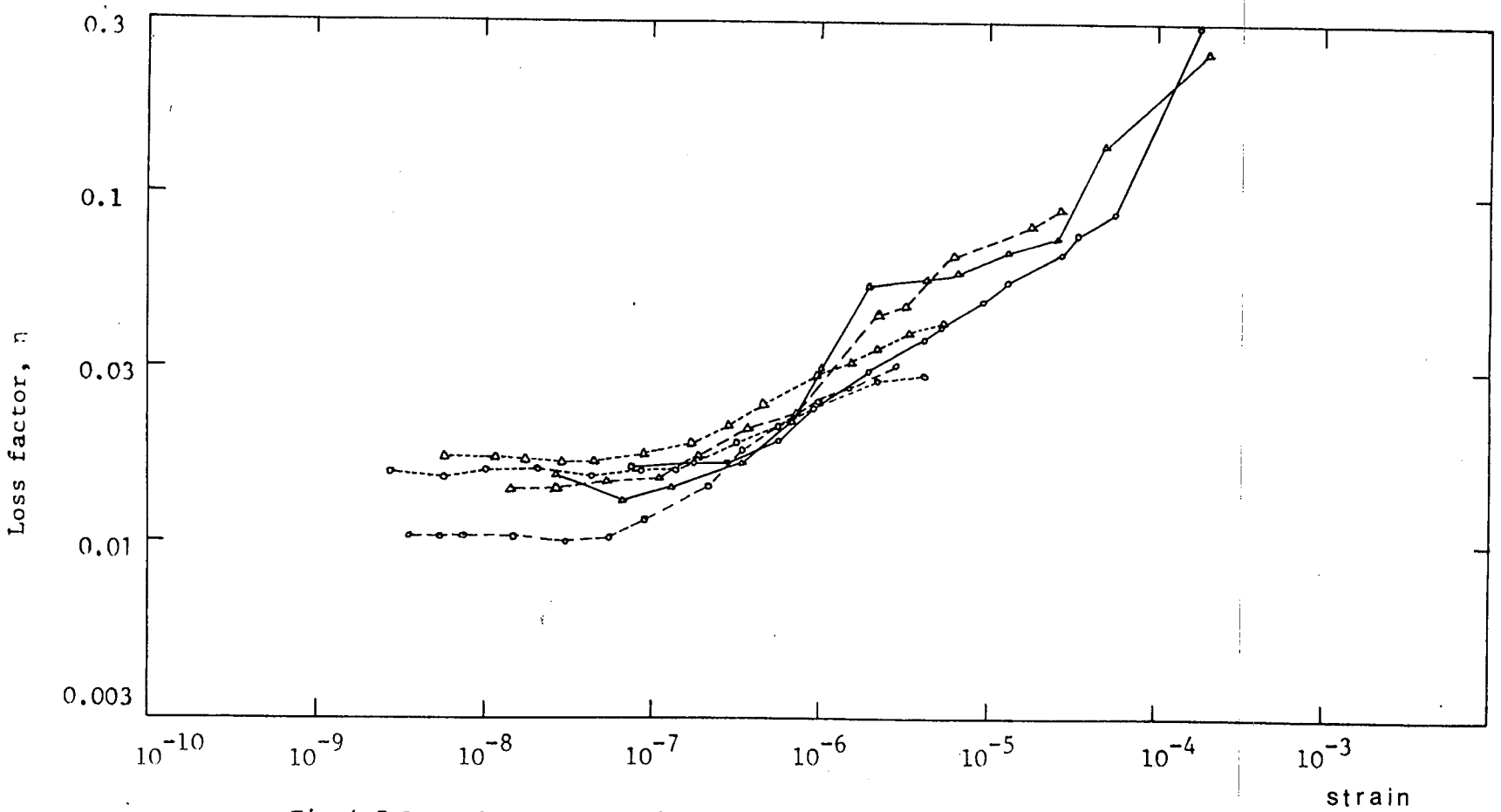

Fig 4.7 Loss factor comparison of dry sand (0.6mm to 1.18mm) subjected to two different hydrostatic pressures

o——o 1.3×10^4 N/m^2

Δ——Δ 3.0×10^3 N/m^2

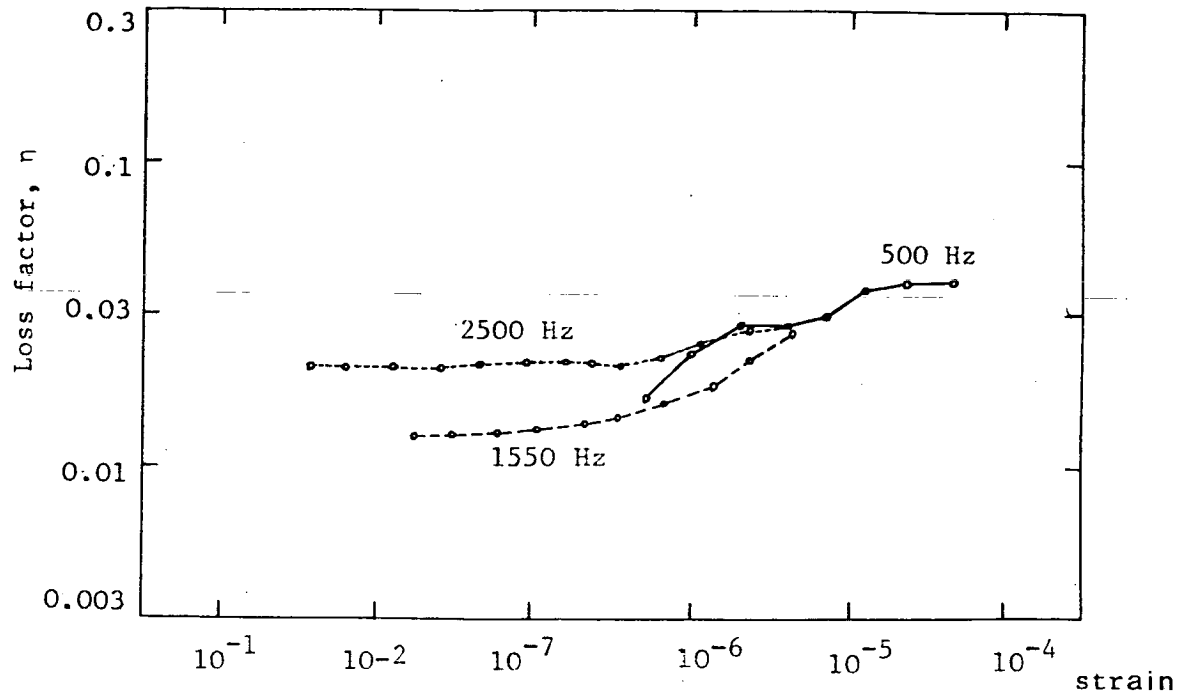

Fig 4.8 Internal loss factor of dry sand (2.36mm to 4.75mm) Hydrostatic pressure: 1.3×10^4 N/m^2

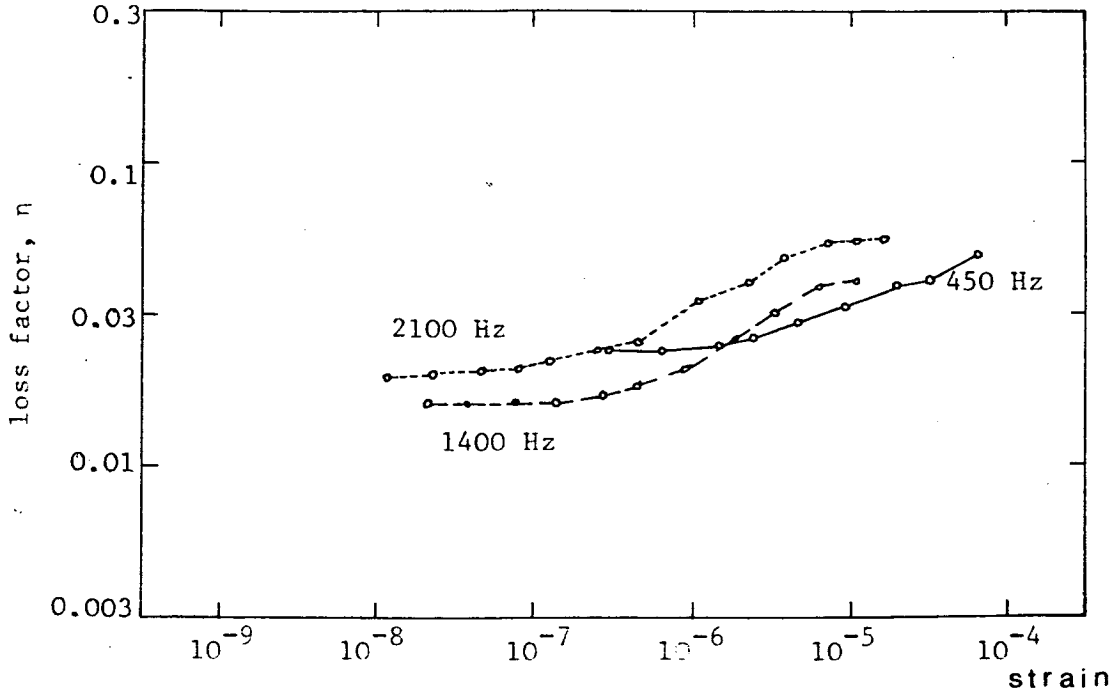

Fig 4.9 Internal loss factor of dry sand (2.86mm to 4.75mm) Hydrostatic pressure: 6.5×10^3 N/m^2

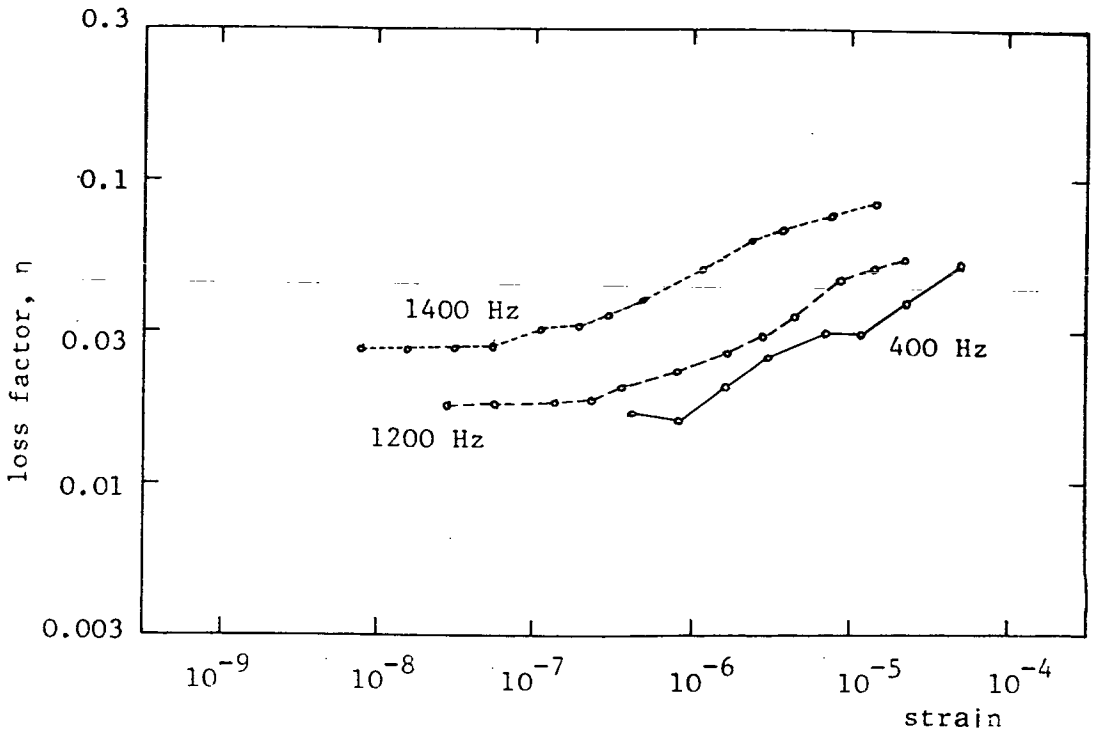

Figure 4.10 Internal loss factor of dry sand (2.86mm to 4.75mm) Hydrostatic pressure: 3×10^3 N/m^2

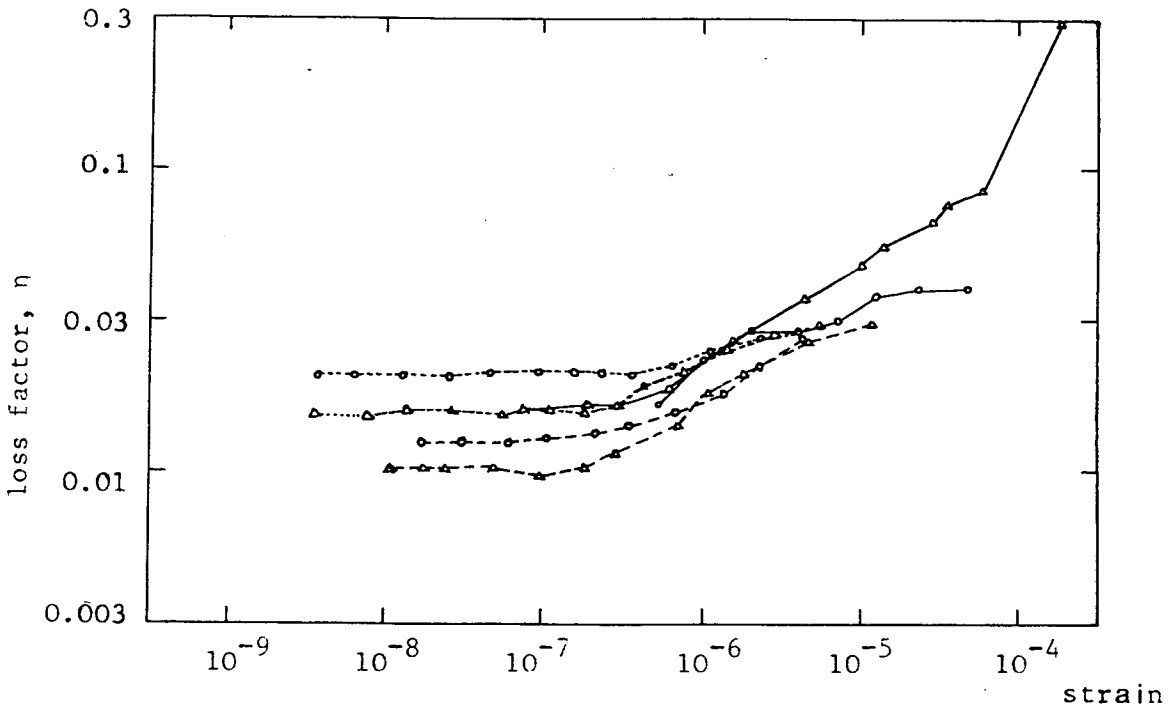

Figure 4.11 Loss factor comparison for different (dry) sand grain sizes. Hydrostatic pressures: 6.5×10^3 N/m^2

2.36mm to 4.75mm

0.6mm to 1.18mm

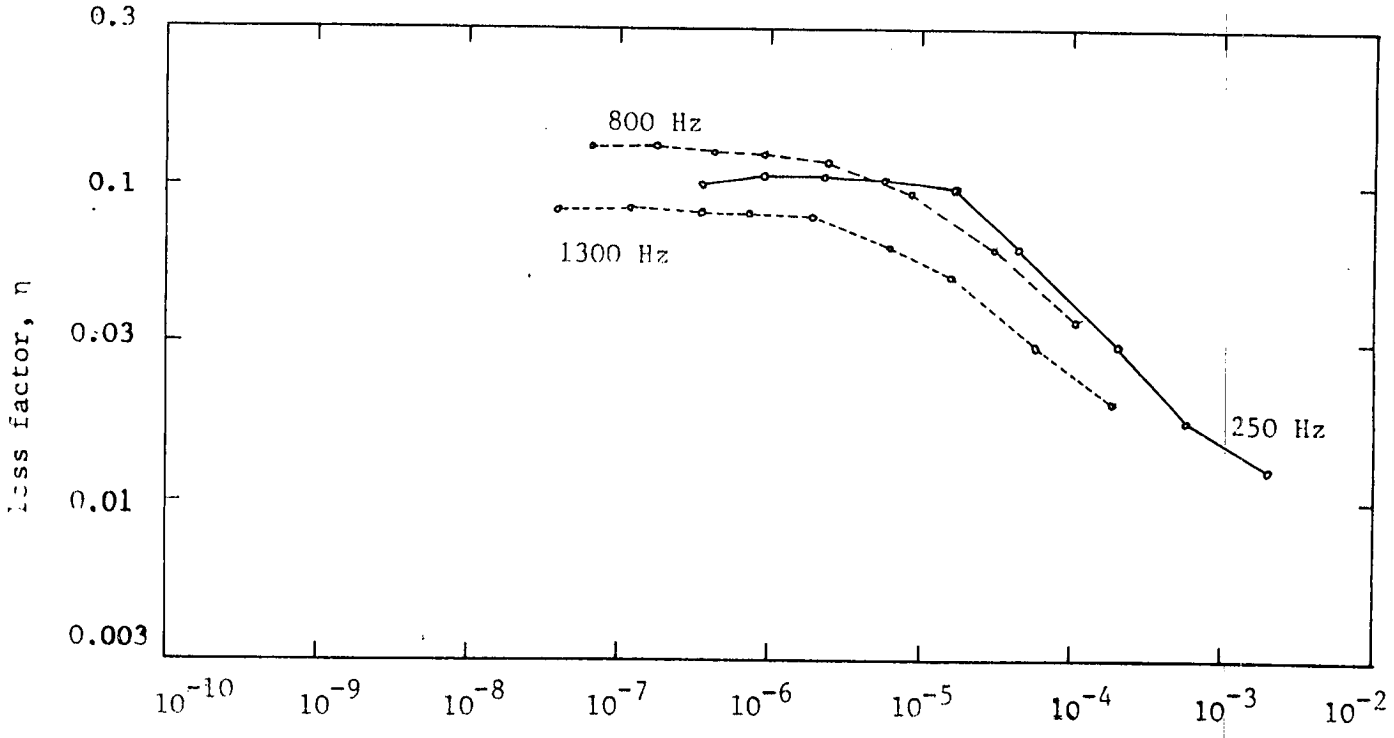

Figure 4.12: Internal loss factor of lead shot (1.5mm to 20mm), Hydrostatic pressure: 3.0×10^3 N/m^2

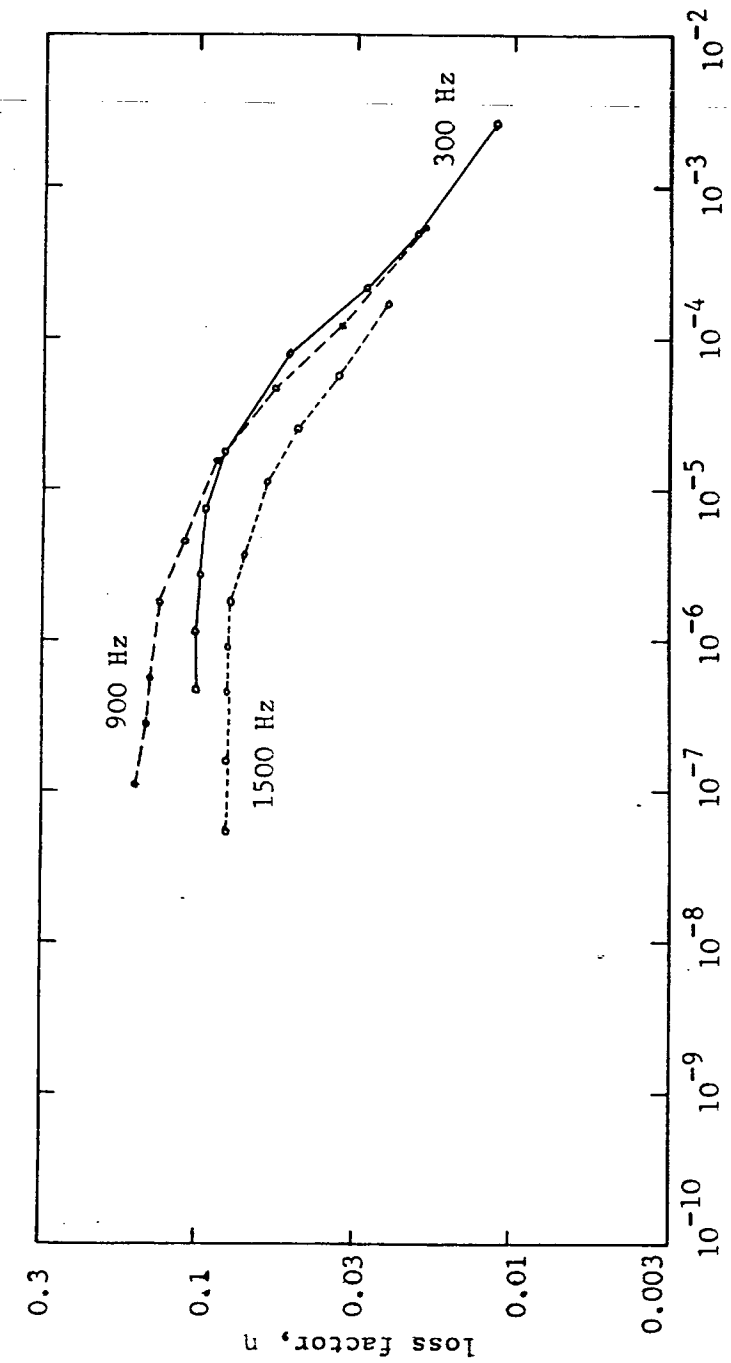

Figure 4.13: Internal loss factor of lead shot (1.5mm to 2.0mm)
Hydrostatic pressure: 6.5×10^3 N/m^2

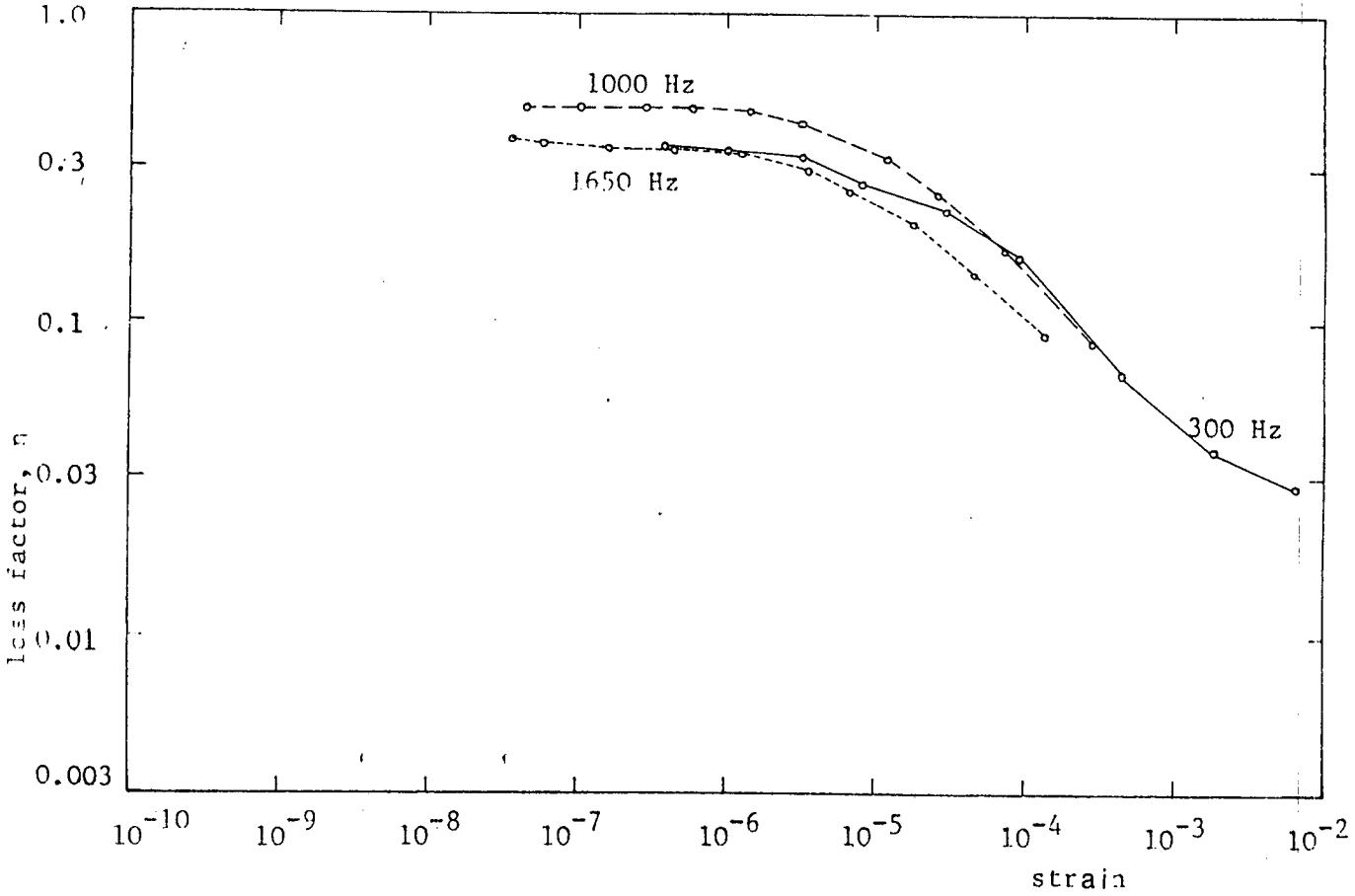

Figure 4.14 Internal loss factor - lead shot (1.5mm to 2.0mm)

Hydrostatic pressure: 1.3×10^4 N/m^2

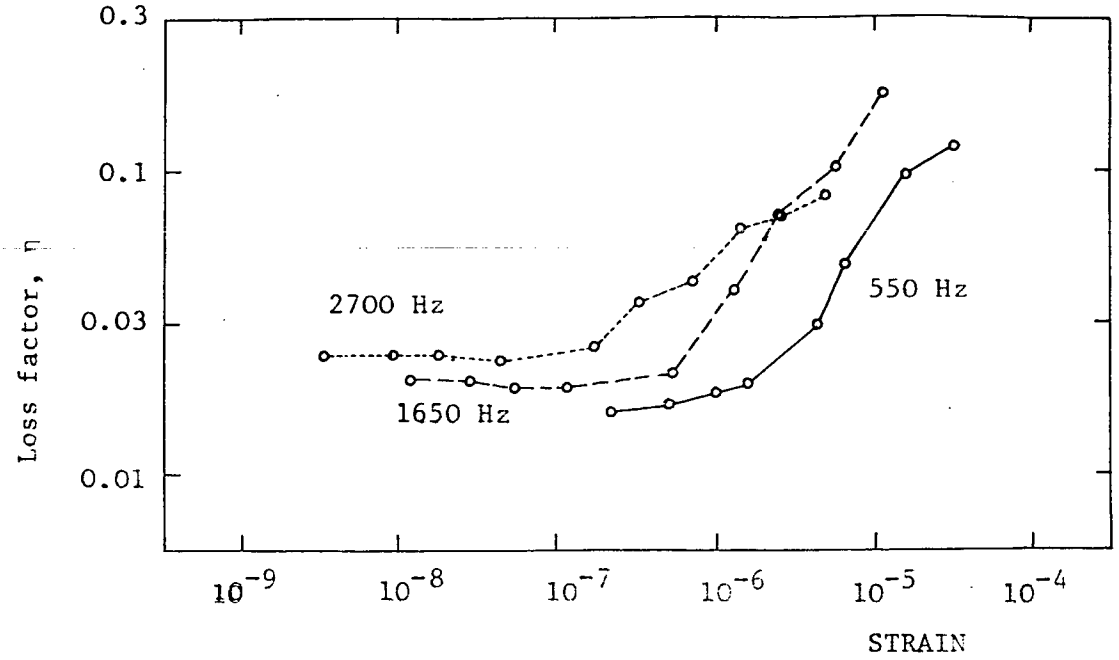

Fig 4.15 Loss factors of glass spheres (Ø1mm to Ø2mm)
Hydrostatic pressure: 1.3×10^4 N/m^2

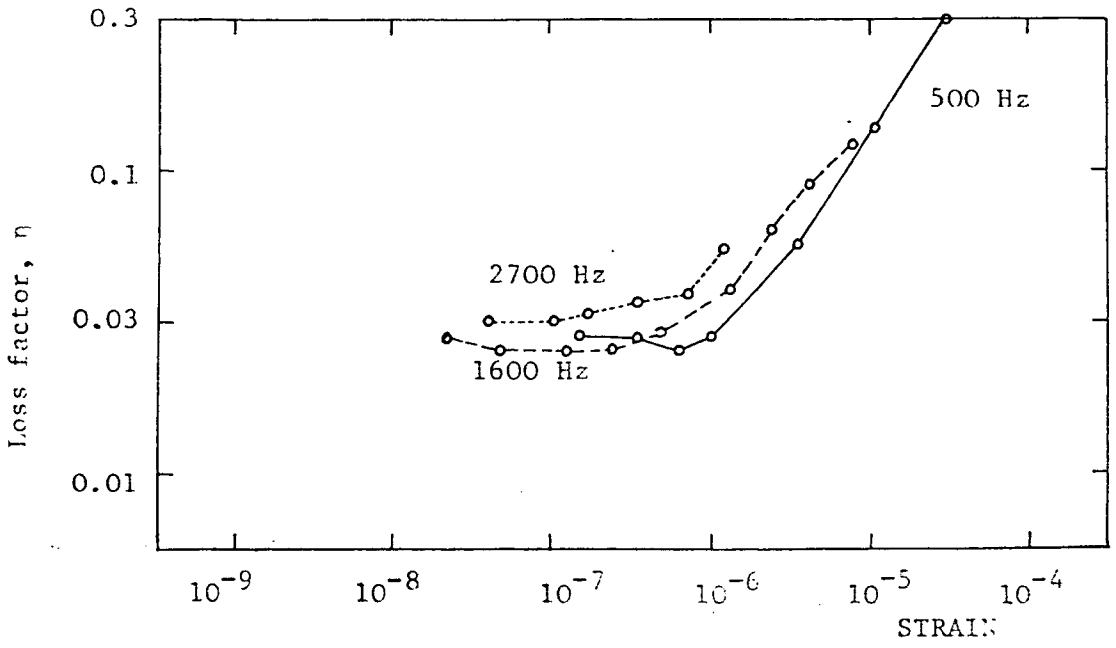

Fig 4.16 Loss factors of glass spheres (Ø 1mm to Ø 2mm)
Hydrostatic pressure 6×10^3 N/m^2

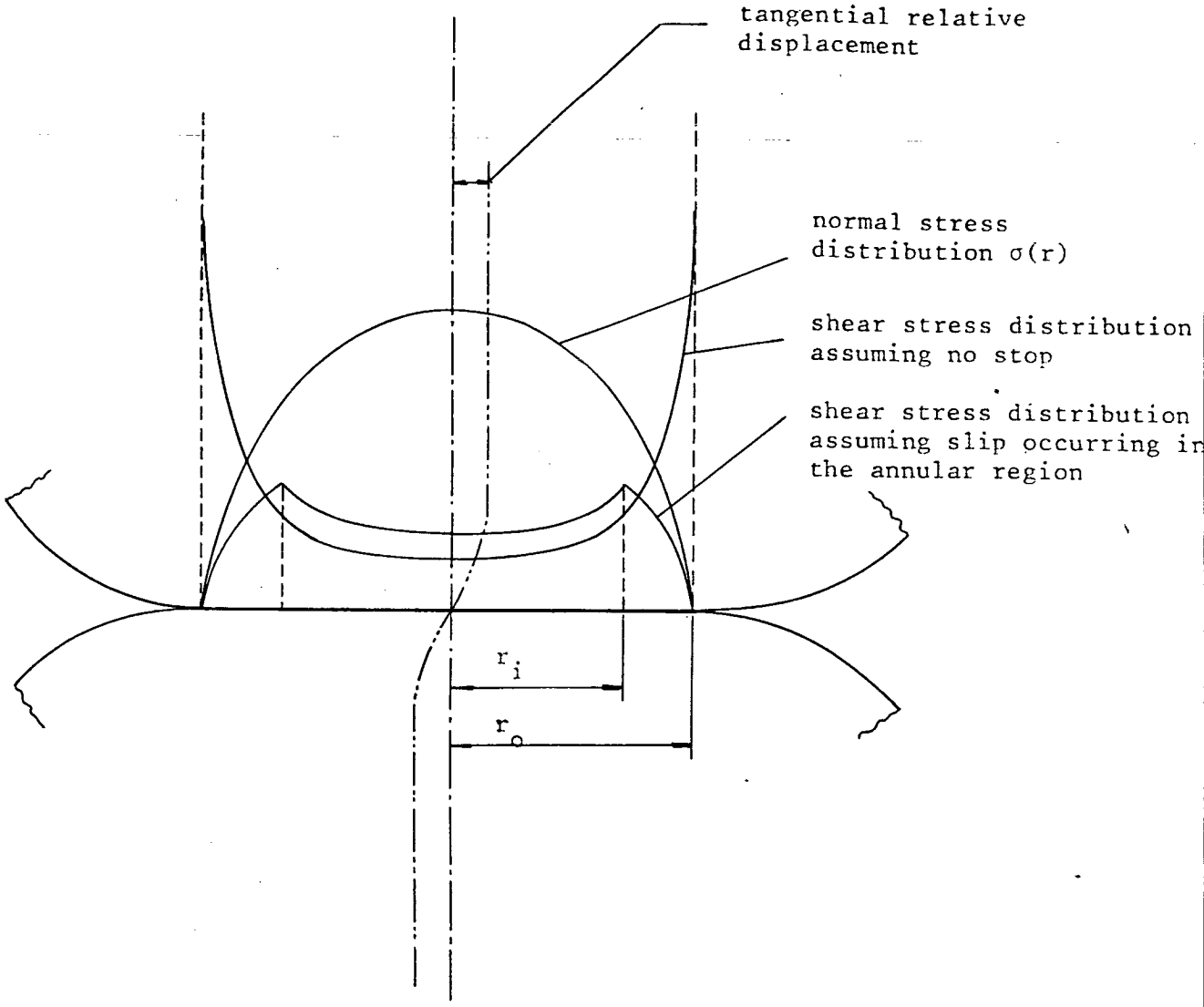

Figure 4.17 Normal and shear stresses distributions over the contact area

CHAPTER 5

SPEED OF ELASTIC WAVES IN GRANULAR MATERIALS

5.1 Introduction

The experimental work on damping of hollow beams filled with sand, as described in Chapter 2, showed that levels of damping were a maximum in distinct frequency regions due to resonances in the granular material. It is interesting to mention that for our configuration the region where the first maximum occurs is around 1000 Hz. This is of great practical importance, since most of the noise energy radiated from machine structures lies in the 500 Hz to 3000 Hz range, so that there is a need for additional structural damping in this range, and a need to know exactly how to tailor the geometry to provide maximum damping at the relevant frequency.

Although the maximised damping peak has a broad shape, covering a wide frequency range, it is desirable to "tune" it to frequencies of interest for any particular application. To do this an accurate knowledge of wave speed values in granular materials is essential.

The available literature is rather imprecise as to the exact speed of waves in sand; quoted values vary between 55 m/s and 150 m/s. Such variation is unacceptable for an accurate prediction of maximum damping frequencies. Also, the influence of parameters such as amplitude of vibration and frequency upon wave speed are very much unknown.

This chapter describes experimental work, carried out to determine an accurate value of wave speed and how longitudinal and shear wave speeds are influenced by amplitude of vibration, frequency, grain size and pressure. A theoretical analysis of wave speeds in a pack of spheres is presented and comparison made with behaviour found experimentally.

5.2 A Review of Measurement Methods and Some Results

5.2.1 The vibrating table method

Some of the earliest work done to measure the speeds of waves in granular materials has been reported by Iida[50]. Specimens to be tested were formed into columns supported by a cellophane tube. The column was placed upright on a vibrating table which could produce either longitudinal or torsional modes of vibration into the specimen. The wave velocity was calculated from resonant frequencies and their corresponding wavelength along the column. A displacement transducer was used at the top of the column to detect the resonant frequencies.

Iida investigated the effect of confining pressures on the wave speeds by using columns of different heights, i.e., the pressure is provided by gravitational forces. This is a limitation to this work; if a partial vacuum had been formed inside the column the pressure range could have been extended and also a more uniform pressure distribution formed throughout the column length.

The experiments were nevertheless useful and accurate control upon amplitude of vibration, frequency and confining pressure - the main parameters to be tested - were achieved although the results are limited to low pressure. The results showed wave speeds to vary only slightly with grain size and wave velocities to be proportional to the sixth root of the confining pressure.

Speeds of about 100 m/s were measured for longitudinal waves and 65 m/s for torsional waves at frequencies around 100 Hz. There is no indication of the amplitude of vibration at which measurements were made.

5.2.2 The pulse propagation method

The second method consists of determining the speed by timing a pulse travelling through a known distance in the specimen. Usually a column of the specimen is used with displacement transducers placed at both ends. Since impact times are of the order of one millisecond, the time taken by the pulse to propagate from one end to the other must be much higher to avoid inaccuracies in time lapse readings. For this reason, column lengths of not less than one metre are recommended. If hydrostatic pressures

are low, grains can easily slide relative to each other and the pulse energy is then quickly dissipated, giving another source of error. The method is limited to high confining pressures and there is no control of amplitude and frequency.

5.2.3 The cross correlation method

The cross correlation method uses an experimental set up similar to the pulse propagation method, except that the excitation is continuous rather than impulsive. By cross correlating the response signals from both ends, a peak is obtained at the time taken by waves to propagate through the column. The peak is sharper if a broad frequency band excitation is used. Discrete frequencies excitation is not possible because the cross correlation function would be of sinusoidal type without showing any distinct peak. Although the method permits control of amplitude and, to some extent, pressure, measurements are only possible in frequency bands, which could also lead to erroneous results if the medium is of a dispersive nature.

5.2.4 The resonant column method

The resonant column method overcomes limitations discussed in the two previous methods. It consists basically of using a column made of thin plastic tube containing the specimen to be tested; vibrations are excited at the top by a shaker while the lower end is fixed to a large mass which assures zero displacement (a node) for all frequencies. Speed is determined from resonant frequencies and their corresponding wavelength distributed along the column. The method is a variation of the vibrating table method, with the advantage of not requiring a vibrating system applied to a table. Accurate amplitude, frequency and pressure control with this method are possible.

5.2.5 Some experimental results

5.2.5.1 Pressure effects

Hardin and Richart[51] carried out quite an extensive series of experiments on wave velocities of sand using the resonant column method. They used a column of 0.275 m high and 3.8 cm in diameter, and displacements during measurements were always less than 2.5×10^{-6} m, which in terms of strain is of the order of 10^{-5}.

For all the sands tested, shear and longitudinal wave velocities varied with the 1/4 power of the confining pressure (pressure range tested: 10^4 N/m^2 to 3×10^5 N/m^2). Several authors report velocity dependence upon pressure varying between 1/3 and 1/6 power, which depends primarily upon the state of consolidation of the specimen.

Duffy and Mindlin[49] describe experimental work in which compressive wave velocities were measured in bars of high tolerance spheres ($\frac{1}{8}$" in diameter, $\pm 10^{-5}$ in. and $\pm 5 \times 10^{-5}$ in. tolerances). They noticed that the power of confining pressure with which the velocity varied was higher for the lower tolerance spheres and also decreased as the confining pressure was increased. Their initial variation at the lower confining pressure was approximately the 1/4 power; their theoretical analysis for a bar of perfect spheres predicted a variation with the 1/3 power. It is therefore quite significant that only a small departure from perfect spheres causes a large departure from theoretical predictions. This means that the wave speed is very sensitive to the number of contacts and possibly to geometrical factors.

5.2.5.2 Grain size effect

Grain size was found by Hardin and Richart[51] to have no effect on the speed of waves in sands. (A similar independence of grain size was found for internal damping measurements - Section 4.3.) Consolidation of the granular material, however, has some effect. Wave speed increases with the density of consolidation, possibly because the number of contacts per unit volume is higher, presenting a more rigid aspect to the propagation of elastic waves. The prediction of the exact effect of consolidation is difficult, given the irregular shape of sand grains. However, in practical applications, consolidation is of secondary importance and has been neglected in the current analysis.

5.2.5.3 Water content effect

The effect of water or any other liquid is to reduce the wave speed because of the added mass which moves with grains. Most experiments on this effect have been carried out at low frequencies and the exact effects of moisture content at higher frequencies is still unknown. At high frequencies, fluid flow through interstices may alter the mechanisms of propagation and dissipation of waves.

Small amounts of water in the granular material can reduce the stiffness of a chain of contacts through which the stress wave travels. The water acts as a lubricant at the contacts and as a result, reductions of up to 15% in the speed has been observed[50], for small percentages of water content.

5.2.5.4 The propagation mechanism of pressure perturbations in granular materials

A packed material of irregularly shaped grains present chains of stress-linked grains which actually transmit pressure perturbations through the material. Elastic moduli of compacted media are therefore usually treated in terms of grain-grain contact properties. In free grained materials, as studied here, slips between grains can occur which have great influence upon speed of waves. Some adjacent grains may have little lateral linkage and, consequently, those grains do not form part of the structure that carries stresses and determines elastic moduli.

Compaction and externally applied hydrostatic pressures have the effect of altering elastic behaviour of contacts to that of a continuously welded material with flat cracks (as is the structure of rocks). This explains the increase in wave speed with pressure. The presence of moisture, even in minute quantities, introduces weaknesses at contacts by preventing "welded contacts" being formed, and consequently wave speed is reduced.

At high pressures (above a few bars) experiments[38] suggest that Hertzian contact theory is the best way to describe the changes in velocity with pressure. Below a certain pressure, contacts loosen and the stresses associated with waves propagating through the material may be higher than the hydrostatic pressure, thus having direct effect upon the formation of the chain of grains responsible for stress transmission.

5.3 Experimental Studies of Speed of Waves in Granular Materials

The discussion presented in the preceding sections of this chapter shows that the effects of pressure on wave speed are reasonably understood, but some doubts still remain about the influence of other parameters, particularly the amplitude of waves. Granular materials when used for filling cavities of machine components for structural damping purposes, are subjected to structural vibrations which can vary by several orders of magnitude throughout the spectrum. This section describes a series of experiments aimed towards an understanding of amplitude effects upon the speed of waves.

5.3.1 Experiment description

The method employed has been the resonant column method as it permits accurate control upon the variables of interest in this study, i.e., amplitude of vibration, frequency and external pressure. Attempts to use pulse propgation and cross correlation methods failed because of their inherent inefficiency in controlling frequency and amplitude.

The experiment set-up for measurements of longitudinal waves was the same as that used for damping measurements and was described in Chapter 4 and shown in figure 4.2. Vibrations were excited at resonant frequencies of the column and speeds determined from their corresponding wavelengths. Measurements were made at the three first resonances which were in the frequency range 300 Hz to 2500 Hz. Resonances were detected by constant observation of the phase angle between force and response and by monitoring the response level.

Shear waves were measured by a similar method after slight modifications to the test rig so that torsional vibrations could be excited. Two shakers connected in opposition to the top disc produced the driving torque (figure 5.1). In order to transmit shear stresses from disc to column, sand grains were glued to the lower face of the disc in contact with the material, thus providing an "indentation" effect capable of transmitting shear forces.

Wavelengths were taken as four times the length of the column for the first mode, 4/3 of the length for the second mode and 4/5 for the third.

5.3.2 Equipment lay-out

Wave speeds were measured on the same equipment as had been used for the damping measurements (figure 5.2). The excitation of torsional waves, without inducing other types of vibration, required a careful balance of both driving forces so that bending deflections would not be induced. A two-channel power amplifier with independent gain controls was used. Two identical force transducers were placed between shaker and disc for monitoring the applied forces. Every precaution was also taken to ensure that the connectors had about the same masses. An accelerometer was attached to each side of the disc for detecting resonances, but response readings were only taken from one of them.

5.3.3 Results of longitudinal wave speed measurements in dry sands

The parameter used to represent amplitude was the maximum strain. This was defined as the ratio between maximum displacement (measured at the top of the column) to one quarter of the wavelength. Results for dry sand (grain diameters 0.6 mm to 1.18 mm) are shown in figures 5.3, 5.4 and 5.5. The main feature of the results is the variation of wave speed with strain, i.e., independent of amplitude at low strains ($< 10^{-6}$). Wave speed gradually drops to lower values as amplitude increases. The speed of longitudinal waves varies from about 50 m/s for very large strains to about 300 m/s at small amplitudes,depending upon the pressure. Comparison with published results suggests disagreement, as values of 50 m/s to 150 m/s are normally quoted in the literature. However, an analysis of the tests which were carried out reveals that most of the results available were obtained from experiments using resonant columns. These vibrate at very low frequencies (large displacements) and very often without external pressure applied. The experiment was repeated simulating these extreme conditions, and as shown in figure 5.6, speed can indeed be as low as 50 m/s at very large strains.

Hardin and Richart's work on wave speeds in sand resulted in values of 250 m/s to 300 m/s at strains of 10^{-5} and pressures of 10^4 N/m^2. These results are in agreement with the present results. It is concluded that amplitude effects are directly related to stresses produced in the material by the propagation of waves. There must, however, be a limit where wave stresses become greater than the hydrostatic pressure, causing failure of the chain grain-grain contacts responsible for the transmission of stresses.

The frequency variation in the tests (ranging from 300 Hz to 2500 Hz) showed no significant alteration in the speed, suggesting that stress propagation mechanisms are not frequency dependent, confirming the hypothesis of pure friction at contacts.

Figures 5.7, 5.8 and 5.9 show wave speed results for sand of larger grain sizes (2.36 mm to 4.75 mm). Conclusions drawn above are still generally valid. Hardin and Richart's results show that grain size does not alter the speed of waves, but the void ratio (defined as the volume proportion of empty space to grain volume) has some effect upon the speed; void ratios of sands are altered by the degree of compaction. Compacting sand increases the number of contacting grains per unit volume, shortening the path through which stresses propagate. Speed variation with grain size is attributed to possible differences in void ratios.

Pressure influence in the low strain region were observed in this experiment to follow 1/4.6 power law for the 0.6 mm to 1.18 mm sand and 1/7 power law for the 2.36 mm to 4.75 mm sand, in contrast to 1/3 power suggested by Duffy and Mindlin's theoretical predictions for a pack of perfect spheres.

5.3.4 Results for longitudinal waves in glass spheres

Sand has irregular grains which renders its transmission and damping properties sensitive to compaction and external pressure. In this experiment tiny glass spheres 1.5 mm to 2mm in diameter were used to study the speed of waves in a medium composed of spherical granules. The glass spheres used are normally used for plate mode shape visualisation and as such were not manufactured to a high degree of tolerance. It is assumed that the material properties (modulus of elasticity, Poisson's ratio and density) of the glass spheres do not vary from those of rock, any deviation in wave speed may be attributed to grain shape and particularly to their curvature at contacts, neglecting possible differences due to compaction.

Figures 5.10 and 5.11 show results for glass spheres in which longitudinal wave speeds are observed to have almost identical values to those of sand. Thus, despite the spherical shape of granules, the wave speed is still about the same as for an irregularly shaped granular medium, so that, as pointed out by Duffy and Mindlin[49], a small tolerance in the

manufacture of the spheres is enough to significantly reduce the wave speed. It is therefore concluded that the looseness of grains is the important parameter influencing wave speed, rather than their precise spherical shape.

5.3.5 Results for longitudinal waves in lead shot

Lead shot was used in this series of experiments to study the effect of density (lead shot is about four times heavier than sand). It is difficult to predict the precise influence of density but as a first approximation it would be expected that wave speed will vary with density to the power $-\frac{1}{2}$ because it is proportional to density and to the elasticity of the granular material as follows:

$$c = \sqrt{\frac{E_{gm}}{\rho}}$$

Thus lead shot should present wave speeds about half as fast as those in sand. The experimental results showed a dependence slightly smaller (figures 5.12, 5.13 and 5.14) which is attributed to the low elasticity of lead compared to that of rock.

5.3.6 Results for torsional waves in sand

Shear wave speed in sand (grain diameters 0.6 mm to 1.18 mm) was measured by the resonant column method as described in 5.3.1 and results are shown in figures 5.15, 5.16 and 5.17. Shear wave speeds are noticed to vary with strain at large amplitudes in a similar manner to longitudinal waves. Torsional wave speeds showed a smaller variation with pressure than was observed for longitudinal waves but this could be due to measurement accuracies. A possible source of error is the long time required by the granular material to accommodate a new mode shape when the excitation frequency is changed.

Torsional wave speed values are of about 160 m/s, i.e., about 60% of longitudinal speeds. This is an interesting conclusion because the relationship between shear and longitudinal waves in granular materials is identical to the one observed in solids.

5.3.7 A summary of amplitude influence upon wave velocity

As described earlier in this chapter, conditions at contacts and their number per unit volume are governed by compaction and external pressure. This dictates the elasticity of the grain-to-grain chain which transmits stress waves through the material. It is also concluded that pressure has great influence because it holds grains together avoiding collapse, due to the stresses induced by the waves themselves. Obviously, the chain strength can be reinforced by compaction because it increases the number of contacts per unit volume of the material.

Assuming force-deformation relations at contacts follow Hertzian contacts, an analysis of normal and tangential components at contacts show they are both inversely proportional to the hydrostatic pressure to the power 1/3, indicating a nonlinear relationship in which speeds are expected to increase with pressure. If hydrostatic pressure is kept constant, however, speeds would be expected to increase with amplitude because forces at contacts produced by the passage of waves have identical effects to those produced by external pressure. Experimental results presented in this section, however, show a different variation with strain. At large amplitudes, forces at contacts can be greater than those produced by the external pressure, causing failure of the rigid chain of contacts.

If one considers the fact that at small strains actual displacements may only be similar to the atomic dimensions, deformations at contacts are no longer expected to account for the elasticity of the granular material. Elastic deformations of the actual grains will then predominate, rendering the wave speed velocity independent of vibration amplitude at low strain levels.

5.3.8 The calculation of wave speed in granular materials

The propagation of waves in granular media as discussed in the preceding section occurs through several main paths of grain-grain contacts. The path framework is of a macroscale nature, determined by the grain size. Values of wave speed obtained from the experiments will represent an average constant speed through the material. It has been assumed that wave speed is independent of the direction of propagation and also of

position within the material, i.e., the material is considered isotropic. The elasticity can therefore be represented in complex form, related to the internal dissipation, as follows:

$$\bar{E} = E(1 + i\eta)$$

E is the Young's modulus and η the loss factor of the granular material. The speed of longitudinal waves is given by

$$c = (E/\rho)^{\frac{1}{2}}$$

where ρ is the density.

5.4 Predictions of Wave Speed in Granular Materials

5.4.1 The Duffy and Mindlin Approach

Duffy and Mindlin carried out wave propagation analysis in a fully consolidated arrangement of spheres which represents a face-centred cubic array (as shown in figure 5.18) and provides the most dense packing. The approach consisted of determining increments of stress, assuming the cube is in equilibrium under the initial stress state. The deformation of the block is obtained from compliance relations of contacts determined from force and the relative incremental displacement as studied in a pair of spheres.

Since each sphere in a face-centred cubic array is in contact with twelve others, thirty-six components of contact force in each sphere will have to be taken into account. Despite half the components being equal pairs (leaving only eighteen to be found, of which six are normal and twelve tangential) the solution of a general three-dimensional problem is a difficult task.

If, however, the cubic array is subjected to a uniaxial variable stress perturbation (σ_a) as well as the constant hydrostatic pressure (σ_o), only three components of contact force (two normal and one tangential) have to be determined. In this case the problem can be expressed in the form as follows:

$$dN_i = f_i(\sigma_o) + g_i(\sigma_a).$$

The coefficients involved (f_i and g_i) depend on the instantaneous values of normal and tangential forces, which makes the above integration rather complex however. Thurston and Deresiewicz have carried out such an integration, and the results (see Appendix A) allow determination of the component forces (as well as the stresses and deformations produced in the cube), which govern the speed of waves in the granular material.

Thurston and Deresiewicz's results were plotted using a computer with quadruple precision since terms involving subtraction require an accuracy of up to 30 digits if strains as low as 10^{-10} are to be analysed. Figure 5.1 shows the variation of the speed of longitudinal waves in a pack of perfect steel spheres 2 mm in diameter (friction coefficient of 0.5) when the pack is subjected to a hydrostatic pressure of 1.6×10^4 N/m^2. Three curves are shown, for β values of 0.1, 0.2 and 0.5. The parameter β represents the tangent of the angle between normal and the tangential components of the contact forces (β = unity for their model). Thurston and Deresiewicz's theory, however, presents singularities for this particular value, so that our computing results had to be limited below 0.5 because the theory is also limited to β values smaller than the (static) friction coefficient. Despite such limitations, the theory is useful in the analysis of the influence of the several parameters.

The main feature of the results, as shown in figure 5.19, is the speed variation with amplitude at large strain, a behaviour opposing that found experimentally. This is probably due to the assumption that gross slip does not take place, which is not the case in practice, since large amplitude waves are capable of producing forces larger than those produced by the hydrostatic pressure. At low strains, speeds are constant, suggesting that relative displacements at contacts are negligible compared with the deformations of the granules themselves. Speeds are noticed to be strongly dependent upon β; longitudinal waves for $\beta = 1.0$ are estimated to be as high as 2000 m/s. Duffy and Mindlin estimated an approximate value for the longitudinal wave speeds (valid for very small wave amplitudes only) so that the approach overcomes singularity problems as β tends to unity. The speed values obtained were of the order of 500 m/s. Their

comparison with experiments carried out on steel spheres of two different tolerances showed a rapid decrease in speed, demonstrating how the theory is sensitive to the looseness of granules in the pack.

Figure 5.20 shows a comparison between theoretical and experimental results for sand 2.36 mm to 4.75 mm, subjected to a hydrostatic pressure of 1.3×10^4 N/m^2. Agreement is achieved for β values between 0.1 and 0.2. For the irregularities of granules of sand, β can assume a wide variety of values, and it is observed from the present experiments that an effective β value for sand lies between 0.1 and 0.2.

5.4.2 The "failure" strain

In the theoretical analysis of wave speeds in granular materials, contact forces were calculated and their variation with strain in the cube observed to compare with forces produced by hydrostatic pressure. It was generally observed that forces due to external pressure are smaller for strains larger than 10^{-6} to 10^{-5}, depending, obviously, upon the magnitude of the pressure. This indicates that gross slip can indeed take place at strains greater than 10^{-6}. As noticed from experimental results, speeds begin to drop at the strain range mentioned above, confirming the failure of the main frame which carries the wave. The incapability of granular materials to take tension due to their loose nature is responsible for the frame failure, as described here.

5.4.3 Brandt's approach

Brandt's approach[52] is somewhat more realistic because it takes into account the shape and arrangement of the granules. Brandt's model is composed of four sizes of spherical particles. Particles of the largest size are distributed randomly and smaller ones placed in the interstices without disturbing the arrangement. The speed is determined from the bulk modulus of the aggregate, which by itself is determined from volume-pressure relationship developed by means of the Hertz theory for the deformation of elastic spheres.

Two parameters are involved in the theory; the void ratio and the average number of contacts per particle. Because of the random distribution of the particles, these parameters were determined empirically; values of 0.393 for void ratio and 8.84 contacts per particle were obtained. It is interesting to compare the 8.84 contacts of the random distribution with 12 contacts for perfect spheres in a face-centred cubic array.

The theory can be extended to aggregates of nonspherical granules, as long as granule surfaces have an average radius of curvature conducive with the Hertzian theory of contact. The average number of contacts is also altered if irregular granules are used. The theory is simplified if a single constant is used to represent the shape dependent parameters. This constant must be determined experimentally.

The speed of longitudinal waves in dry granular materials in Brandt's analysis is proportional to the following parameters:

$$c \propto \frac{k\sigma_o^{1/6}}{\rho^{\frac{1}{2}}\phi^{\frac{1}{2}}(1-\phi)^{\frac{1}{2}}}$$

where k is the constant, σ_o the external pressure, ρ the density and ϕ the porosity, i.e., fraction of void volume per unit volume of the material.

This result confirms some of the experimental observations, particularly the porosity or the compaction, the pressure dependence to the power 1/6 and the influence of density upon wave speed (from the lead shot results).

5.5 Conclusions

The present experimental work has broadened the understanding of the parameters influencing wave velocity in granular materials, particularly with regard to vibrational amplitude where a two regime dependence was observed according to the strain produced by the waves. At large amplitudes, speeds drop with strain due to the greater forces being produced by the

waves than those supplied by the external pressure. Gross slip then takes place, destroying the main structure of grain-grain contacts through which the waves are transmitted in the material. This effect causes a reduction of the wave speed. Below a certain strain (which in most cases was found to lie between 10^{-6} and 10^{-5}) the hydrostatic pressure is capable of holding together the granular material and wave speed is then noticed to be constant with strain. A possible reason for this is related to elastic deformations of grains which may predominate over contact deformations.

The main conclusion with regard to the amplitude influence is that it is directly related to the pressure caused by the waves themselves.

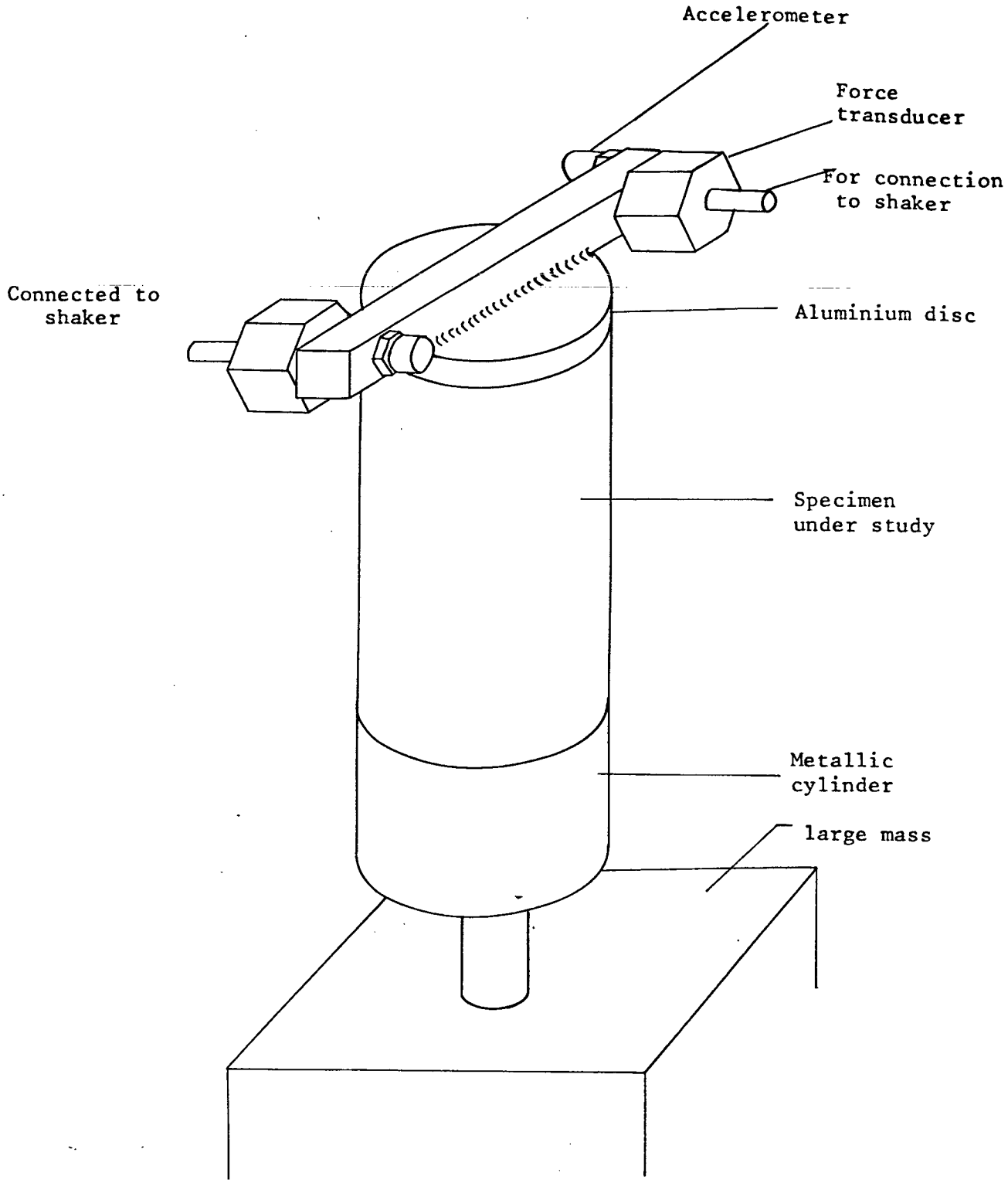

Fig 5.1 Experiment set-up for measurement of torsional wave speed

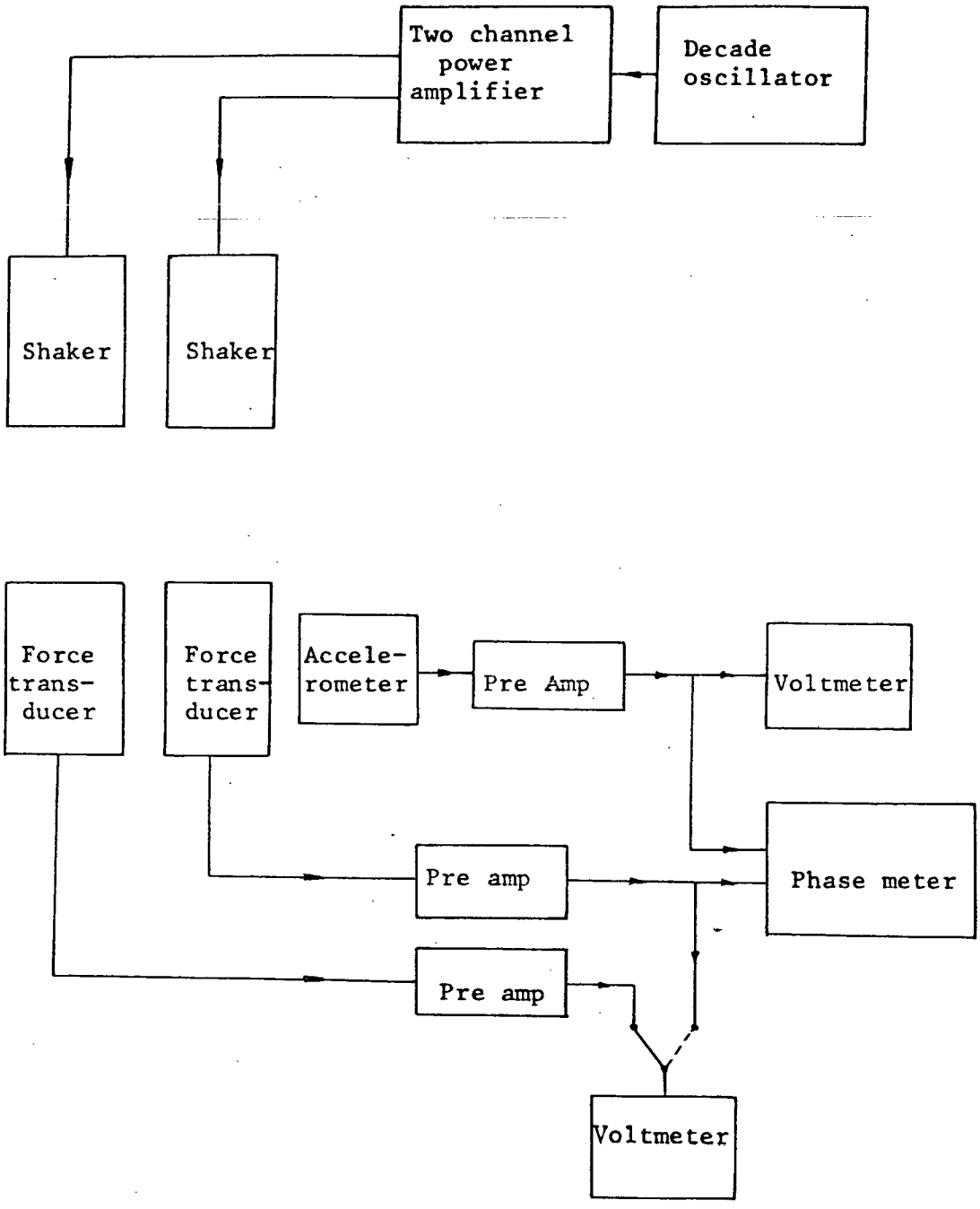

Fig 5.2 Equipment Layout

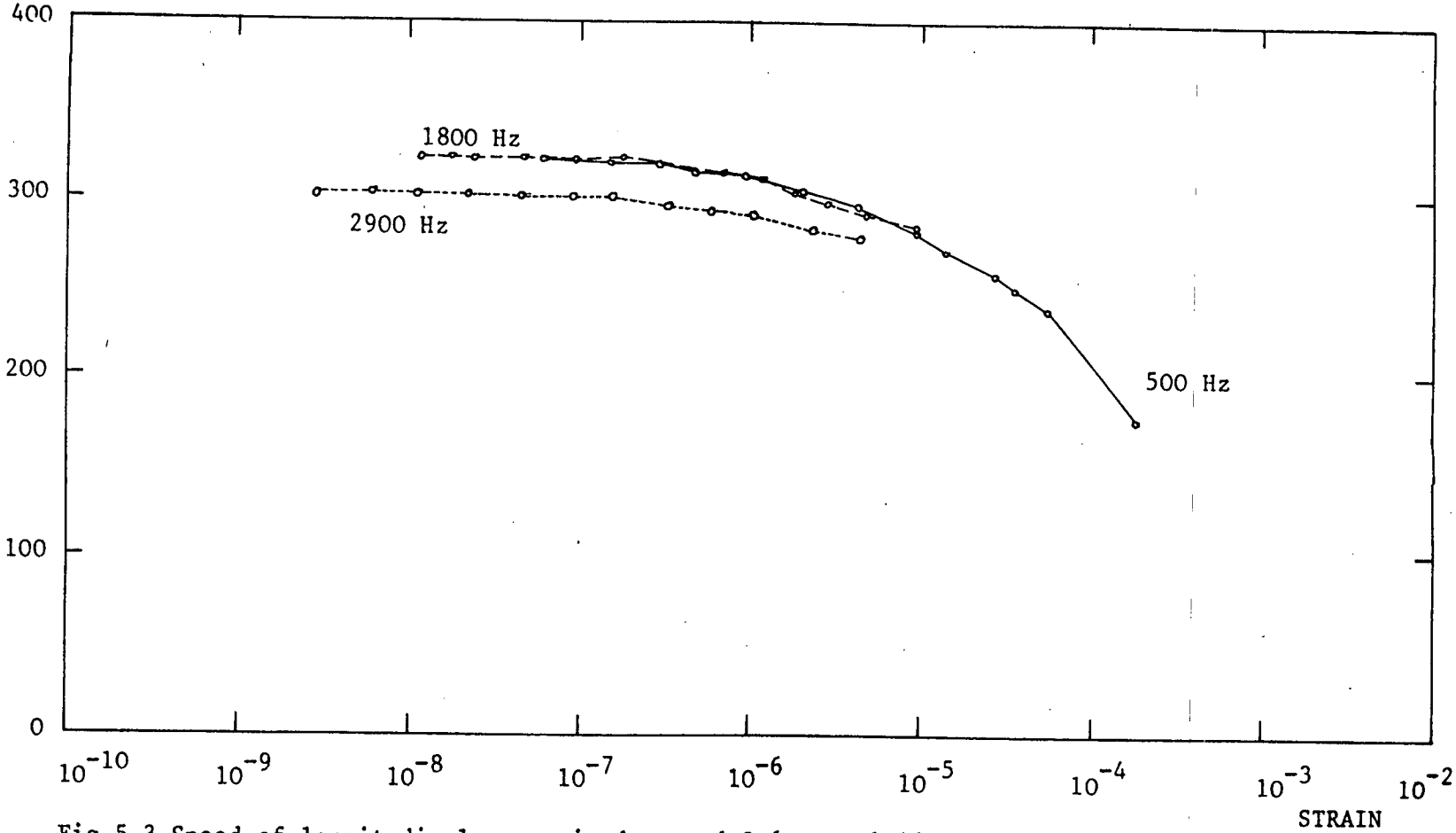

Fig 5.3 Speed of longitudinal waves in dry sand 0.6mm to 1.18mm of grains diameter subjected to hydrostatic pressure of 1.3×10^4 N/m^2

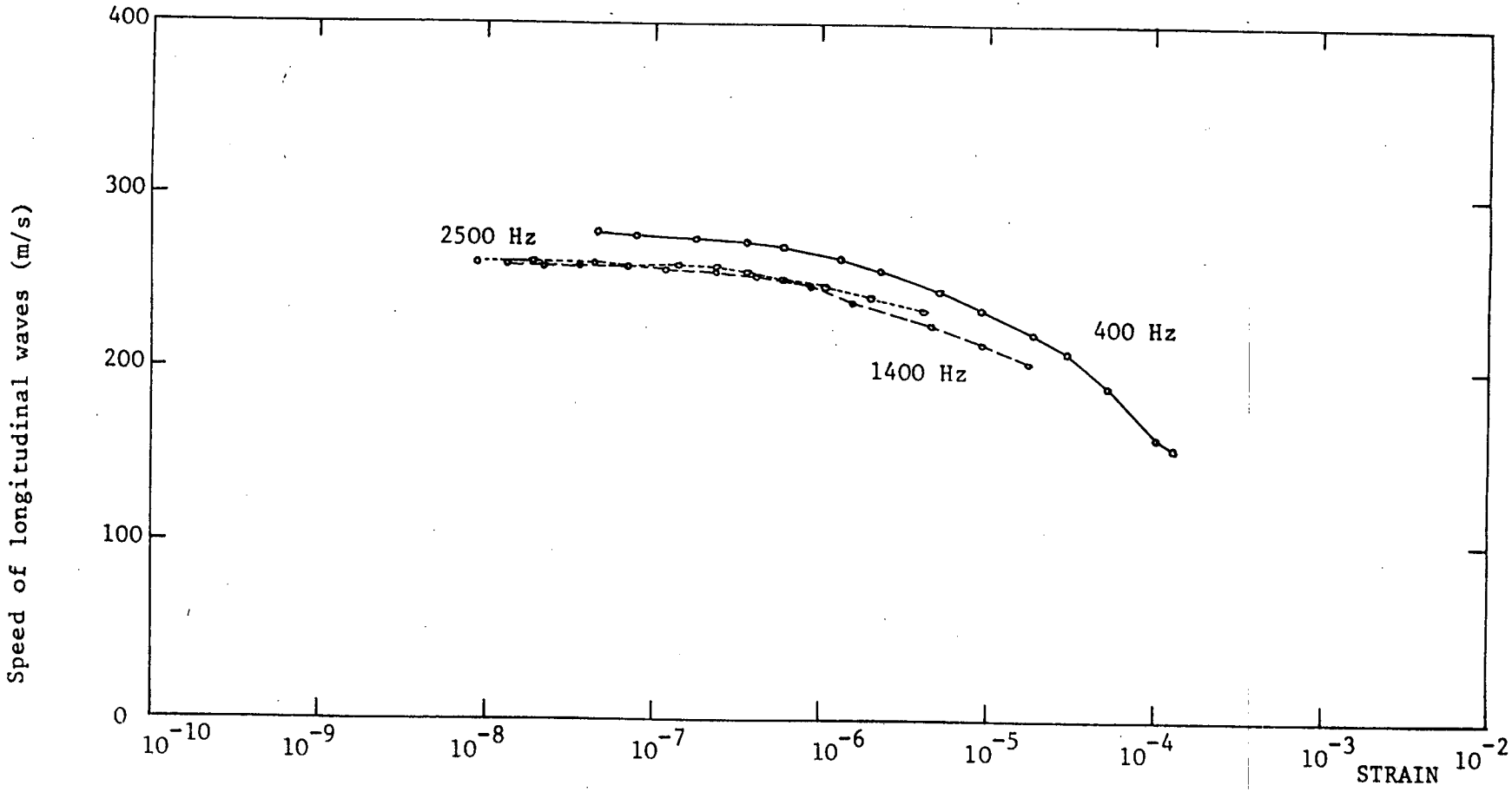

Fig 5.4 Speed of longitudinal waves in dry sand 0.6mm to 1.18mm, subjected to hydrostatic pressure of 6×10^3 N/m^2

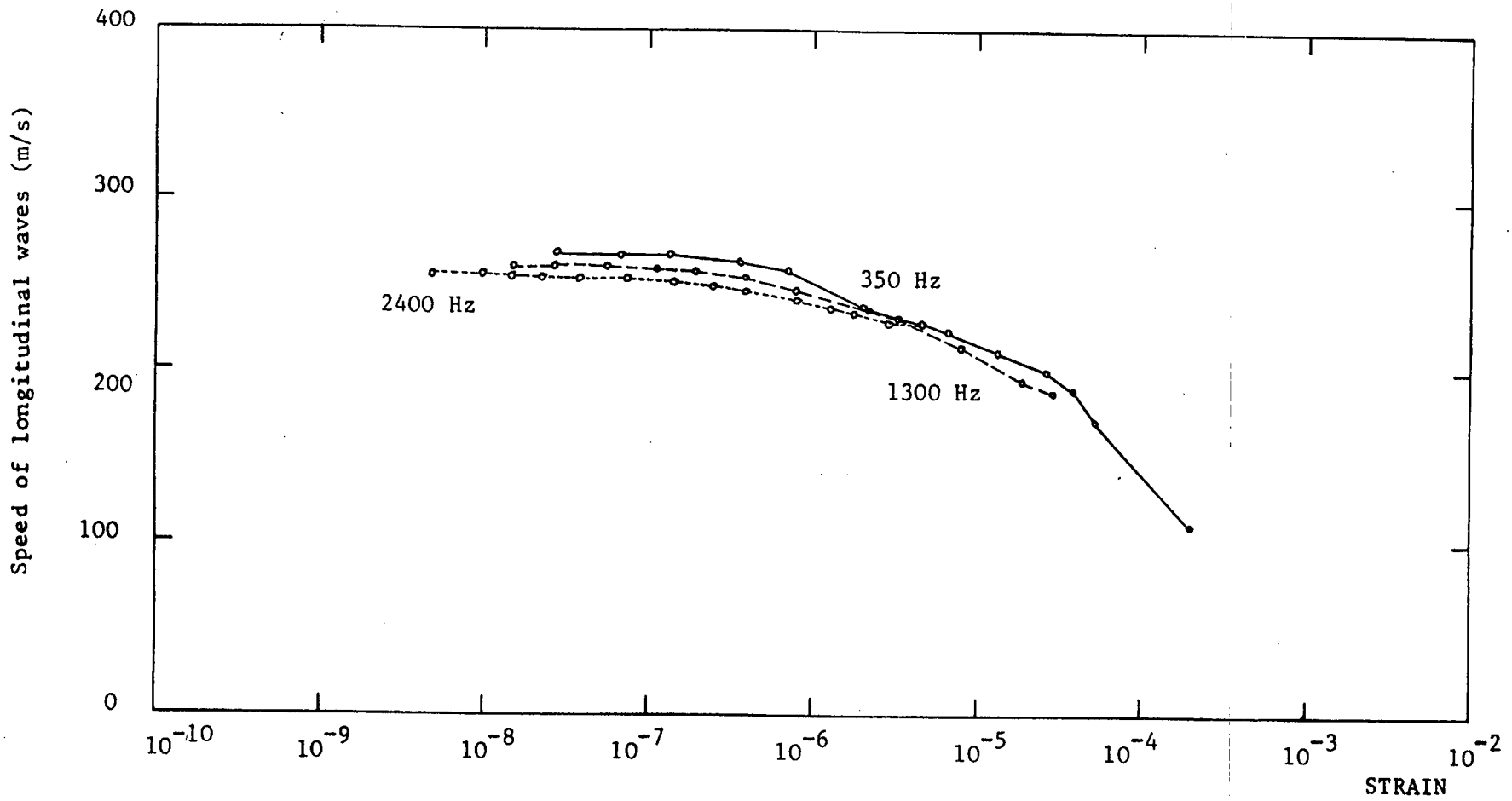

Fig 5.5 Speed of longitudinal waves in dry sand 0.6mm to 1.18mm, subjected to hydrostatic pressure of 3×10^3 N/m^2

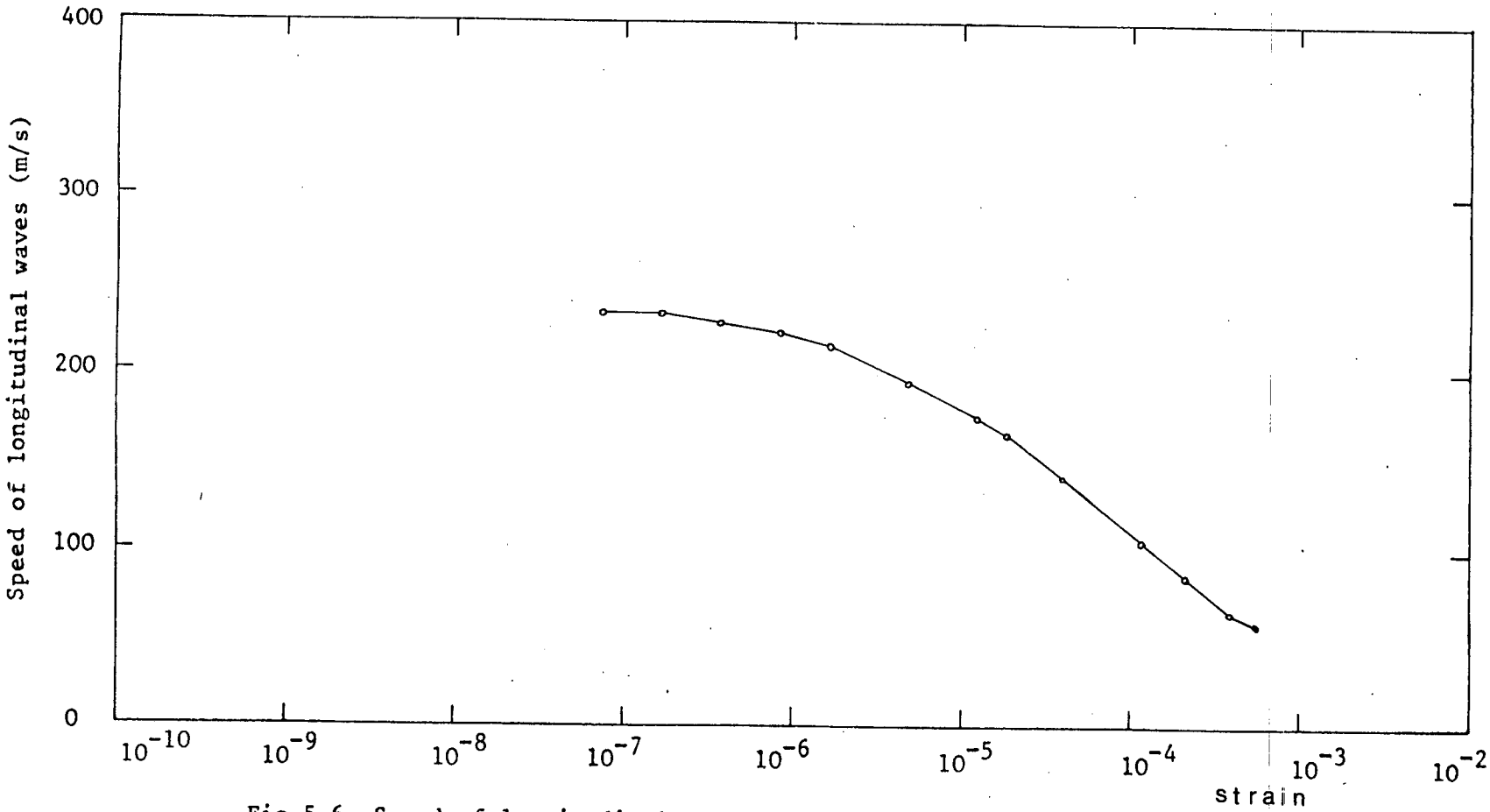

Fig 5.6 Speed of longitudinal waves in dry sand 0.6mm to 1.18mm, subjected to no external pressure

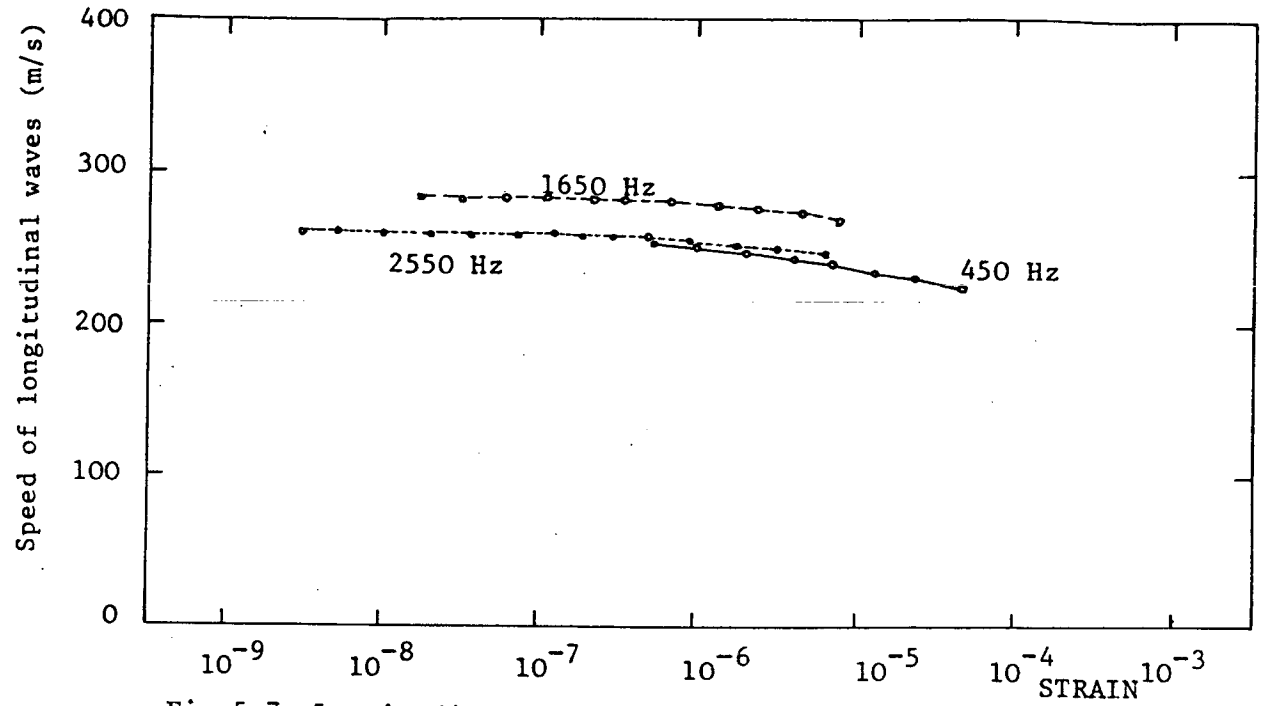

Fig 5.7 Longitudinal wave speed in dry sand (2.36mm to 4.75mm) subjected to hydrostatic pressure: 1.3 x 10^4 N/m^2

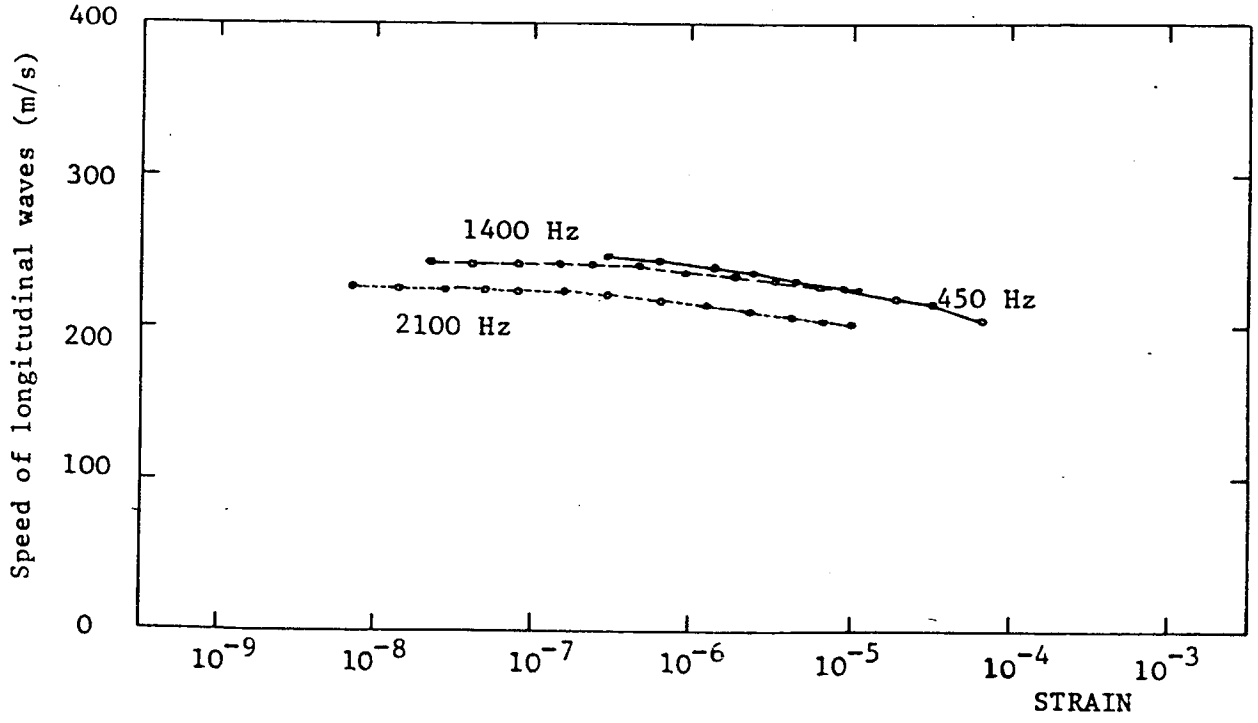

Fig 5.8 Longitudinal wave speed in dry sand (2.36mm to 4.75mm) subjected to hydrostatic pressure: 6 x 10^3 N/m^2

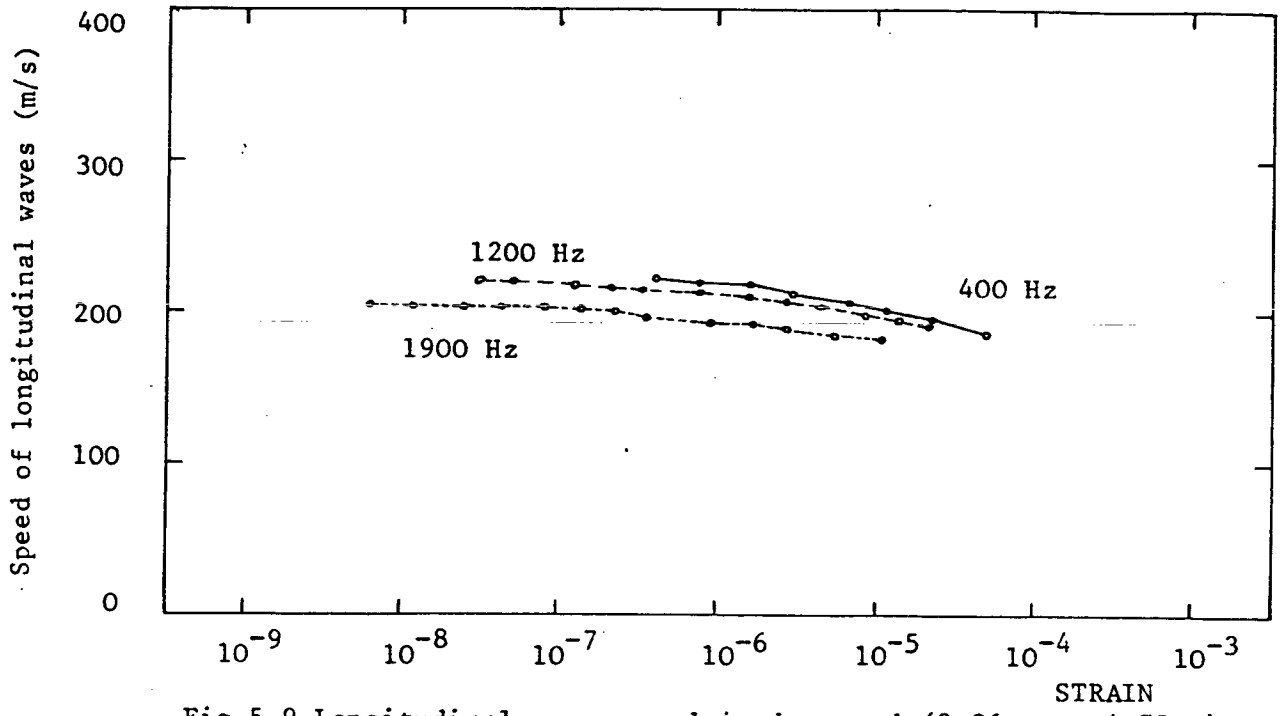

Fig 5.9 Longitudinal wave speed in dry sand (2.36mm to 4.75mm) subjected to hydrostatic pressure 3×10^3 N/m^2

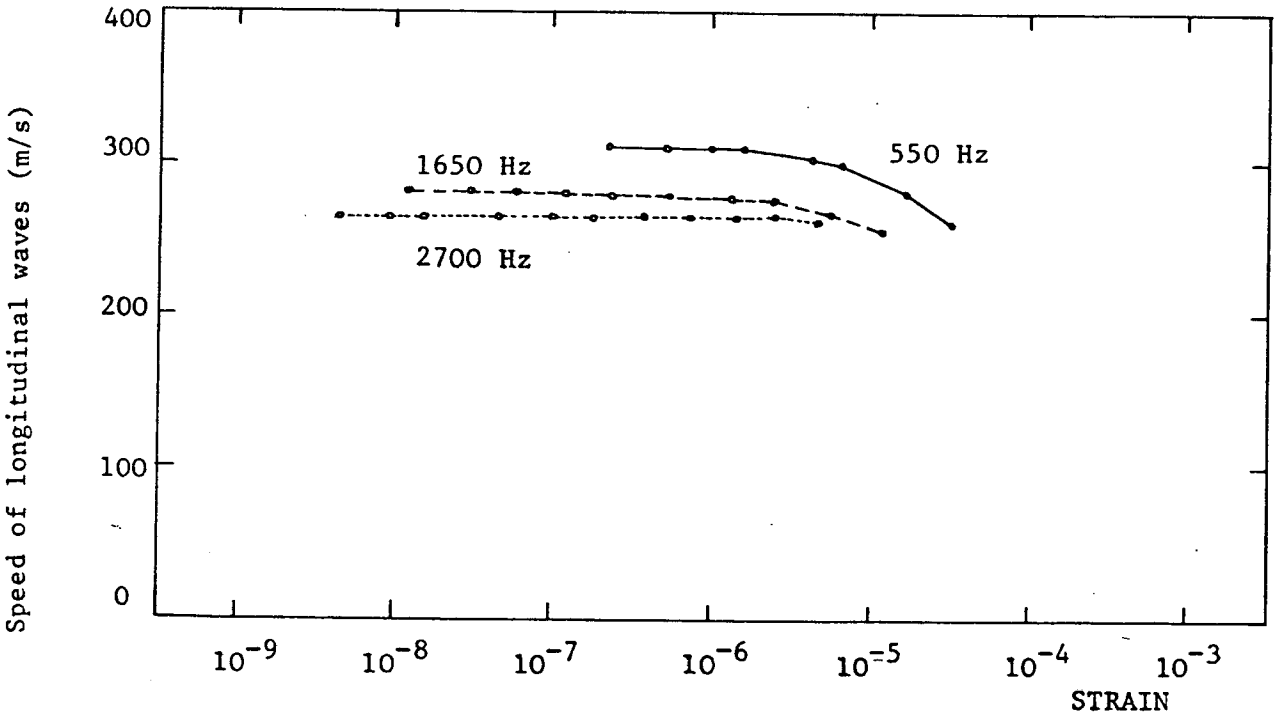

Fig 5.10 Longitudinal wave speeds in glass spheres, subjected to hydrostatic pressure 1.3×10^4 N/m^2

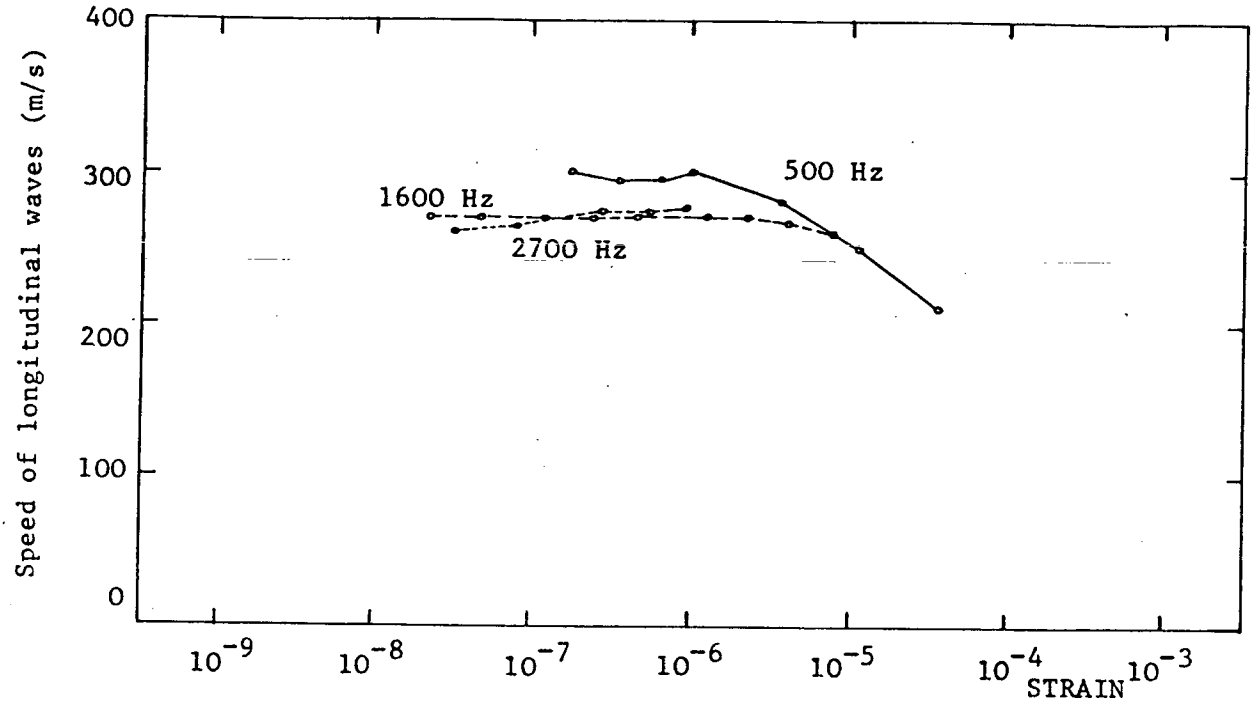

Fig 5.11 Longitudinal wave speeds in glass spheres, subjected to hydrostatic pressures of 6 x 10^3 N/m^2

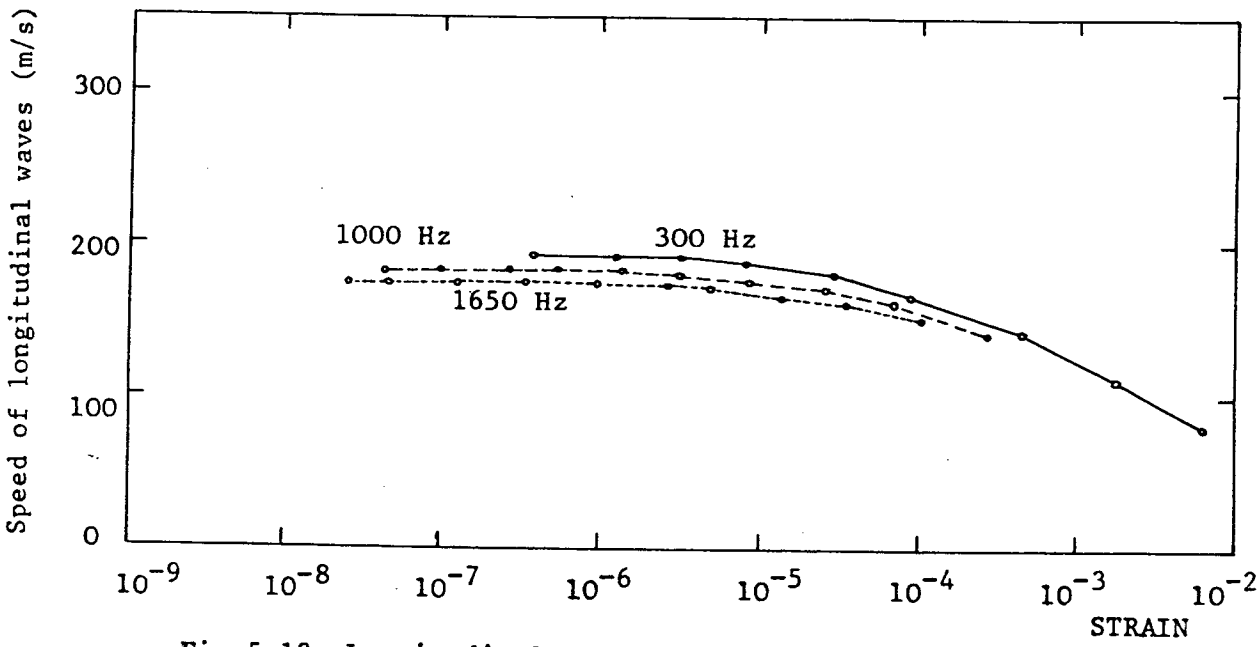

Fig 5.12 Longitudinal wave speeds in lead shot, subjected to hydrostatic pressure of 1.3 x 10^4 N/m^2

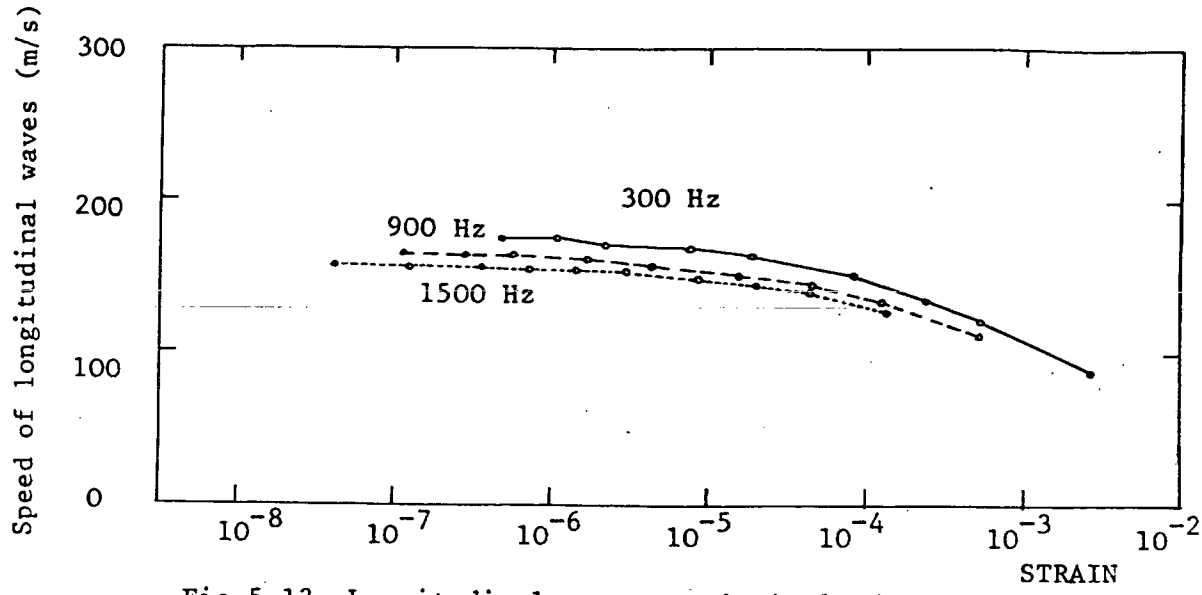

Fig 5.13 Longitudinal wave speeds in lead shot, subjected to hydrostatic pressure of 6×10^3 N/m^2

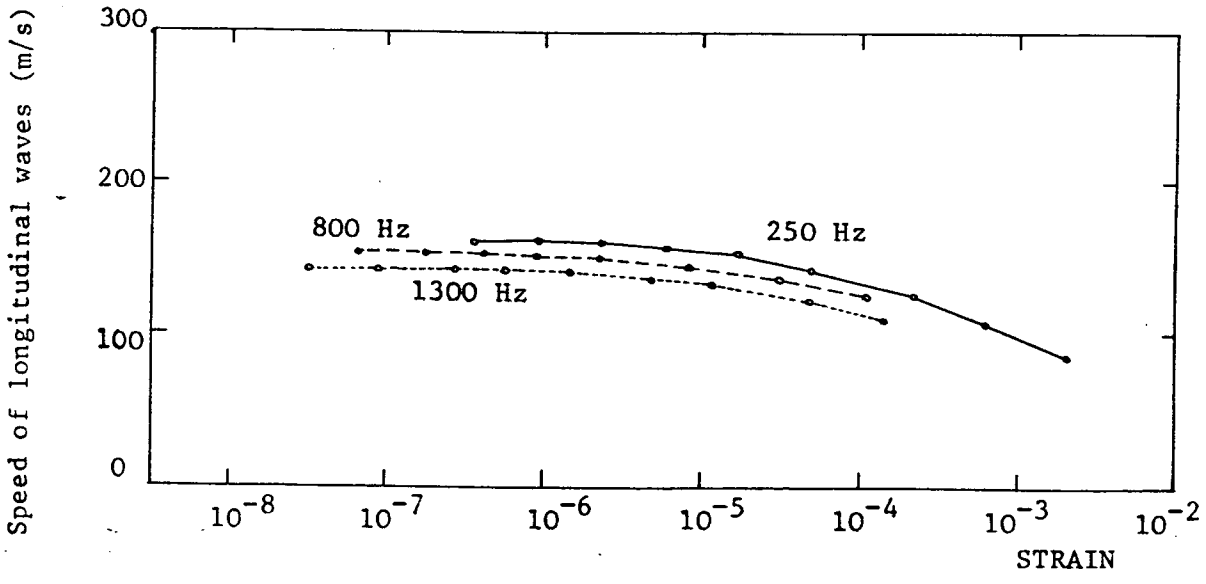

Fig 5.14 Longitudinal wave speeds in lead shot, hydrostatic pressure 3×10^3 N/m^2

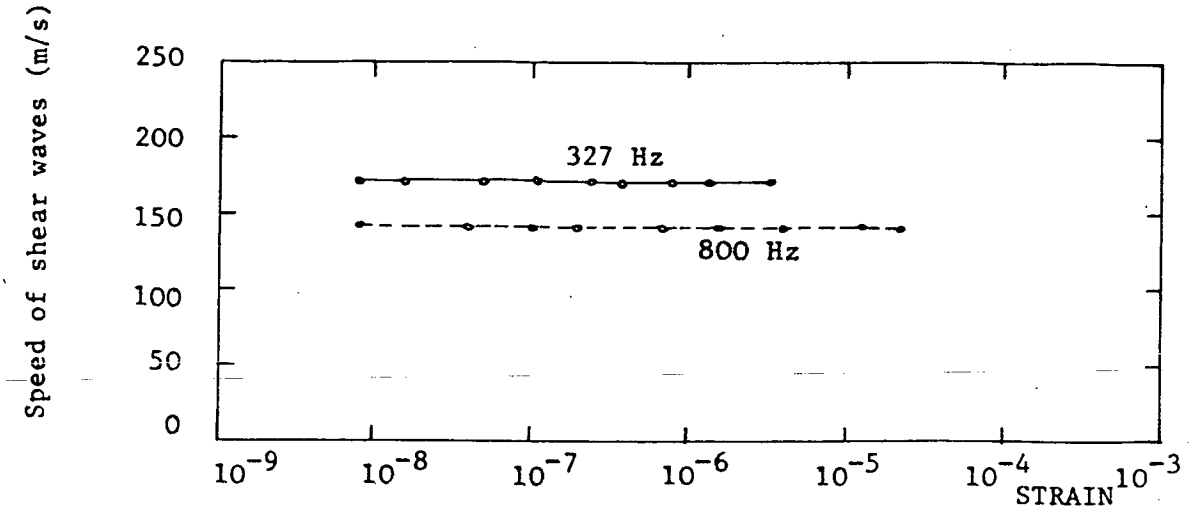

Fig 5.15 Torsional waves in dry sand (0.6mm to 1.18mm)
Hydrostatic pressure: 1.3×10^4 N/m^2

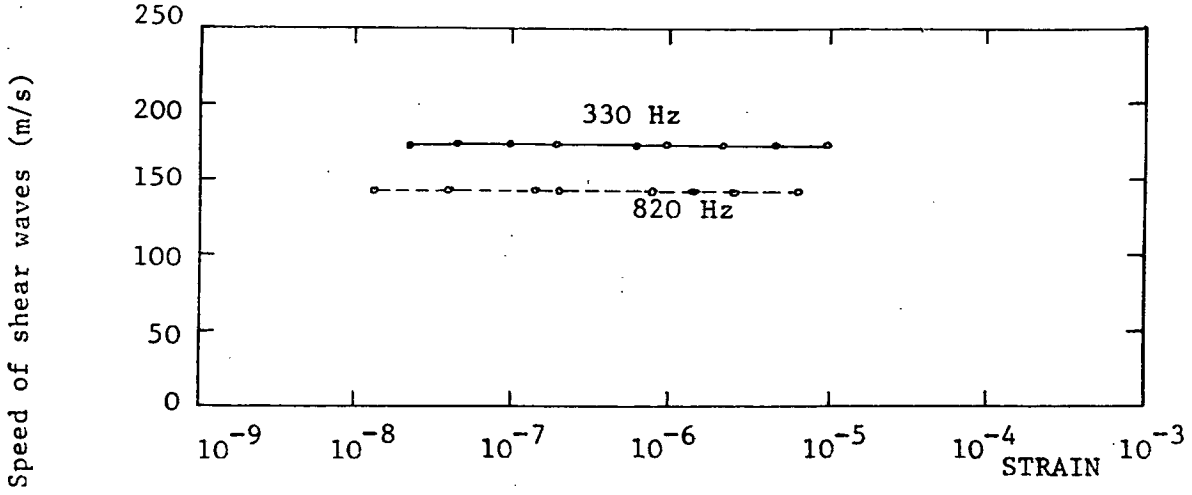

Fig 5.16 Shear Waves in dry sand (0.6mm to 1.18mm)
hydrostatic pressure: 6×10^3 N/m^2

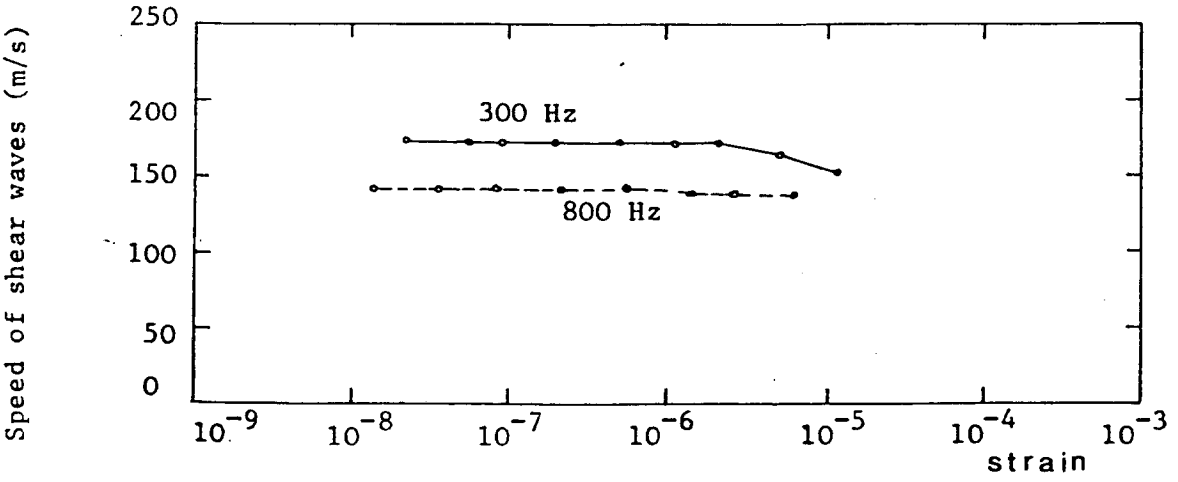

Fig 5 17 Shear mass in dry sand (0.6mm to 1.18mm)
hydrostatic pressure of 3×10^3 N/m^2

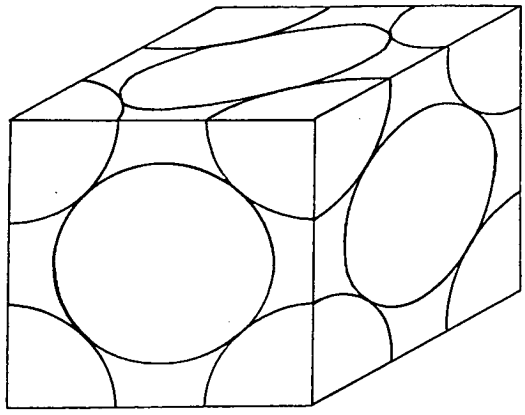

Fig 5.18 Element of volume of a face-centred cubic array of spheres

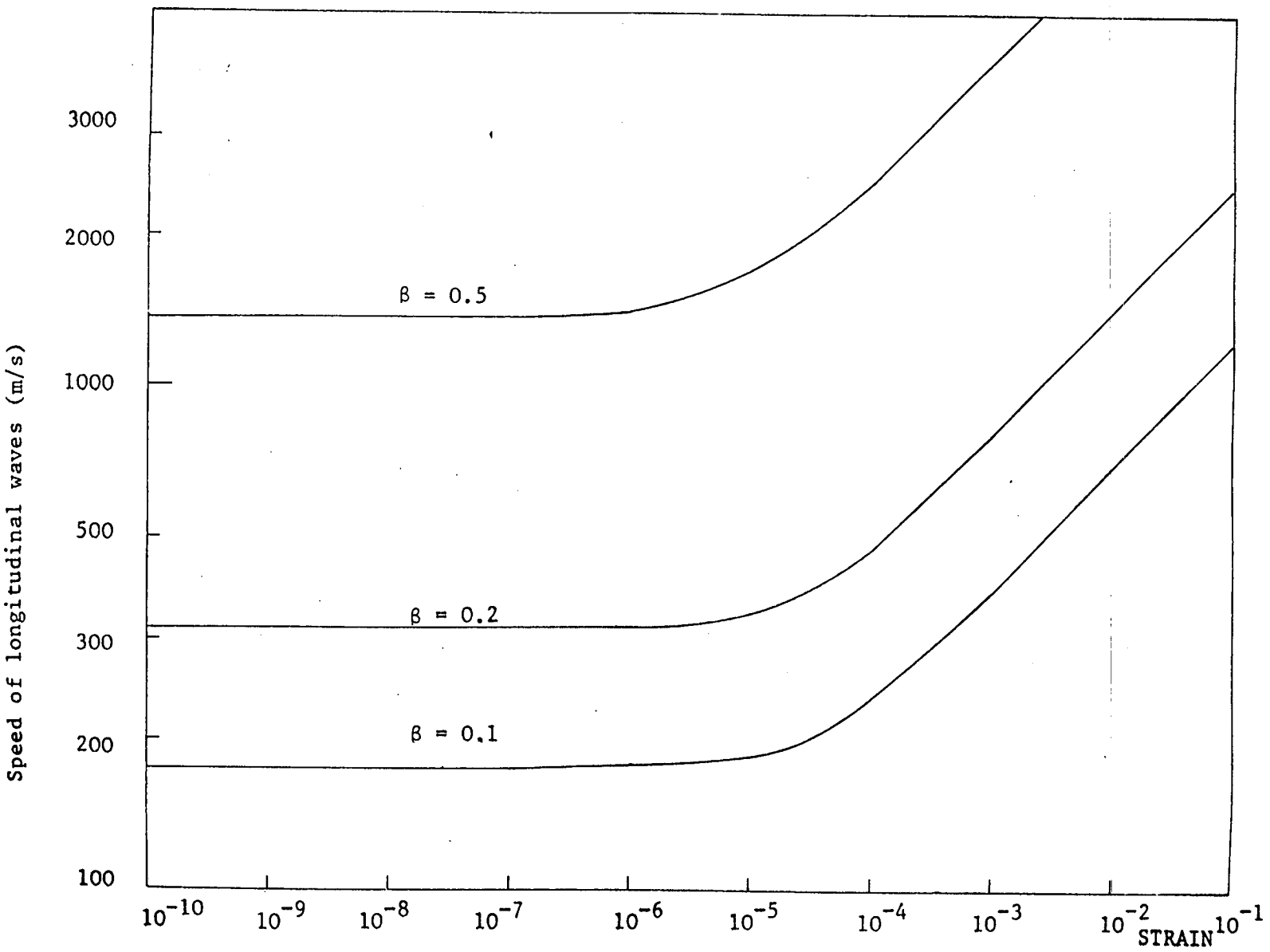

Fig 5.19 Theoretical variation of speed with β and strain (Duffy and Mindlin model)

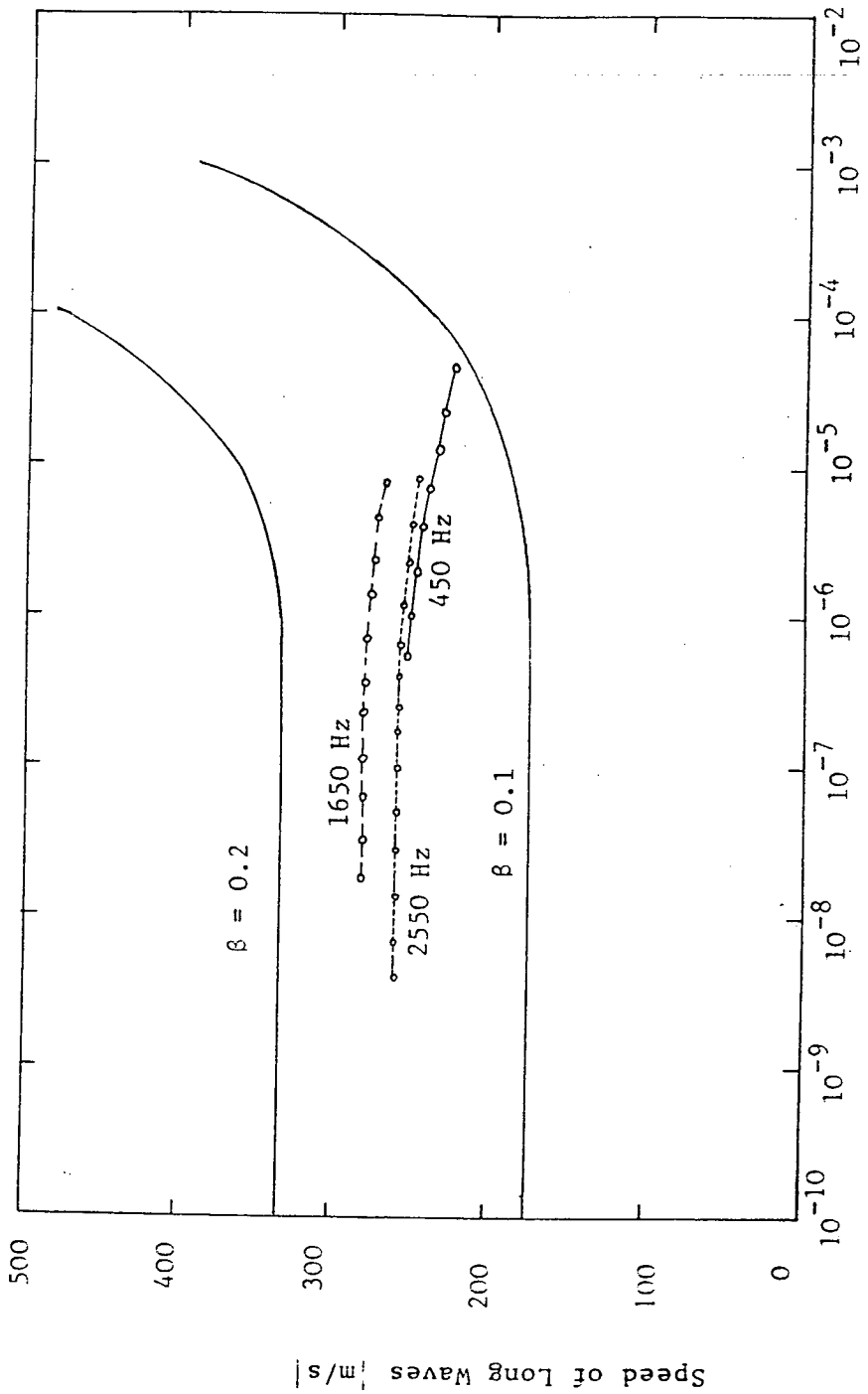

Fig 5.20
Comparison between theoretical (β= 0.1 and β= 0.2) and experimental results for the speed of long waves on sand (2.30 to 4.75mm). Hydrostatic pressure 1.3×10^4 N/m^2

CHAPTER 6

THEORETICAL ANALYSIS

6.1 Introduction

The series of experiments on the damping of hollow beams filled with sand, described in Chapter 3, has led to the observation that regions of maximum damping occur at frequencies with wavelengths directly associated with the internal dimensions of the beam cavities. Maximum damping was observed when the cavity dimensions were equal to one-half the longitudinal wavelength, such that antinodal points were formed at the surfaces of the cavity (other regions of maximum damping were observed for $\lambda = \frac{3}{4}, 1\frac{1}{4}, 1\frac{3}{4}$, etc.). In these regions the transfer of energy from the beam to the sand, and consequently the damping, is maximised.

Later experiments on the speed of waves in sand showed that under certain conditions longitudinal waves can travel at speeds up to 300 m/s, which is almost three times the speed normally quoted in the literature (100 m/s). Thus a different number (or fraction) of standing waves may be occurring and be the actual cause for the maximum damping. A theoretical study of the conditions at which damping of structures filled with granular materials is maximised is presented in this chapter.

6.2 Basic Expressions

6.2.1 Flexural wave equation for beams with a uniformly distributed load

A segment of a beam having a uniformly distributed load is shown in fig. 6.1. The load is assumed to be of constant magnitude along the beam length, and is given by

$$\text{Load} = \bar{Z} \frac{\partial \xi}{\partial t} dx$$

where $\bar{Z}$ is the impedance (per unit length of the beam) of the granular material at the surface of the cavity.

Summing the moments gives:

$$F(x) + \tfrac{1}{2}\bar{Z}\frac{\partial \xi(x,\, t)}{\partial t}\, dx - \frac{\partial M(x,\, t)}{\partial x} = 0 \qquad (6.1)$$

where $F(x)$ is the shear force; $M(x)$, the moment and $\xi(x, t)$ the beam displacement. Summing the forces:

$$\bar{Z}\,\frac{\partial \xi(x,\, t)}{\partial t} + \frac{F(x)}{\partial x} + \rho_s \frac{\partial^2 \xi(x,t)}{\partial t^2} = 0 \qquad (6.2)$$

If the moment is written in terms of beam flexural stiffness B $(= EI)$,

$$M(x) = -EI\,\frac{\partial^2 \xi(x,\, t)}{\partial x}\,,$$

a new classical beam equation is obtained, which takes into account the effect of the reaction forces produced by the granular material, i.e.,

$$EI\,\frac{\partial^4 \xi(x,t)}{\partial x^4} + \left[\rho_s + \frac{\bar{Z}}{j\omega}\right]\frac{\partial^2 \xi(x,t)}{\partial t^2} = 0 \qquad (6.3)$$

ρ_s represents the beam mass per unit length, $\omega = 2\pi f$ and f the frequency.

6.2.2 Impedance expression for a column of granular material

Assuming flexural wavelength is much larger than the cavity dimensions of a beam filled with granular material an expression for the impedance of the granular material is determined by considering the column of material contained in a short section of the beam along which the reaction forces exerted on the beam walls by the granular material are considered constant, see fig. 6.2.

The material inside the cavities is also assumed to be in contact with the walls throughout the period of vibration, including when the wall is moving away from the material (fig. 6.3). As the beam deforms in flexural modes, the forces acting at both ends of the column are identical in direction and magnitude. Impedance expressions can then be developed,

beginning with the longitudinal wave equation in rods,

$$\frac{\partial^2 \zeta}{\partial y^2} = \frac{1}{c^2} \frac{\partial^2 \zeta}{\partial t^2}$$

whose solution is of the form

$$\zeta(y, t) = Ae^{j(\omega t - \bar{k}y)} + Be^{j(\omega t + \bar{k}y)}$$

where ζ is the particle displacement, A and B are constants, and $\bar{k}$ is the longitudinal wavenumber in complex form for taking into account the internal damping of the granular material.

From boundary conditions, one obtains,

at $y = 0$, $$j\bar{k}ES\left[A - B\right] = F_o \tag{6.5}$$

and at $y = \ell$, $$j\bar{k}ES\left[Ae^{-j\bar{k}\ell} - Be^{j\bar{k}\ell}\right] = -F_o \tag{6.6}$$

S represents the cross-sectional area of the column, given by $d\Delta x$, and E is the Young's modulus of the granular material. From equations (6.5) and (6.6), the constants A and B can be isolated, as follows,

$$A = -\frac{F_o}{j\bar{k}ES}\left[\frac{1 + e^{j\bar{k}\ell}}{e^{-j\bar{k}\ell} - e^{j\bar{k}\ell}}\right] \tag{6.7}$$

and

$$B = \frac{-F_o}{j\bar{k}ES}\left[\frac{1 + e^{-j\bar{k}\ell}}{e^{-j\bar{k}\ell} - e^{j\bar{k}\ell}}\right]. \tag{6.8}$$

Substituting A and B into equation (6.4), gives,

$$\zeta(y=0) = \frac{-F_o}{\bar{k}ES}\left[\frac{1 + \cos \bar{k}\ell}{\sin \bar{k}\ell}\right]e^{j\omega t} \tag{6.9}$$

and

$$\zeta(y=\ell) = \frac{-F_o}{\bar{k}ES}\left[\frac{1 + \cos \bar{k}\ell}{\sin \bar{k}\ell}\right]e^{j\omega t} \tag{6.10}$$

from which impedance expressions are obtained,

$$\bar{Z}_{(y=0)} = \frac{-\bar{k}ES}{j\omega}\left[\frac{\sin \bar{k}\ell}{1 + \cos \bar{k}\ell}\right] \tag{6.11}$$

and

$$\bar{Z}_{(y=\ell)} = \frac{-\bar{k}ES}{j\omega}\left[\frac{\sin \bar{k}\ell}{1 + \cos \bar{k}\ell}\right]. \tag{6.12}$$

The impedance at both ends of the column is the same, so that the total reaction force acting upon the beam will be twice the force exerted by one side only.

6.2.3 Impedance expression including internal damping

If internal damping of the material (η_{gm}) is taken into account, the wavenumber $\bar{k}$ of longitudinal waves can be expressed in the simplified form (see section 6.3.1):

$$\bar{k} = k(1 - j\eta_{gm}/2).$$

This approximation deviates from exact values only by about 4% when $\eta_{gm} = 0.5$.

Its substitution into the impedance expression (equation (6.11) or (6.12)) leads to:

$$\bar{Z}_{(y=0)} = \bar{Z}_{(y=\ell)} = \frac{-kES}{j\omega}\left[\frac{\sin k\ell - j \sinh k\ell\eta_{gm}/2}{\cos k + \cosh k\ell\eta_{gm}/2}\right]. \tag{6.13}$$

6.2.4 The new flexural wave equation

If the impedance expression is substituted into the beam wave equation (equation (6.3)), one obtains:

$$\frac{\partial^4 \xi(x,\ t)}{\partial x^4} + \frac{1}{E_{beam} I_{beam}} \left[\rho_s + \frac{2kE_{gm}}{\omega^2} \frac{\sin k\ell - j \sinh k\ell\eta_{gm}/2}{\cos k\ell + \cosh k\ell\eta_{gm}/2} \right] \frac{\partial^2 \xi(x,t)}{\partial t^2}$$

$$= o \qquad (6.14)$$

The validity of the above equation can be checked by letting the frequency tend to zero, in which case the second term inside brackets reduces to

$$\frac{k^2 E_{gm} d\ell}{\omega^2} = \rho_{gm} d\ell$$

which is the column mass per unit length (along the beam), as expected at low frequencies. The granular material therefore behaves only as an added mass.

6.3 Damping Prediction in Hollow Beams Filled with Granular Materials

6.3.1 From the beam flexural wavenumber

One of the methods used for expressing the damping of vibrating beams consists of calculating real and imaginary parts of the beam wavenumber, which in this case are given by,

$$\bar{k}^4 = \frac{\omega^2}{(EI)_{beam}} \left[\rho_s + \frac{2kE_{gm} d}{\omega^2} \frac{\sin k\ell - j \sinh k\ell\eta_{gm}/2}{\cos k\ell + \cosh k\ell\eta_{gm}/2} \right]. \qquad (6.15)$$

Since the imaginary part is small compared to the real part, the fourth root can be approximated to

$$\bar{k}_{beam} = k_{beam}[1 - j\eta_s/4]$$

where η_s is the loss factor of the beam, which can therefore be calculated as follows

$$\eta_s \simeq 4 \frac{k_{imag}}{k_{real}} .$$

The error involved in this approximation is less than 10% in the magnitude of $\bar{k}$ when $\eta_s = 0.5$.

An example of real and imaginary parts of the flexural wavenumber for a hollow beam filled with granular material of density 1500 kg/m^3 and loss factor 0.1, is shown in fig. 6.4.

Figure 6.5 shows the loss factor prediction of a beam filled with sand. Regions of maximum damping are evident when $k\ell = \pi, 3\pi, 5\pi,$ which correspond to cavity dimension (ℓ) being equal to one half, one and a half, and two and a half wavelengths.

A column as shown in fig. 6.3, with impedance given by:

$$\bar{Z} = \frac{dkE_{gm}}{\omega} \frac{\sinh k\ell\eta_{gm}/2 - j\sin k\ell}{\cos k\ell + \cosh k\ell\eta_{gm}/2}$$

shows a maximised real part for the same $k\ell$ values as those mentioned above. The resistance to vibration produced by the granular material produces maximum absorption of energy. It is assumed in the analysis that once energy is absorbed it is totally dissipated within the material.

Two sharp peaks are observed at $k\ell = \pi$. These are considered to be of a purely mathematical origin, stemming from the approximation made for the internal damping to the granular material ($\bar{k} = k(1 - i\eta_{gm}/2)$. The effect disappears as $k\ell$ assumes larger values.

6.3.2 From impedance expressions

Impedance expressions give a rather simpler method of calculating the impedance. The results may not be as accurate, however, since the inertia of the structure itself is not included. The prediction of damping is via the loss factor definition, thus energy dissipated per cycle and beam vibratory energy must be stipulated.

Assuming all the energy transferred to the granular material is dissipated within the material itself, the energy dissipated per cycle can be expressed as:

$$E_{diss}/\text{cycle} = \frac{Re}{\omega} \{\text{Veloc.}_{beam} \times \text{Force}^{*}_{beam}\}$$

or

$$E_{diss}/\text{cycle} = |V_{beam}|^2 \frac{Re}{\omega} \{\bar{Z}_{gm}\}$$

per unit length of the beam. The vibratory energy of the beam is given by:

$$E_{vib} = \tfrac{1}{2}(\rho.S)_{beam}|V_{beam}|^2$$

and loss factor by:

$$\eta_s = \frac{Re\{\bar{Z}_{gm}\}}{\omega(\rho S)_{beam}} .$$

Substituting equation (6.16) into the above equation, gives:

$$\eta_s = \frac{2kE_{gm}d}{\omega^2(\rho S)_{beam}} \frac{\sinh k\ell\eta_{gm}/2}{\cos k\ell + \cosh k\ell\eta_{gm}/2} . \qquad (6.16)$$

An example of loss factors predicted by this method is shown in fig. 6.6 and a comparison with the previous method (section 6.3.1) is given in fig. 6.7.

The present method assumes that the dynamic behaviour of the structure is not affected by the reaction forces provided by the granular material, which in some cases may exceed beam inertia forces. Despite this, agreement between both methods is very good.

6.3.3 Comparison with experimental results

Theoretical predictions require accurate estimation of the speed of longitudinal waves in the granular material, which as discussed in Chapter 5, varies significantly with the amplitude of the waves. It is therefore

essential to determine the amplitude of vibration of the structure (assuming it is of the same order of magnitude as amplitude of waves in the material). This is necessary so that the speed of waves can be specified at the various frequencies at which predictions are made.

It was observed during damping measurements of sand-filled beams that their surface displacements were of the order of 10^{-4} m at 100 Hz and 10^{-8} m at 3000 Hz. Considering their internal dimensions were 5×10^{-2} m, strains in the granular material were of the order 10^{-3} at low frequencies, and 10^{-7} at high frequencies. The main objective of this chapter is to predict levels and frequencies at which maxima of beam damping occur; strains for this particular region are 10^{-5} to 10^{-6}, and according to experimental results, longitudinal wave speeds vary between 250 m/s and 300 m/s.

The expressions presented above predict that maximum damping occurs at frequencies two or more times higher than those observed experimentally, as can be seen in fig. 6.8. Thus the expressions were considered inadequate to model the physical problem.

It was assumed in the derivation of the expressions that the filling material was always in contact with the walls of the cavity and that energy transfers existed in both stress states, i.e., when the structure was being compressed by the material and when it was moving away from it. Obviously, the loose grain characteristics of granular materials make it incapable of resisting tensional stresses so that the boundary conditions assumed may not represent the actual physical problem. Modifications were therefore made to the expressions detailed as follows in section 6.4.

6.4 Damping Predictions in Hollow Beams Filled with Granular Material - Assuming Improved Boundary Conditions

6.4.1 Impedance expressions

Again analysing a section of the beam containing a column of the filling material, this time, however, with the boundary conditions of one end free (force term vanishes) and the other end forced (the force being that exerted by the beam). Figure 6.9 shows the segment under study.

Applying boundary conditions to the solution of the longitudinal wave equation,

$$\zeta(y, t) = Ae^{j(\omega t - \bar{k}y)} + Be^{j(\omega t + \bar{k}y)}$$

one obtains

$$\text{at } y = 0, \qquad j\bar{k}ES[A - B] = F_o \tag{6.17}$$

$$\text{and at } y = \ell, \qquad Ae^{-j\bar{k}\ell} = Be^{j\bar{k}\ell} \tag{6.18}$$

From equations (6.17) and (6.18), constants A and B can be isolated; their expressions are:

$$A = \frac{F_o e^{j\bar{k}\ell}}{j\bar{k}ES\left[e^{j\bar{k}\ell} - e^{-j\bar{k}\ell}\right]}$$

$$B = \frac{F_o e^{-j\bar{k}\ell}}{j\bar{k}ES\left[e^{j\bar{k}\ell} - e^{-j\bar{k}\ell}\right]} .$$

The displacement expression at $y = 0$ (where the force is applied) is

$$\zeta_{(y=0,t)} = \frac{F_o e^{j\omega t}}{j\bar{k}ES}\left[\frac{e^{j\bar{k}\ell} + e^{-j\bar{k}\ell}}{e^{j\bar{k}\ell} - e^{-j\bar{k}\ell}}\right] . \tag{6.19}$$

The impedance expression is therefore as follows:

$$\bar{Z}_{(y=0)} = -\frac{\bar{k}ES}{j\omega}\tan \bar{k}\ell$$

or

$$\bar{Z}_{(y=0)} = -\frac{kES}{j\omega}\left[\frac{\sin 2k\ell - j \sinh k\ell\eta_{gm}}{\cos 2k\ell + \cosh k\ell\eta_{gm}}\right]. \tag{6.20}$$

Equation (6.20) contains the internal loss factor of granular material, η_{gm}, expressed in the form of a complex longitudinal wavenumber, $\bar{k} = k(1 - j\eta_{gm}/2)$, as discussed in 6.3.2.

6.4.2 Damping prediction from impedance expression

It was shown in section 6.3 that damping predictions by both the flexural wavenumber and the impedance methods gave almost identical results. The predictions made in this section will, therefore, be restricted to the impedance method only because of the simpler calculations and determination of the influence of the several parameters involved.

The loss factor as derived in section 6.4.2 is

$$\eta_s = \frac{\mathrm{Re}\{\bar{Z}_{gm}\}}{2\pi f(\rho S)_{beam}}$$

and substituting equation (6.20), one obtains,

$$\eta_s = \frac{kE_{gmd}}{\omega^2(\rho S)_{beam}} \left[\frac{\sinh k\ell\eta_{gm}}{\cos 2k\ell + \cosh k\ell\eta_{gm}}\right] \qquad (6.21)$$

The similarity of the resultant equation with equation (6.16) is apparent (see fig. 6.10), except at the maximum damping frequencies, which are half the values previously obtained. The damping levels are also half the values given by equation (6.16) because of the assumption that energy is transferred during half the period of vibration only, i.e., at the compression stage.

6.4.3 Comparison with experimental results

Equation 6.21 is compared with experimental results in Figs. 6.11, 6.12 and 6.13. This time the agreement between maximum damping frequencies is very close, indicating that the model representing the physical problem is more accurate. It can also be seen that measured damping levels agree at low frequencies with predicted values assuming internal loss factor of sand of 0.05 - 0.1. Experiments carried out on columns of sand, as described in chapter IV resulted in internal loss factor values dependent upon the stain. strains associated to high amplitudes of vibrations at low frequencies are

such that loss factors are indeed of the order of 0.1. It can then be concluded that the model predicts the damping of beams filled with granular materials with good accuracy at low frequencies. At higher frequencies, experimental curves present a broad shape approaching the theoretical curve for internal loss factors much higher than values obtained in laboratory.

The influence of parameters related to the damping of granular materials will be discussed next.

6.4.3.1 Amplitude of waves

Experiments on longitudinal waves speed in sand indicate that speed varies significantly with amplitude. For intance, sand (0.6mm to 1,18mm in diameter) subjected to a hydrostatic pressure of 6×10^3 N/m^2, have speed of 150 m/s when the strain is 10^{-4} and it increases to 250 m/s at strains of 10^{-6}.

This non linear regime may cause a broadening of the damping curve.

A record of beams displacement amplitudes show that the strain of the granular material, which is roughly estimated by the ratio beam displacement to cavity length, is of the order of 10^{-6} at frequencies around 1000 Hz. An example of beam acceleration and displacement levels measured during the series of experiments on sand filled beams are shown in Figs. 3.19 and 3.30.

The transition between the two regimes thus lies in the frequency region where the first damping peak occurs and it is therefore expected that amplitude of vibration have only a minor effect upon the damping curve broadening.

6.4.3.2 Pressure effect

The granular material trapped inside cavities of beam tested in vertical position are subjected to pressure varying from zero at the top to about 22500 N/m^2 at the lower end. The beam is 1,5m long.

Experiments on longitudinal waves speed in sand carried out for several hydrostatic pressures showed some variation in the results. For constant strains of 10^{-6}, for instance, speed varies from 220 m/s for no external applied pressure to 300 m/s for a pressure of 13.000 N/m^2. It would therefore be expected some influence upon the damping curve. However, a comparison of results for beams positioned horizontal and vertically shows that only in some cases horizontal beams present a slightly broader damping peak, apart from being shifted towards lower frequencies. See figures 3.14, 3.15 and 3.18.

This leads to the conclusion that pressure variation has some influence to such broad damping peak observed experimentally but may not be the predominant parameter.

6.4.3.3 Comparison between measured and predicted maximum damping frequencies

The damping of three of the beams studied experimentally was predicted and results are compared in Figures 6.11, 6.12 and 6.13 . A good agreement is observed for peak damping frequencies, particularly for predictions assuming a very high internal loss factor for the granular material. This confirms the hypothesis that damping maximization is caused by resonances in the material, but its inability to react to tensional stresses causes a free-end effect as the walls of the structure moves away from the material. The frequency of the first damping peak is given by

$$f_{max} = \frac{C\ell}{4\ell}$$

Cavities accommodate one quarter of a wavelength for the first damping peak.

This work also explains the incertainty with regard to the mechanisms of damping described in the literature. Kerwin[28] for instance, suggested the possibility of maximum damping being caused by shear wave resonances whose half wavelength matched quite closely the internal dimension of the cavity.

Heckl[21], however, suggested that maximum damping occurs when cavities accommodate three-quarters of a wavelength. It must be mentioned that the reason for such divergencies was probably the lack of accurate information about the speed of waves in granular materials.

6.4.3.4 Comparison between damping levels

As longitudinal wavelength is higher than cavity dimensions at low frequencies,grains inside the beam move almost in phase with its walls. The impedance of a segment of material is low in this frequency region and little energy is transfered to it from the beam. It is being assumed that the granular material dissipates all the energy absorved.
Damping thus is very low at low frequencies as can be seen is Figs. 6.11, 6.12 and 6.13.

As the frequency increases, impedance is maximized at the resonances of the material and consequently damping peaks are observed at these frequencies

The first peak occurs when the cavity dimension is one-quarter of the wavelength.

Figures 6.11 to 6.13 show that theoretical results become closer to measured values when predictions are made assuming internal loss factors are of the order of unity. This observation can be explained in terms of inability such materials have to transmit tension stresses. During the propagation of waves through granular materials it is expected that compression stresses mantain their half sine shape whereas this may occur for tensios tresses. Their amplitudes are reduced with respect to compression stresses such that standing waves resultant are different than those existent in a homogeneous and isotropic material.

The material thus behaves as it has much higher internal loss factor than values measured in laboratoty.

This explains the broad shape of peaks in the experimental damping curres.

6.5 Conclusions

Theoretical models presented for analysis and determination of the actual mechanism of damping of hollow beams filled with granular material showed that maximun damping occurs when cavities accommodate one-quarter of a longitudinal wavelength in the filling material. This is caused by the inabibity of the material to resist tensional forces, which produces a "free-end" effect to the material as the beam wall moves away.

The model is accurate enough to determine the mechanism of damping and the maximum damping frequency. Agreement between theoretecal and experimental results is satisfactory if it is assumed that granular materials have internal damping (of the order of unity) much higher than actual values measured in laboratory. The reason lies in the fact that granular materials do not transmit tension stresses as efficiently as for compression stresses.

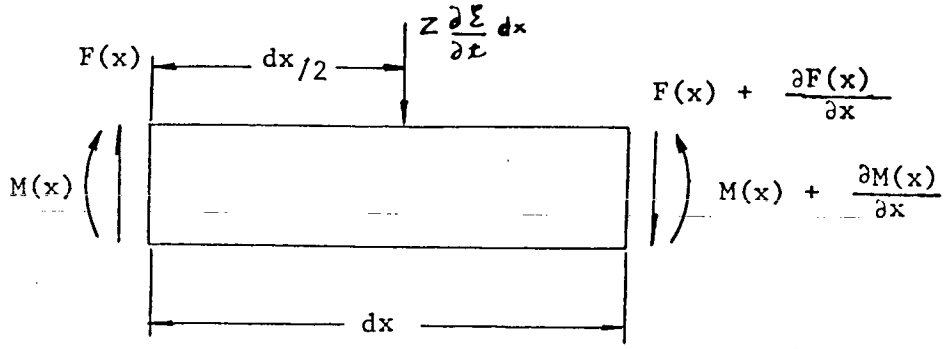

Figure 6.1

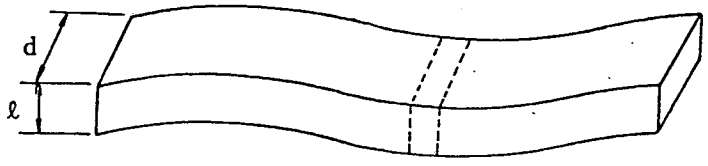

Figure 6.2

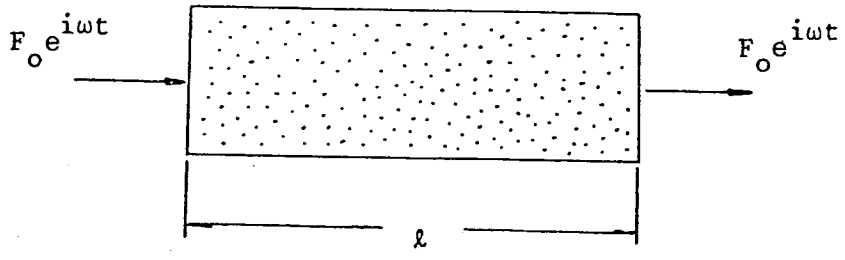

Figure 6.3

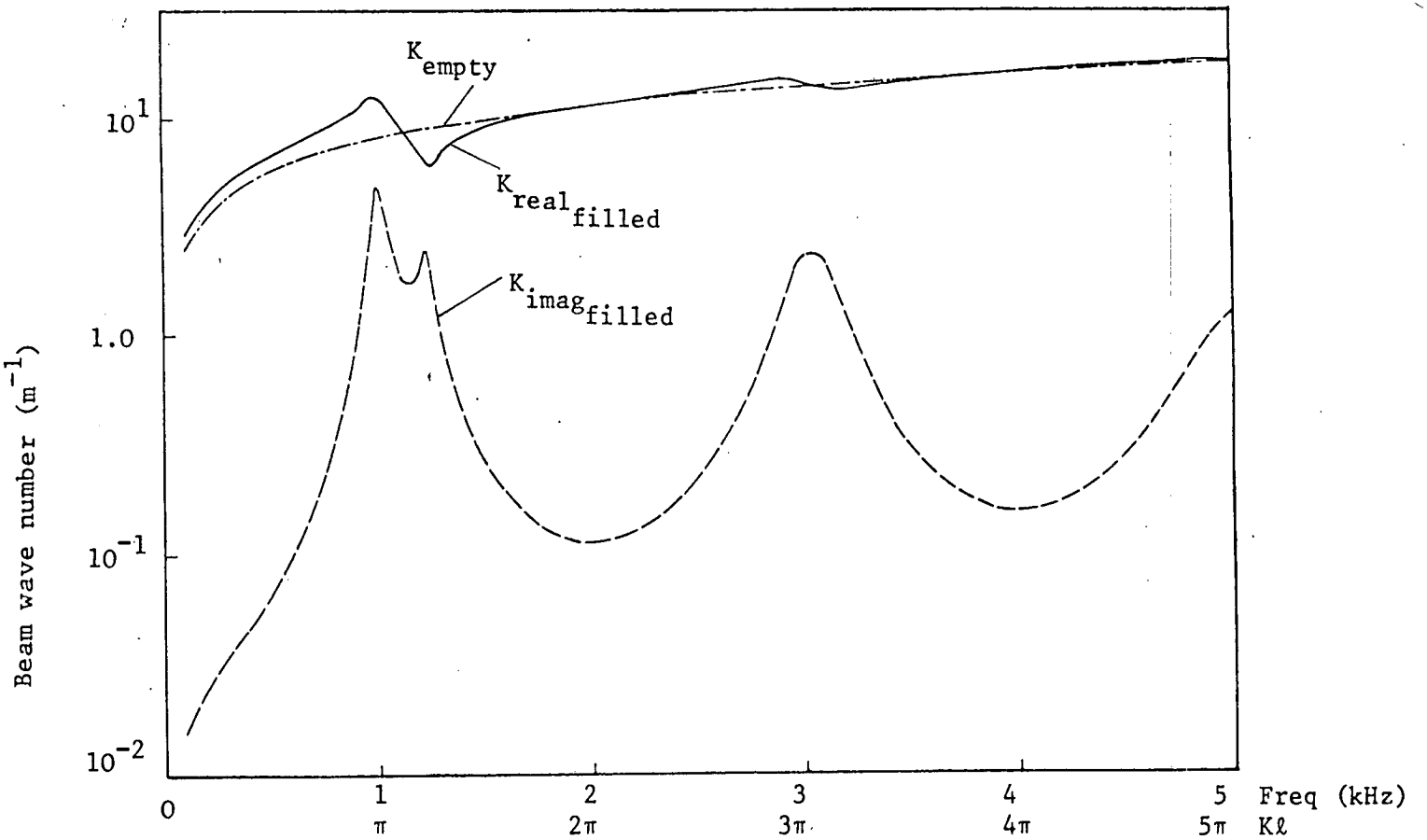

Fig 6.4 Wavenumber of a beam 2"x2"x $\frac{1"}{8}$, empty and filled with granular material having relative density 1.5, loss factor 0.1 and speed of longitudinal waves 100 m/s.

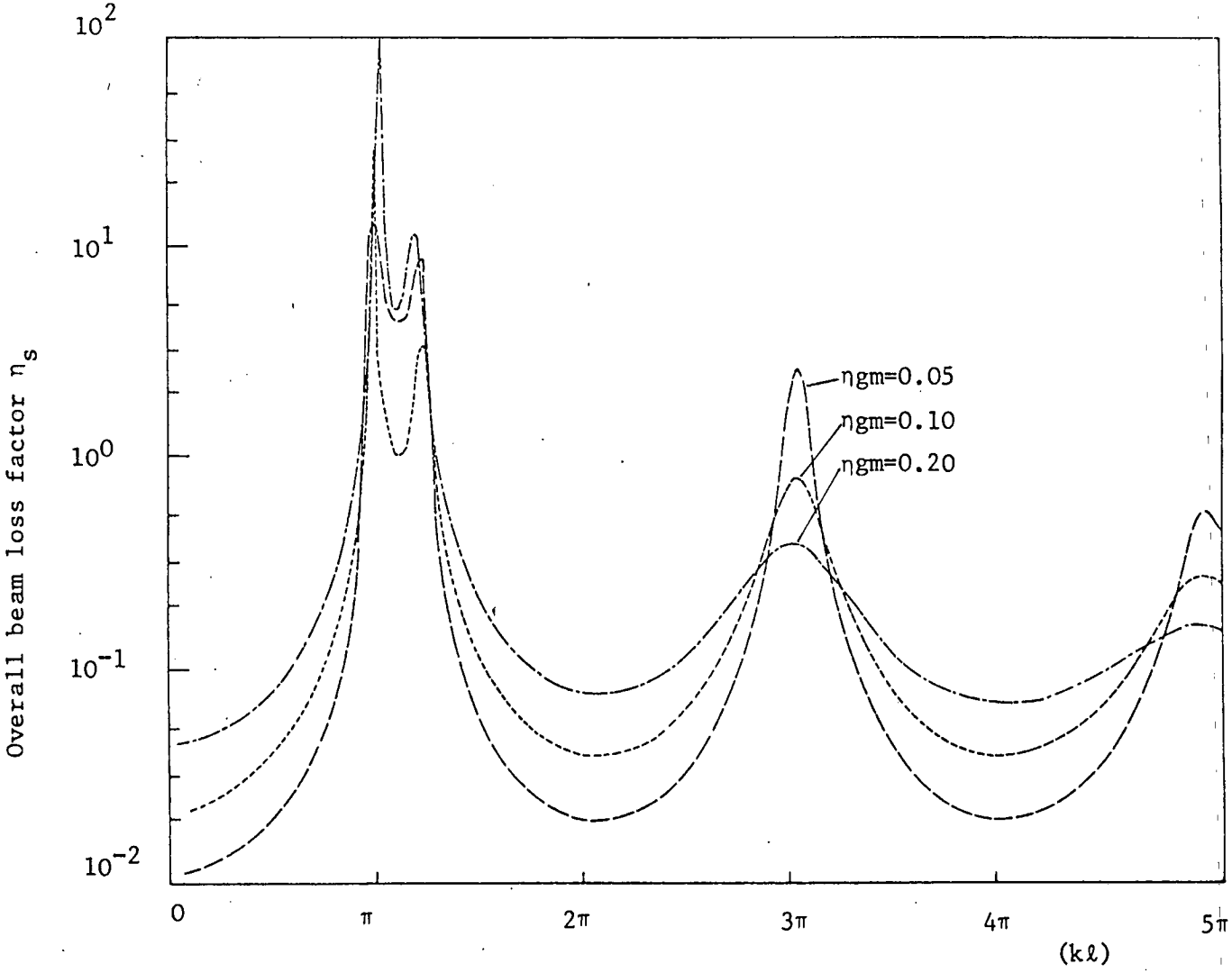

Fig 6.5 Damping prediction of hollow beam (2"x2"x $\frac{1}{8}$" - 1.5 long) filled with granular material. Predicted from beam flexural wave numbers.

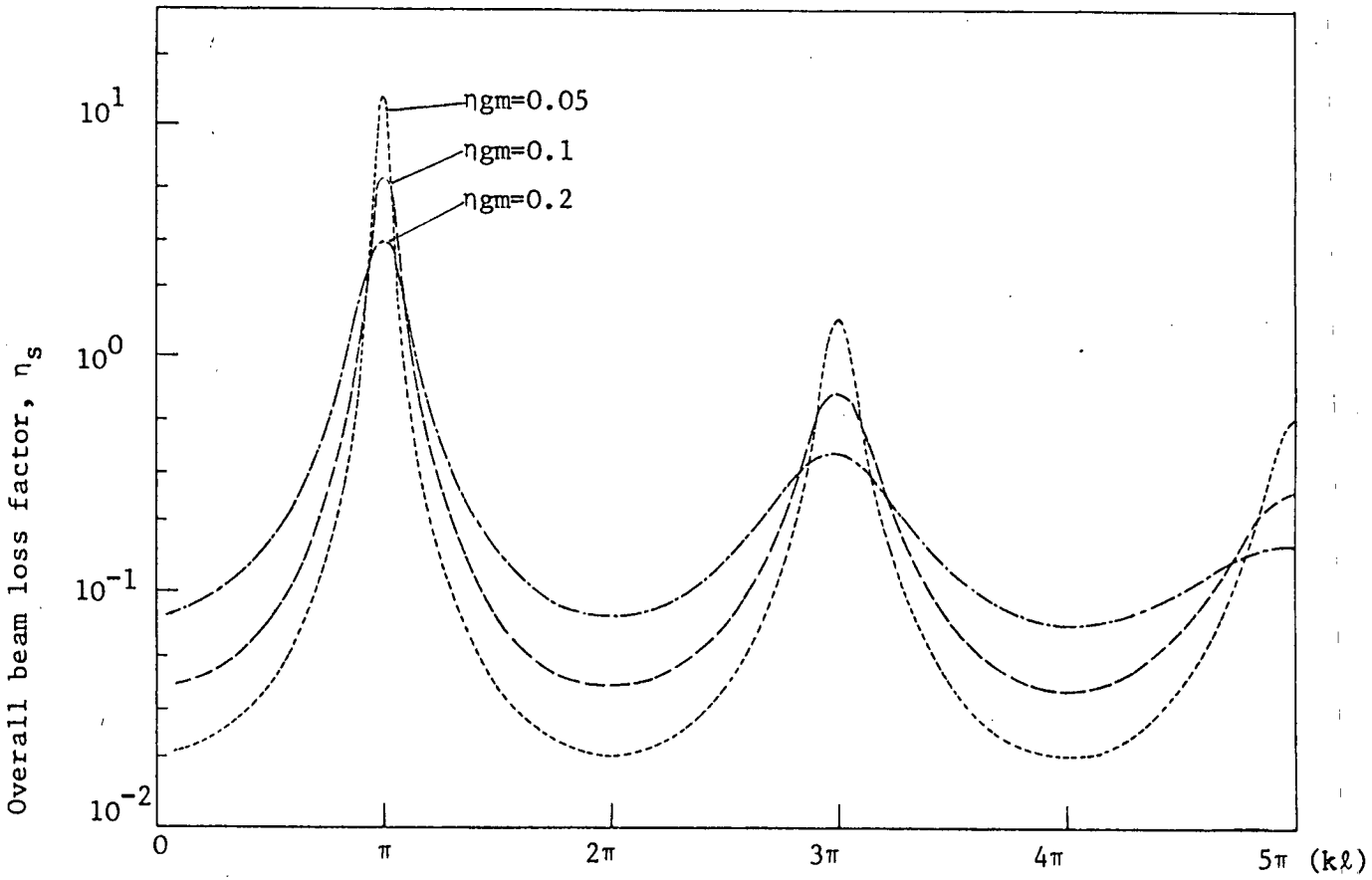

Fig 6.6 Damping prediction of hollow beam (2"x2"x $\frac{1"}{8}$ - 1.5m long) filled with granular material, predicted from impedance expression.

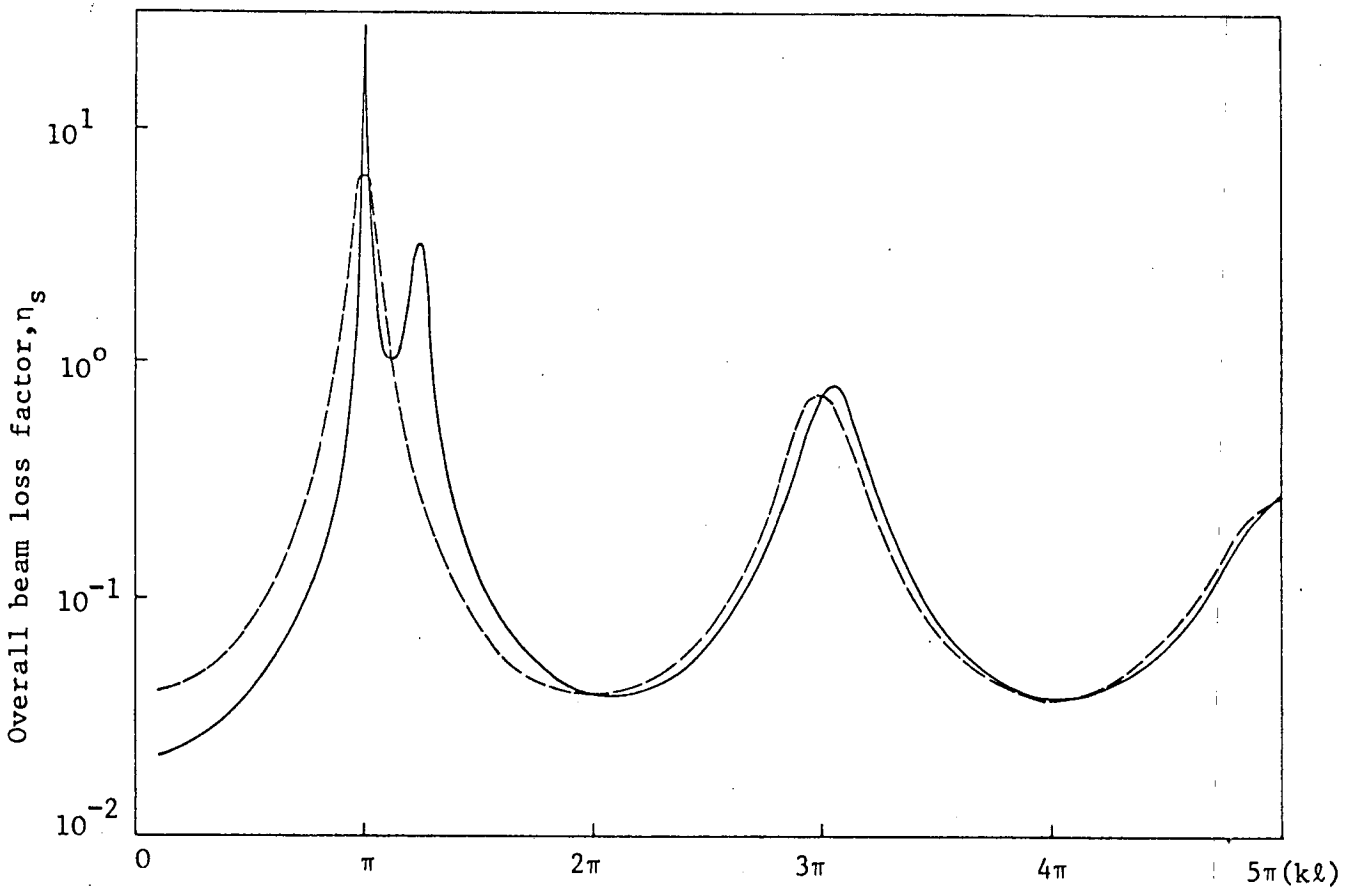

Fig 6.7 Comparison of damping prediction from the two methods

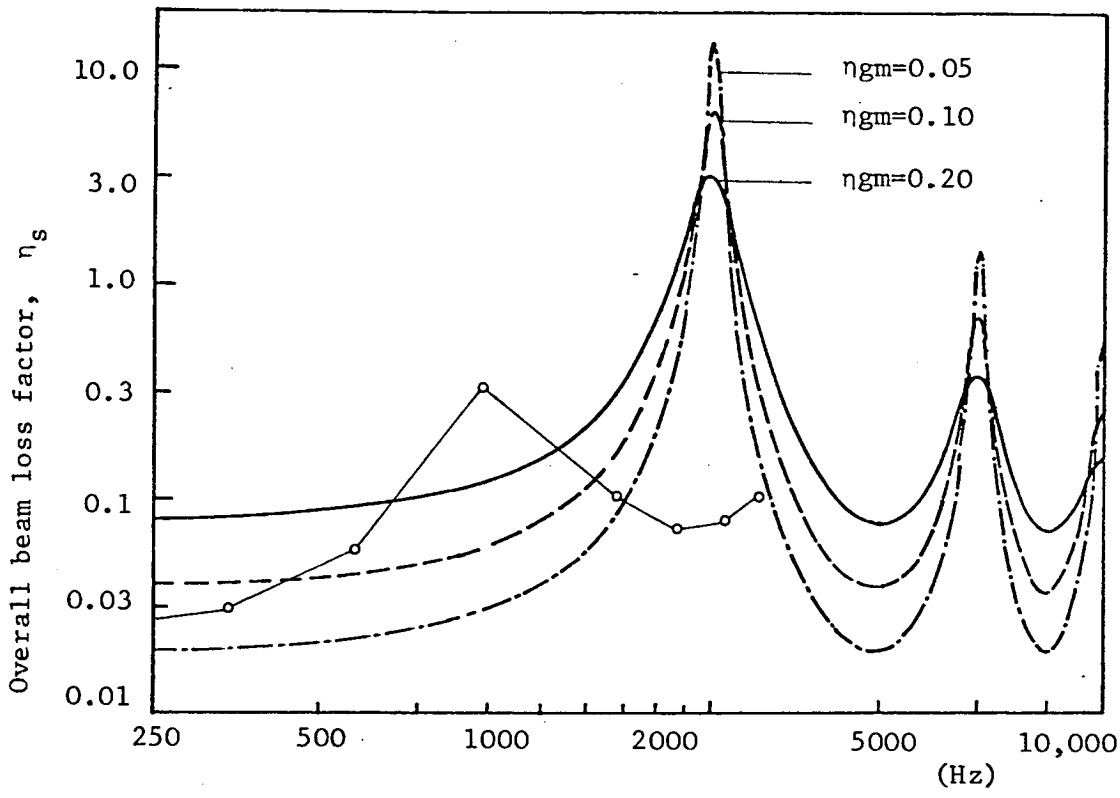

Fig 6.8 Overall loss factor of a beam 2"x2"x $\frac{1"}{8}$ (1.5m long) filled with granular material of 1.5 relative density and speed of longitudinal waves of 250 m/s comparison between theoretical and experimental results.

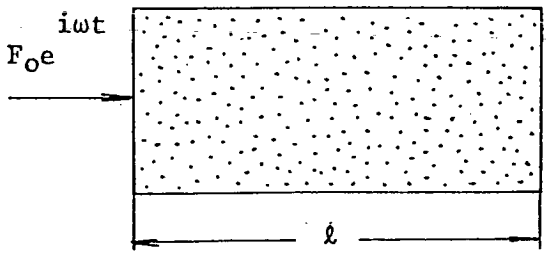

Figure 6.9

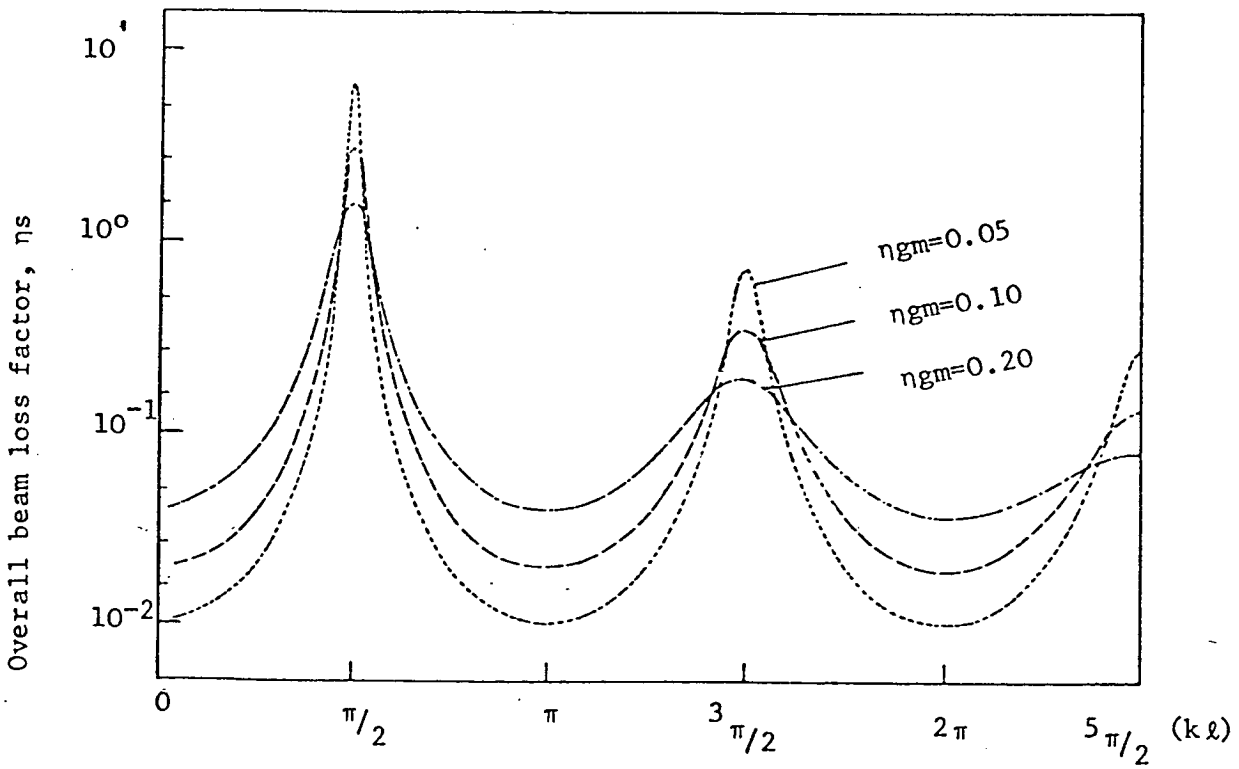

Fig 6.10 Damping prediction of a hollow beam (2"x2"x $\frac{1}{8}$" 1.5m long) filled with granular material. Predicted from impedance expression.

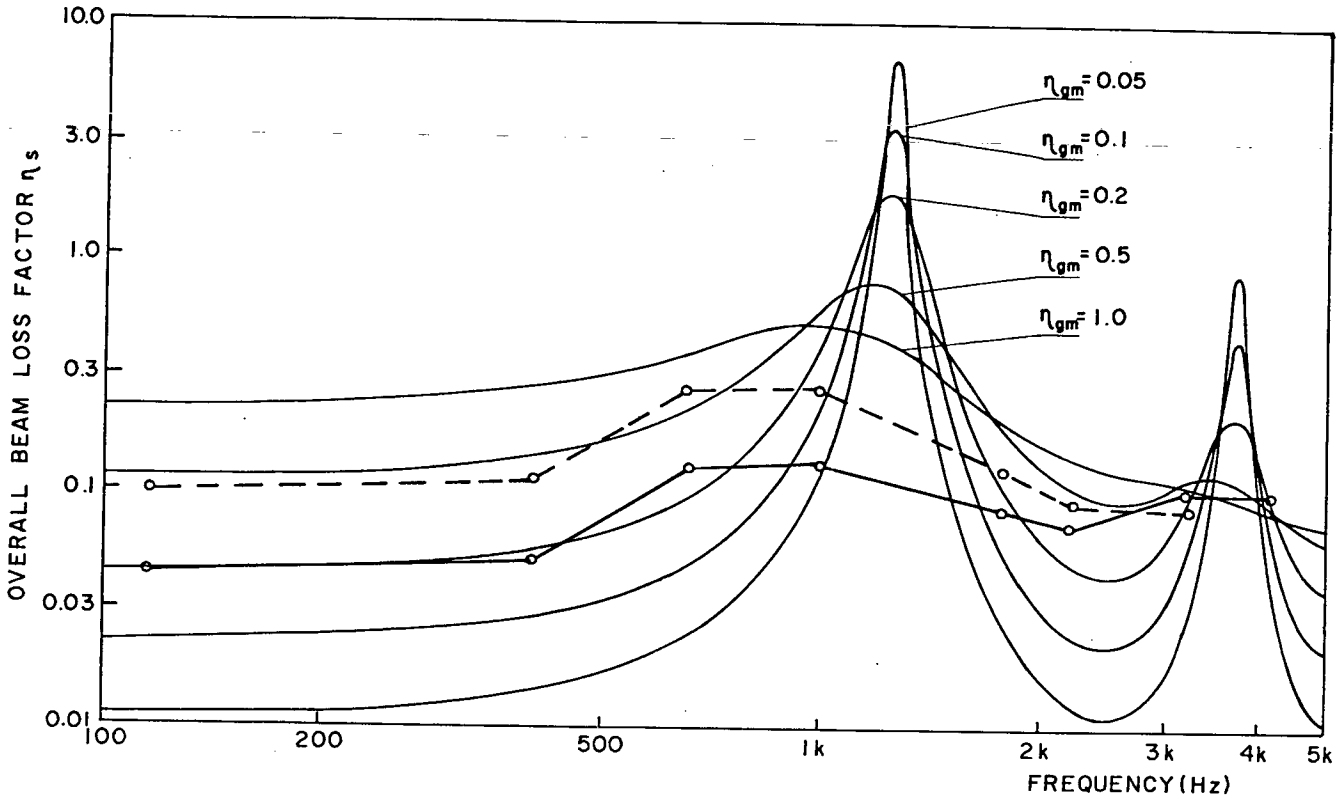

Fig.6.11. Comparison between experimental and predicted loss factor of a beam 2" x 2" x 1/8" - 1,5 m long, filled with dry sand (relative density 1.5 and speed of longitudinal waves, 250 m/s)
o——o Experimental values for beam in vertical position
o– – –o Beam in horizontal position

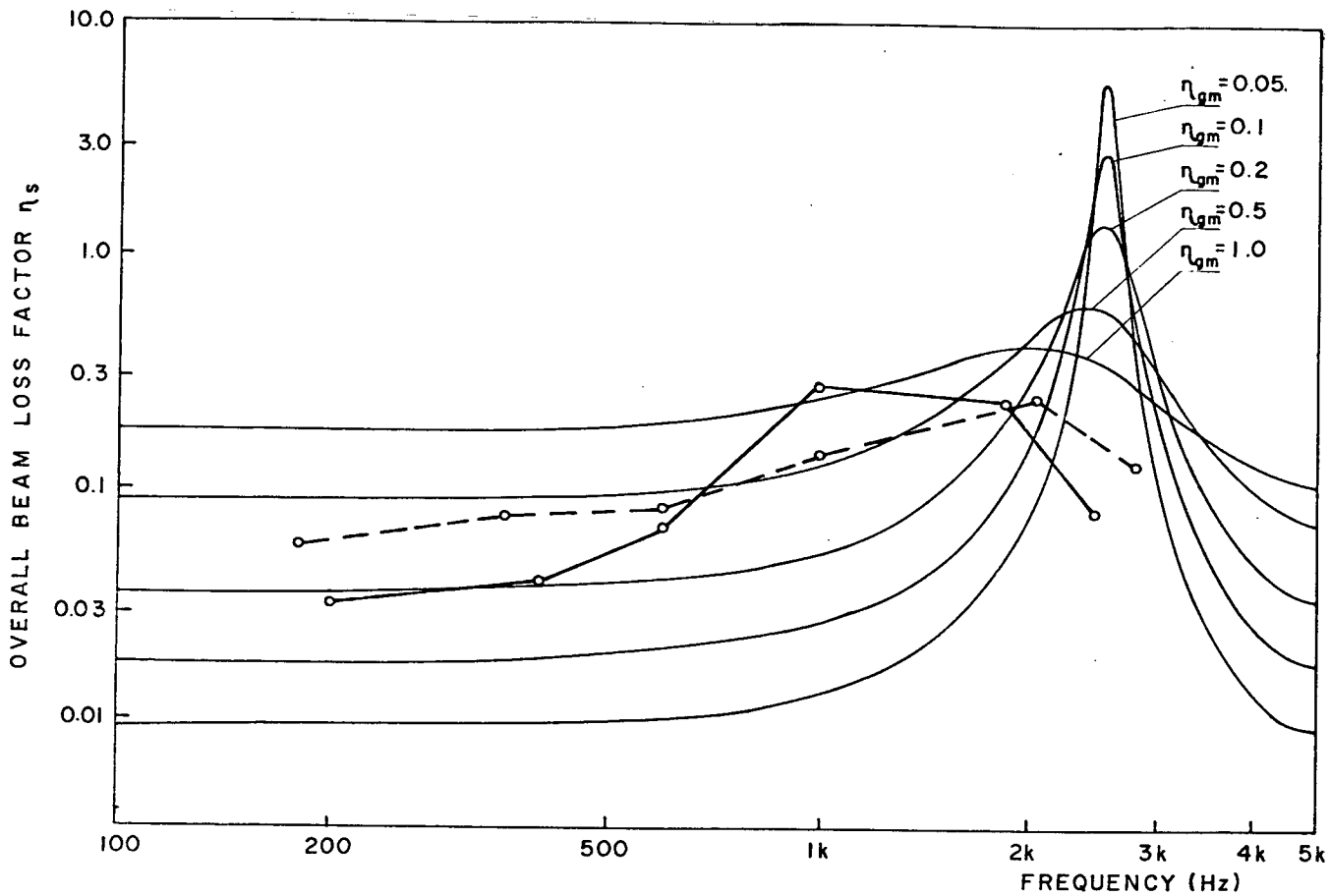

Fig.6.12. Comparison between experimental and predicted loss factor of a beam 2" x 1" x 1/8" - 1.5 m long, filled with dry sand (relative density 1.5 and speed of longitudinal waves, 250m/s).

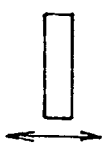

o——o Experimental values for beam in vertical position

o- - -o Beam is horizontal position

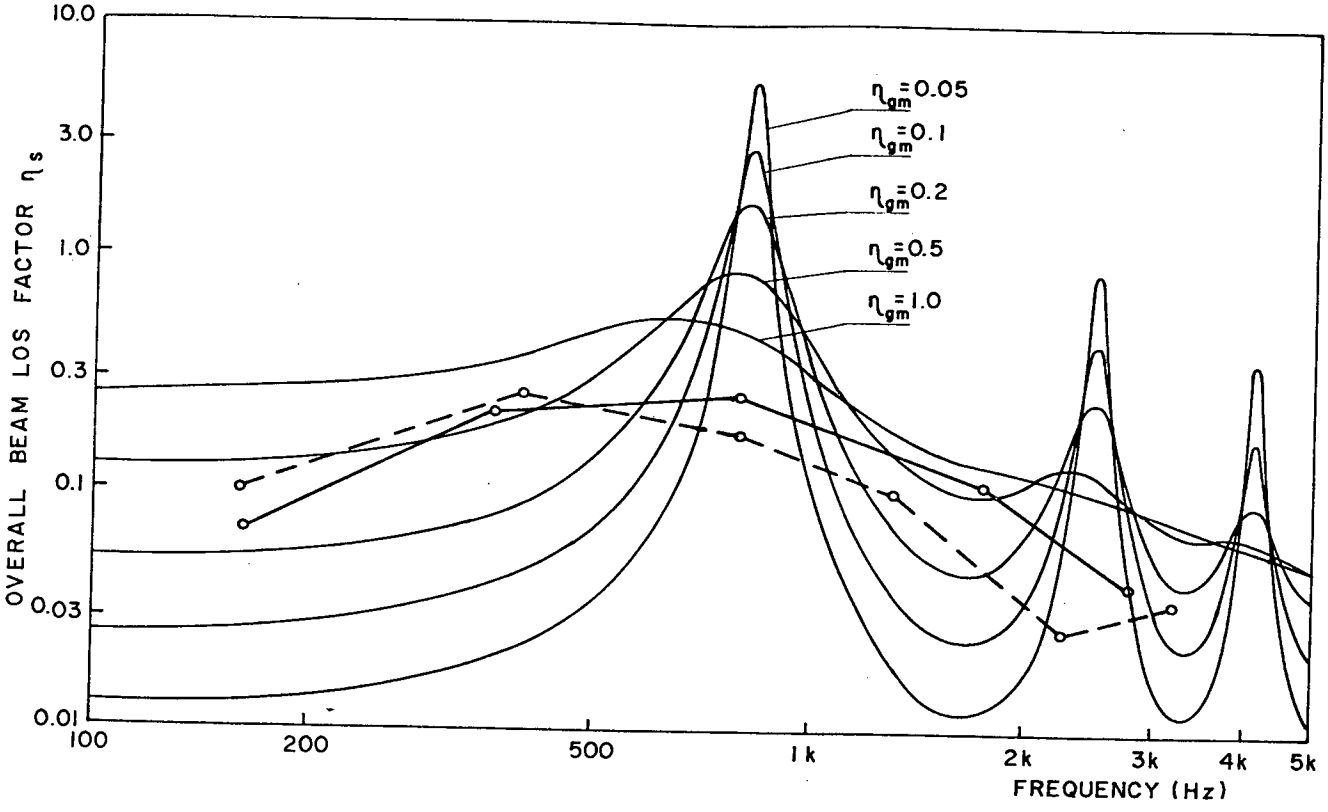

Fig.6.13. Comparison between experimental and theoretical loss factors of a beam 3" x 2" x 1/8" - 1.5 m long, filled with dry sand (relative density 1.5 and speed of longitudinal waves,250 m/s)

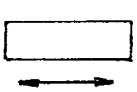

Experimental values for beam in vertical position

Beam in horizontal position

CHAPTER 7

CONCLUSIONS

The broad review on the mechanisms of energy dissipation of machine components (Chapter 2) has led to the conclusion that most of the energy is dissipated in the joints by friction. Experimental measurements of typical machines such as presses and drop forges have shown frequency dependent loss factors varying from about 10^{-1} at 300 Hz to about 10^{-2} at 3000 Hz. The precise nature of the mechanisms involved are to some extent unknown. Previous works on dry frictional damping in joints show that reasonably high levels can occur at the large relative displacements, usually associated with low frequency vibrations. For small relative displacements (high frequencies) negligible energy is dissipated. Thus, dry frictional damping is only significant at the lower end of the spectrum. The loss factors of the order of 10^{-2} occurring at high frequencies in machine structures may be attributed to the viscous damping produced by films of lubricant oils trapped at joint gaps or impurities such as corrosion by-products and humidity which present viscous behaviour.

Most of the acoustic energy radiated from machine structures is in the medium frequency range so that for noise control this is the range where addition of structural damping is useful. This makes the use of granular materials an important damping technique because high loss factors can be achieved at mid-frequencies and also the damping can be maximised at certain frequencies corresponding to resonant conditions in the structure. Maximum levels of damping are obtained when the internal dimension of cavities are equal to one quarter, three quarters, one and a quarter, etc. of the longitudinal wavelength in the material. Thus, the frequency at which optimum conditions are obtained can be selected to be any desired value by proper specification of the internal dimension of the cavities.

Energy dissipation and hence the damping is caused because reaction forces generated by the material oppose the structural motion, absorbing energy in the process and dissipating it into heat within itself.

The damping of granular materials was found to have two distinct regimes related to the amplitude of the vibrational waves. At large amplitudes,

Coulomb friction at grain contacts is the dominant source of energy dissipation, while at low amplitudes, damping is totally provided by the dissipation taking place inside grains in the form of material damping.

Experimental studies on the speed of waves in granular materials have shown that the amplitude of waves also presents a two regime characteristic related to the strain produced by the waves. As granular materials are held together by forces at contacts generated by pressure (either externally applied or that due to its own weight) this causes the build-up of a chain of grain-grain contacts through which waves propagate. For low amplitudes of vibration the forces generated at contacts by such waves are, normally, much smaller than those produced by the external pressure. Thus the chain of contacts is not affected by the waves. Large amplitude waves, however, can produce the collapse of the chain, which reduces the effective elasticity of the granular material, and so reduces the wave speed.

Theoretical analysis of the damping of hollow beams filled with granular materials has shown that loss factors are dependent upon the density of the filling material, leading to the conclusion that denser materials, such as lead shot, are preferable.

The possibility of tuning the maximum damping frequency to any desirable value by altering cavity size is the main feature of granular material damping. The tuning can be achieved by the introduction of spacers inside cavities, positioned one quarter of the longitudinal wavelength at which maximum damping is required. If the structure is solid, boxes filled with granular material can be attached at antinodal points, to achieve similar results.

It is considered that further work is needed to investigate the practical validity of granular material damping treatments:

The columns of drop forges represent a typical application. The acoustic energy is radiated from these components with levels around 700 Hz. A treatment with cavity spacings of 8 cm is suggested to maximise damping at this frequency. Granular materials can also be useful to provide damping improvements in the walls of buildings which have a poor transmission loss at their first resonance. Granular materials are suitable for the absorption of very intense sounds because of the occurrence of gross slip.

A sound level of 120 dB has an RMS pressure of 20 N/m^2, which is high enough to produce gross slip at contacts if the material is subjected to low external pressures. Granular materials could, therefore, be used in the walls of close fitting enclosures as an alternative to conventional enclosure walls with a high mass and stiffness. For a wall made entirely of supported granular material sound waves would have to pass directly through the granular material rather than be transmitted by flexural vibrations as in stiff walls.

APPENDIX A: The Duffy and Mindlin Approach for the Study of Waves in Granular Materials

The Duffy and Mindlin approach for the analytical study of speed of waves in a pack of perfect spheres considers a unit cube in a face-centred cubic arrangement. Each sphere in the array is in contact with twelve others, so that there are thirty-six independent rectangular components of contact forces per sphere. For homogeneous state of stress, forces are diametrically opposed, contacts are equal and oppositely directed, and as a result, the number of independent components is reduced to eighteen (six normal, N, and twelve tangential, T).

The incremental relative displacement between centres of spheres is given by each component of incremental contact force multiplied by the associated instantaneous compliance, as follows:

$$d\alpha_i = C_i dN_i$$

and

$$d\theta_i = S_i dT_i$$

where C_i, S_i are normal and tangential compliances, respectively, and α_i, θ_i are normal and tangential relative displacements.

The incremental strains in the array are expressed in terms of the relative displacements of centres of spheres, so that stress-strain relations are determined when the incremental contact forces are found in terms of stresses applied to the unit cube.

For an initial hydrostatic pressure σ_o, all initial contact forces between spheres are purely normal, with magnitude,

$$N_o = R^2 \sigma_o \sqrt{2}$$

where R is the radius of the spheres.

If one-dimensional waves only are assumed to propagate through the granular material whose amplitude of stress is σ_a, the number of components of contact forces is reduced to three (two normal and one tangential), which can be expressed in the form:

$$dN_1 = f_1 d\sigma_o + g_1 d\sigma_a$$

$$dN_2 = f_2 d\sigma_o + g_2 d\sigma_a$$

$$dT = f_3 d\sigma_o + g_3 d\sigma_a$$

where f and g are functions of compliance.

The analysis is restricted to constant obliquity of contact forces at each contact, i.e., $dT/dN = \beta$, and it is also assumed that β is less than or at most equal to the coefficient of friction of the contact.

Thurston and Deresiewicz[54] have carried out the integration of the above equation resulting in expressions as follows:

$$(1 + N_1/N_o)^{2/3} = \beta k + (1 - \beta k)(1 + N_2/N_o)^{2/3}$$

$$T_2 = \beta N_2$$

and

$$1 + N_1/N_o = (2\sigma_a/\sigma_o + 3\beta)/[(1 + 3\beta)\xi^3 - 1] .$$

An expression for σ_a was also found as follows:

$$\sigma_a = \frac{\sigma_o}{2} [(\lambda - 1)/(\lambda - \xi^2)]^{3/2}[(1 - \beta)\xi^3 + 1] - (2 - \beta)$$

and for the strain

$$\varepsilon = \tfrac{3}{4} \frac{1 + k\beta}{1 - k\beta} \left[\frac{2(1 - \nu)^2}{3G^2}\right]^{1/3} \sigma_o^{2/3} \left(\frac{\xi^2 - 1}{\lambda - \xi^2}\right)$$

where $\xi = ((N_o + N_2)/(N_o + N_1))^{1/3}$,

$k = (2 - \nu)/2(1 - \nu)$,

and $\lambda = (1 - k\beta)^{-1}$

ν is the Poisson's ratio and G the shear modulus of the material of the spheres.

REFERENCES

1. RICHARDS, E.J. 1981 "On the prediction of impact noise. III: Energy accountancy in industrial machines". J. Sound Vib., Vol. 76, No. 2, pp. 187-232.

2. RICHARDS, E.J., WESTCOTT, M.E. and JEYAPALAN, R.K. 1979 "On the prediction of impact noise. Part II: Ringing noise". J. Sound Vib. Vol. 65, No. 3, pp. 419-451.

3. SKUDRZYK, E. 1980 "The mean-value method of predicting the dynamic response of complex vibrators". J.A.S.A. Vol. 67, No. 4, pp. 1105-1135.

4. RICHARDS, E.J.,CARR, I. and WESTCOTT, M.E. 1982 "On the prediction of impact noise. Part V: The noise from drop hammers", paper submitted for publication in J. Sound Vib.

5. LAZAN, B.J. 1968 "Damping of materials and members in structural mechanics", Pergamon Press, London.

6. KAELBLE, D.H. 1964 "Micromechanisms and phenomenology of damping in polymers", ASTM special technical publication no. 378. Symposium on "Internal friction, damping and cyclic plasticity", Chicago, 22nd June 1964.

7. STIMPSON, G. and LENZI, A. 1980 ISVR Internal Report.

8. ASTM - Draft 5 revised - Test method for measuring vibration damping properties of materials.

9. O'CONNOR, J.J. and JOHNSON, K.L. 1963 "The role of surface asperities in transmitting tangential forces between metals", Wear, Vol. 6, pp. 118-139.

10. ANDREW, C., COCKBURN, J.A. and WARING, A.E. 1967-68 "Metal surfaces in contact under normal forces: some dynamic stiffness and damping characteristics". Proc. Institution of Mechanical Engineers, Vol. 182, Pt. 3K, pp. 92-100.

11. BEARDS, D.F. 1975 "Some effects of interface preparation on frictional damping in joints". Int. Journal Mach. Tool Des. Res., vol. 15, pp. 77-83.

12. TABOR, D. 1959 "Junction growth in metallic friction". Proc. Royal Soc., vol. 251 (series A), page 378.

13. RABINOWICZ, E. 1960 "Practical approach to friction coefficients". Product Engineering, Sept. pp. 51-53.

14. EARLS, S.W.E. and PHILPOT, M.G. 1967 "Energy dissipation at plane surfaces in contact". Journal Mech. Eng. Sci. vol. 9, No. 2, pp. 86-97.

15. ITO, Y. and MASUKO, M. 1971 "Experimental study on the optimum interface pressure on a bolted joint considering the damping capacity". Proceedings 12th Int. MTDR Conference.

16. GOODMAN, L.E. and KLUMPP, J.H. 1956 "Analysis of slip damping with reference to turbine-blade vibration". Journal of Appl. Mech., Trans. ASME, pp. 421-429.

17. EARLS, S.W.E. and BEARDS, C.F. 1970 "Some aspects of frictional damping as applied to vibrating beams". Int. J. Mach. Tool Des. Res., vol. 10, pp. 123-131.

18. MENTEL, T.J. 1964 "Viscoelastic boundary damping of beams and plates". J. App. Mech., Trans. ASME, pp. 61-71.

19. MENTEL, T.J. 1967 "Joint interference layer damping". J. Eng. Ind., Trans. ASME, pp. 797-805.

20. ITO, Y. and MASUKO, M. 1975 "Study on the damping capacity of bolted joints - effects of the joint surfaces condition". Bulletin JSME, vol. 18, no. 117, pp. 319-326.

21. CREMER, L. and HECKL, M. 1973 "Structure-borne sound". Springer-Verlag, New York.

22. JONES, D.I.D., NASHIF, A.D. and ADKINS, R.L. 1967 "Effect of tuned dampers on vibrations of simple structures". AIAA Journal, vol. 5, no. 2, pp. 310-315.

23. TROCHIDIS, A. 1977 Ph.D. Thesis "Korperschalldampfung Durch Viskositatsverluste in Gasschichten Bei Doppelplatten". Univ. of Berlin.

24. MOSER, M. 1980 "Damping of structure-borne sound by the viscosity of a layer between two plates". Acustica, vol. 46, pp. 210-217.

25. STIMPSON, G. and LENZI, A. 1980 "Report on the damping properties of four samples of high density metals". ISVR internal report.

26. HALLIWELL, N.A. 1979 "Laser-Doppler measurement of vibrating surfaces: a portable instrument". J. Sound Vib. vol. 62, no. 2, pp. 312-315.

27. WOLF, N.D. 1962 "Results of loss factor measurements on concrete beams using a viscoelastic or sand damping system". ASD-TDR-62-717. Wright-Patterson AFB, Ohio.

28. KERWIN, E.M. 1964 "Macromechanisms of damping in composite structures". Paper published at the 67th Annual Meeting of ASTM on Internal Friction Damping and Cyclic Plasticity. ASTM-STP No. 378.

29. KUHL, W. and KAISER, H. 1952 "Absorption of structure-borne sound in building materials with and without sand-filled cavities". Acustica, vol. 2, pp. 179-188.

30. GORDON, R.B. and DAVIS, L.A. 1968 "Velocity and attenuation of seismic waves in imperfectly elastic rock". Journal of Geophysical Research, vol. 73, no. 12, pp. 3917-3935.

31. ATTEWELL, P.B. and RAMANA, Y.V. 1966 "Wave attenuation and internal friction as functions of frequency in rocks". Geophysics, vol. 31, no. 6, pp. 1049-1056.

32. WALSH, J.B. 1966 "Seismic wave attenuation in rock due to friction". Journal of Geophysical Research, Vol. 71, no. 10, pp. 2951-2959.

33. WINKLER, K., NUR, A. and GLADWIN, M. 1979 "Frictional and seismic attenuation in rocks". Nature, vol. 277, pp. 528-531.

34. JACKSON, D.D. and ANDERSON, D.L. 1970 "Physical mechanisms of seismic wave attenuation". Rev. Geophys. Space Phys. Vol. 8, no. 1, pp. 1-63.

35. MASON, W.P. 1971 "Internal friction in moon and earth rocks". Nature, vol. 234, December, pp. 461-463.

36. MAVKO, G.M. 1979 "Frictional attenuation and an inherent amplitude dependence". Journal of Geophysical Research, vol. 84, pp. 4769-4775.

37. BYERLEE, J.D. 1967 "Frictional characteristics of granite under high confining pressure". Journal of Geophysical Research, vol. 27, no. 14, pp. 3639-3648.

38. WARREN, N. and ANDERSON, O.L. 1973 "Elastic properties of granular materials under uniaxial compaction cycles". Journal of Geophysical Research, vol. 78, no. 29, pp. 6911-6925.

39. HALL, J.R. and RICHART, F.E. 1963 "Dissipation of elastic wave energy in granular soils". Journal of the Soil Mechanics and Foundations Division, Proc. ASCE, November, SM6, pp. 27-56.

40. HARDIN, B.O. 1965 "The nature of damping on sands". Journal of Soil Mechanics and Foundations Division, Proc. ASCE, January, pp. 63-97.

41. RICHART, F.E. Jr., HALL, J.R. and WOODS, R.D. 1970 "Vibrations of Soils and Foundations". Prentice-Hall Inc., N.J.

42. GOLDSMITH, W. 1960 "Impact, The Theory and Physical Behaviour of Colliding Solids", Edward Arnold (publishers) Ltd., London.

43. TIMOSHENKO, S. and GOODIER, J.N. 1949 "Theory of Elasticity". McGraw-Hill Book Co., New York.

44. MINDLIN, R.D. and DERESIEWICZ, H. 1953 "Elastic spheres in contact under varying oblique forces". J. App. Mechanics, Trans. ASME, September, pp. 327-344.

45. MINDLIN, R.D., MASON, W.P., OSMER, J.F. and DERESIEWICZ, H. 1951 "Effects of an oscillating tangential force on the contact surfaces of elastic spheres". Proc. 1st US National Congress of App. Mechanics, New Jersey.

46. JOHNSON, K.L. 1955 "Surface interaction between elastically loaded bodies under tangential forces". Proc. Royal Soc. (A), vol. 230, pp. 531-549.

47. GOODMAN, L.E. and BROWN, C.B. 1962 "Energy dissipation in contact friction: constant normal and cyclic tangential loading". J. App. Mech. Trans. ASME, vol. 29, pp. 17-22.

48. JOHNSON, K.L. 1961 "Energy dissipation at spherical surfaces in contact transmitting oscillating forces". Journal Mechanical Engineering Science, vol. 3, no. 4, pp. 362-368.

49. DUFFY, J. and MINDLIN, R.D. 1957 "Stress-strain relations and vibrations of a granular medium". J. App. Mechanics, Trans. ASME, December, pp. 585-593.

50. IIDA, K. 1939 "Velocity of elastic waves in a granular substance". Bull. Earthquake Research Inst., vol. 17, pp. 783-808.

51. HARDIN, B.O. and RICHART, F.E. 1963 "Elastic wave velocities in granular soils". J. Soil Mech. and Foundations Division. Proc. ASCE, February, pp. 33-65.

52. BRANDT, H. 1955 "A study of the speed of sound in porous granular media". J. App. Mechanics, Trans. ASME, December, pp. 479-486.

53. SKUDRZYK, E. 1968 "Simple and complex vibratory systems". Pennsylvania State University Press, State College, PA.

54. THURSTON, C.W. and DERESCIEWICZ, H. 1959 "Analysis of a compression test of a model of a granular medium". Journal of App. Mech., Trans. ASME, June, pp. 251-258.